Schweizerische Eidgenossenschaft
Confédération suisse
Confederazione Svizzera
Confederaziun svizra

Federal Department of the Environment, Transport, Energy and Communications DETEC

**Swiss Federal Office of Energy SFOE**
Energy Research and Cleantech Division

**Final report from 16.05.2025**

# OrtsNetz


**Source:** ©EKZ 2023

**Date:** 16.05.2025

**Location:** Bern

**Publisher:**
Swiss Federal Office of Energy SFOE
Energy Research and Cleantech
CH-3003 Bern
www.bfe.admin.ch

**Subsidy recipients:**
Power Systems Laboratory, ETH Zurich
Physikstrasse 3, CH-8092 Zurich
www.psl.ee.ethz.ch

Bits to Energy Lab, ETH Zurich
Weinbergstrasse 56/58, CH-8092 Zurich
www.bitstoenergy.com

Elektrizitätswerke des Kantons Zürich
Ueberlandstrasse 2, CH-8953 Dietikon
www.ekz.ch

**Authors:**
Katharina Kaiser, Power Systems Laboratory, ETH Zurich, kkaiser@ethz.ch
Markus Kreft, Bits to Energy Lab, ETH Zurich, mkreft@ethz.ch
Matteo Guscetti, Power Systems Laboratory, ETH Zurich
Dr. Gustavo Valverde, Power Systems Laboratory, ETH Zurich, gustavov@ethz.ch
Dr. Ludger Leenders, Elektrizitätswerke des Kantons Zürich
Dr. Marina González Vayá, Elektrizitätswerke des Kantons Zürich, marina.gonzalezvaya@ekz.ch
Prof. Dr. Thorsten Staake, Bits to Energy Lab, ETH Zurich, tstaake@ethz.ch
Prof. Dr. Gabriela Hug, Power Systems Laboratory, ETH Zurich, ghug@ethz.ch

**SFOE project coordinators:**
Karin Söderström, karin.soederstroem@bfe.admin.ch
Michael Moser, michael.moser@bfe.admin.ch

**SFOE contract number:** SI/502271-01

# Summary

The increasing deployment of decentralized renewable energy sources and the electrification of the transport and heating sectors place great demands on the distribution grid. To meet these challenges, the OrtsNetz pilot project explored the use of time-dependent grid usage tariffs and automated load control to help avoid power peaks in the low-voltage grid and ease the integration of decentralized sources. In this context, the project investigated and compared (i) changes in customer behavior due to tariff signals, (ii) automated load control of large appliances (electric water heaters, heat pumps, and electric vehicles) via tariff signals, and (iii) direct control of these flexible loads by the distribution grid operator based on central optimization.

The pilot project was implemented in the municipality of Winkel, located in the canton of Zurich. Flexible loads from three transformer stations were controlled, with one station assigned to each OrtsNetz scheme. The first two settings were based on indirect load control: a pre-planned Time-of-Use tariff and a fully dynamic real-time tariff able to adapt to different grid situations. In a third scheme, loads were directly controlled using a centralized optimization. In return, the customers received a reduced constant grid-usage tariff for providing flexibility to the distribution system operator. For technical feasibility, the control in all three schemes was limited to blocking or unblocking the power consumption of flexible loads.

A total of 630 customers received a new tariff for the project. Out of these, 546 participated without a control device. For automatic control of electric water heaters and heat pumps, 64 load control devices were installed at customer houses. Additionally, 42 customers registered their electric vehicles to be used as flexible loads.

The manual change in energy consumption in response to the novel tariffs was generally low, on the order of a few percent. A significant difference in the reaction exists between customers who actively signed up to the project (Opt-in) and those who were passively enrolled (Not Opt-out). This difference in engagement is also observable in the interaction with participant surveys, the OrtsNetz platform, and the voluntary market for local solar power. Survey respondents were generally happy with the project and expressed a high desire for novel tariffs. In turn, they expect savings on their electricity bill.

The analysis of the automated load control shows that in summer, the dynamic real-time tariff achieved the largest reductions of feed-in peaks, followed by the direct load control scheme and the Time-of-Use tariff. In winter, the direct load control achieved peak reductions when comparing the peaks during the pilot with the ones observed with the standard well-known ripple control. However, none of the OrtsNetz schemes could reduce the consumption peaks in winter compared to a setting without any control of flexible loads.

The findings on customer behavior are limited by the best-accounting policy implemented in the project, which ensured that participants could only accumulate savings and never spend more. Nonetheless, the project results have major implications for the use of novel tariffs. While pilot projects and Opt-in offers may suggest strong customer reactions, the real impact of such tariffs must be evaluated among the wider public and may show substantially lower effects.

Regarding automated load control, the project results show that the technology for deploying direct and indirect load control schemes is ready and that the dynamic real-time tariff and direct load control outperform the Time-of-Use tariff. Simulation results indicate that the dynamic tariff scheme and direct load control performance could be enhanced to achieve higher peak reductions in summer and winter. Furthermore, it is expected that a larger fleet of controllable electric vehicles would make the benefits of these schemes more evident.

# Zusammenfassung

Der steigende Einsatz dezentraler erneuerbarer Energiequellen sowie die Elektrifizierung des Transport- und Wärmesektors stellen grosse Anforderungen an das Verteilnetz. Zur Bewältigung der entstehenden Herausforderungen hat das Pilotprojekt OrtsNetz den Einsatz von zeitabhängigen Netznutzungstarifen und automatisierter Laststeuerung untersucht, um Leistungsspitzen im Niederspannungsnetz zu vermeiden und die Integration dezentraler Quellen zu erleichtern. In diesem Kontext untersuchte und verglich das Projekt (i) Verhaltensänderungen von Kundinnen und Kunden durch Tarifsignale, (ii) die automatisierte Laststeuerung wichtiger Verbraucher (Boiler, Wärmepumpen und Elektrofahrzeuge) mit Hilfe von Tarifsignalen und (iii) die direkte Ansteuerung dieser flexiblen Lasten durch den Verteilnetzbetreiber auf Basis einer zentralen Optimierung.

Das Pilotprojekt wurde in der Gemeinde Winkel im Kanton Zürich durchgeführt. An drei Transformatorstationen wurden flexible Lasten gesteuert, wobei jede Station einem OrtsNetz-Steuerungsansatz zugeordnet war. Die ersten beiden Ansätze basierten auf einer indirekten Laststeuerung: einem im Voraus festgelegten Time-of-Use-Tarif und einem dynamischen Echtzeittarif, der sich an unterschiedliche Netzsituationen anpassen kann. In einem dritten Ansatz wurden die Schaltbefehle mit Hilfe einer zentralen Optimierung festgelegt. Hier erhielten die Kundinnen und Kunden für die Bereitstellung von Flexibilität einen günstigeren Einheitstarif. Auf Grund von technischen Rahmenbedingungen beschränkte sich die Steuerung in allen drei Ansätzen auf das Sperren oder Freigeben der Leistungsaufnahme flexibler Lasten.

Insgesamt erhielten 630 Kundinnen und Kunden im Rahmen des Projekts einen neuen Tarif. Von diesen nahmen 546 ohne eine automatisierte Steuerung teil. Für die Steuerung von Boilern und Wärmepumpen wurden 64 Lastschaltgeräte in den Häusern der Kundinnen und Kunden installiert. Zusätzlich haben 42 Kundinnen und Kunden ihre Elektrofahrzeuge als flexible Lasten angemeldet.

Die manuelle Änderung des Energieverbrauchs als Reaktion auf die neuen Tarife war im Allgemeinen gering und lag im einstelligen Prozentbereich. Es besteht ein signifikanter Unterschied in der Reaktion von den Kundinnen und Kunden, die sich aktiv für das Projekt angemeldet haben (Opt-in), und jenen, die passiv aufgenommen wurden (Not Opt-out). Dieser Unterschied in der Aktivität ist auch in der Interaktion mit den Teilnehmerumfragen, der OrtsNetz-Plattform und dem freiwilligen lokalen Solarstromhandel zu beobachten. Die Umfrageteilnehmerinnen und -teilnehmer waren im Allgemeinen mit dem Projekt zufrieden und äusserten ein grosses Interesse an neuartigen Tarifen. Im Gegenzug erwarten sie Einsparungen bei ihrer Stromrechnung.

Die Analyse der automatisierten Laststeuerung zeigt, dass der dynamische Echtzeittarif im Sommer die grössten Reduzierungen bezüglich der Einspeisespitzen erzielte, gefolgt von der direkten Laststeuerung und dem Time-of-Use-Tarif. Im Winter konnte die direkte Laststeuerung Bezugsspitzen im Vergleich zur weit verbreiteten Rundsteuerung senken. Im Vergleich zu einer Messphase ohne Steuerung der flexiblen Lasten konnten die OrtsNetz-Ansätze die Bezugsspitzen im Winter jedoch nicht reduzieren.

Die Erkenntnisse zu Verhaltensänderungen von Kundinnen und Kunden sind durch die im Projekt umgesetzte Bestabrechnung eingeschränkt, die sicherstellte, dass den Teilnehmerinnen und Teilnehmern keine Mehrkosten entstehen konnten. Nichtsdestotrotz ergeben sich aus den Projektergebnissen wichtige Schlussfolgerungen bezüglich der Nutzung neuartiger Tarife. Während Pilotprojekte und Opt-in-Angebote auf starke Reaktionen der Kundinnen und Kunden hindeuten könnten, muss der tatsächliche Einfluss solcher Tarife in der breiten Öffentlichkeit evaluiert werden, wobei die Auswirkungen wesentlich geringer ausfallen könnten.

Bezüglich der automatisierten Laststeuerung zeigen die Projektergebnisse, dass sowohl die direkte als auch die indirekte Laststeuerung technisch umsetzbar sind und dass der dynamische Echtzeittarif und die direkte Laststeuerung zu einer höheren Senkung der Leistungsspitzen führen als der Time-of-Use-Tarif. Simulationsergebnisse deuten darauf hin, dass die Steuerung über den Echtzeittarif und die direkte Steuerung weiter optimiert werden könnten, um höhere Spitzensenkungen im Sommer und Winter zu erzielen. Darüber hinaus ist davon auszugehen, dass der Mehrwert dieser Ansätze mit einer höheren Anzahl an steuerbaren Elektrofahrzeugen steigt.

# Résumé

Le déploiement croissant d'énergie renouvelables décentralisées et l'électrification des secteurs du transport et du chauffage sollicitent fortement le réseau électrique de distribution. Pour relever ces défis, le projet pilote OrtsNetz a exploré l'utilisation de tarifs d'utilisation du réseau variables dans le temps et la mise en place d'un contrôle automatisé de la charge afin d'éviter les pics de puissance sur le réseau basse tension. Le projet a étudié et comparé : (i) les changements de comportement des consommateurs dus aux signaux tarifaires, (ii) le contrôle automatisé de la consommation des principaux appareils électroménagers (chauffe-eau électriques, pompes à chaleur et véhicules électriques) via des signaux tarifaires, et (iii) le contrôle direct de ces appareils par l'opérateur du réseau de distribution avec l'aide d'une optimisation centralisée.

Le projet pilote a été mis en œuvre dans la municipalité de Winkel, située dans le canton de Zurich. Les charges flexibles de trois transformateurs ont été contrôlées. Plus précisément, un schéma de contrôle du projet OrtsNetz a été implémenté par transformateur. Les deux premiers schémas étaient basés sur un contrôle indirect de la charge : un tarif prédéfini à l'avance qui varie en fonction de l'heure et un autre tarif dynamique capable, cette fois-ci, de s'adapter en temps réel aux changements dans le réseau. Dans un troisième schéma, les charges étaient directement contrôlées à l'aide d'une optimisation centralisée. Les consommateurs recevaient en fait un tarif d'utilisation du réseau réduit et constant pour les récompenser leur fléxibilité. Pour des raisons techniques, le contrôle des charges était limité au blocage ou déblocage de la puissance électrique que celles-ci pouvaient consommer.

Au total, 630 consommateurs ont bénéficié d'un nouveau tarif pendant ce projet. Parmi eux, 546 ont participé sans dispositif de contrôle. 64 contrôleurs automatisés de chauffe-eau et pompes à chaleur ont aussi été installés chez des consommateurs. De plus, 42 participants ont accepté que leurs véhicules électriques soient utilisés comme charges flexibles.

Le changement manuel de la consommation d'énergie en réponse aux nouveaux tarifs était généralement faible, de l'ordre de quelques pourcents. Il y a une différence importante entre les consommateurs qui se sont volontairement engagés dans le projet (Opt-in) et ceux qui ne sont simplement pas désinscrits (Not Opt-out, notamment visible dans la participation aux enquêtes menées auprès des participants et au marché de l'énergie solaire locale, ainsi que dans l'utilisation de la plateforme OrtsNetz. Les consommateurs répondants aux enquêtes étaient généralement satisfaits du projet et ont exprimé leur envie d'obtenir de nouveaux tarifs. En retour, ils espèrent réaliser des économies sur leur facture d'électricité.

En été, le tarif dynamique capable de s'adapter en temps réel est celui qui a réduit le plus les pointes d'injection, suivi par le système de contrôle direct de la charge et le tarif d'utilisation variable en fonction de l'heure. En hiver, le contrôle direct de la charge a permis de réduire les pointes de consommation observées pendant le projet pilote en comparaison avec celles observées avec l'utilisation de télécommande centralisée conventionnelle. Cependant, aucun des schémas OrtsNetz n'a pu réduire les pointes de consommation en hiver par rapport à un scénario sans aucun contrôle des charges.

Les conclusions sur le comportement des clients sont restreintes par la politique mise en œuvre lors de ce projet garantissant aux participants uniquement des économies sur leur facture d'électricité. Néanmoins, les résultats du projet ont des implications majeures pour l'utilisation de nouveaux tarifs. Alors que les projets pilotes et les offres Opt-in peuvent suggérer une forte implication des consommateurs, l'impact réel de ces tarifs doit être évalué auprès d'un public plus large ce qui peut montrer des effets substantiellement plus faibles.

En ce qui concerne le contrôle automatisé de la charge, les résultats du projet montrent qu'il est technologiquement possible de déployer des systèmes de contrôle directs et indirects. De plus, le tarif dynamique capable de s'adapter en temps réel et le contrôle direct de la charge sont plus performants qu'un tarif variable prédéfini à l'avance. Les résultats de la simulation indiquent que les performances du tarif dynamique et du contrôle direct de la charge pourraient être améliorées. En outre, à l'avenir, davantage de véhicules électriques devraient être connectés au réseau de basse tension ce qui pourrait rendre les avantages de ces schémas tarifaires plus évidents.

# Main findings

- The manual response of customers to tariff changes was generally small and dominated by opt-in participants.
- The automated load control schemes achieved slight injection peak reductions in summer. The dynamic tariff and direct control can adjust better to varying inflexible load profiles than the Time-of-Use tariff.
- In winter, the pilot results indicate no clear advantages of the evaluated schemes regarding reducing consumption peaks. It is expected that a larger fleet of controllable electric vehicles and further improvements in the control schemes make the benefits of the dynamic tariff and direct control more evident.

For a more comprehensive list of the main findings, please refer to Section 5.

# Contents

# Abbreviations

| | |
|---|---|
| **API** | Application Programming Interface |
| **BESS** | Battery Energy Storage System |
| **DLC** | Direct Load Controller |
| **DSM** | Demand Side Management |
| **DSO** | Distribution System Operator |
| **EV** | Electric Vehicle |
| **EWH** | Electric Water Heater |
| **FEDRO** | Federal Roads Office |
| **HES** | Head End System |
| **HP** | Heat Pump |
| **KKT** | Karush-Kuhn-Tucker |
| **LCD** | Load Control Device |
| **LCMA** | Load Control Master Agent |
| **LCSA** | Load Control Service Agent |
| **LSTM** | Long Short-Term Memory |
| **MAE** | Mean Absolute Error |
| **MILP** | Mixed Integer Linear Programming |
| **MIQP** | Mixed Integer Quadratic Programming |
| **MSD** | Most Similar Day |
| **PLC** | Power Line Communication |
| **PV** | Photovoltaic |
| **P2P** | Peer-to-Peer |
| **RL** | Reinforcement Learning |
| **SFH** | Single Family Home |
| **SM** | Smart Meter |
| **SoC** | State of Charge |
| **TECA** | Total Energy Correctly Assigned |
| **TS** | Transformer Station |
| **ToU** | Time-of-Use |
| **WP** | Work Package |

# 1 Introduction

## 1.1 Background information and current situation

Current efforts towards decarbonization and increased sustainability are fundamentally reshaping the electricity sector. Conventional power plants running on fossil fuels are replaced with distributed, renewable energy sources, which are more volatile and intermittent. These changes challenge traditional supply-side approaches to balancing supply and demand. Simultaneously, the electrification of transport and heating increases electricity demand, putting extra stress on the distribution grid during peak times and necessitating costly grid expansions [1].

Enabled by the progressing digitization, Demand Side Management (DSM) is a means to address these challenges. Instead of adapting supply to a given demand, the flexibility present in many devices is used to adapt their demand to available supply, shifting peaks in demand to those in supply or flattening demand curves in general. In particular, the heating and transportation sectors exhibit considerable flexibility. Heating systems can use thermal inertia to store energy, and batteries in Electric Vehicles (EVs) are typically connected to the grid for longer periods than they require for charging, allowing flexibility during the charging process. Due to these beneficial properties, demand-side flexibility has been incorporated in the revision of the StromVG [2] and is already grounded in the “NOVA” concept for grid planning.

## 1.2 Purpose and objectives of the project

The overall goal of OrtsNetz was to define and evaluate approaches that facilitate the integration of renewable energy sources into the future’s low-voltage grid by using appropriate tariff schemes and flexible loads. The project aimed to reduce power peaks in the low-voltage grid, considering system costs, practicability, and the fair distribution of costs and benefits.

Specifically, the project had the following goals:

- Evaluate the acceptance and manual response of customers to time-varying tariffs. Such findings help to determine how novel tariffs may be deployed in the future and what changes in energy consumption can be expected from customers’ responses.
- Develop and quantify the effectiveness of centralized and price-based approaches for automated control of large electrical appliances. Based on this, future demand response offers can be appropriately designed.
- Test the developed control approaches in a real-world pilot and determine if existing communication infrastructure can be used for real-time control settings. The real-world application gives relevant insights regarding the required steps for the rollout on a larger scale.

To this end, the project studied different DSM approaches and evaluated their effectiveness in promoting grid-friendly behavior of the consumers. Two main strategies were compared (see Fig. 1): In a direct load control setting (strategy 1), the Distribution System Operator (DSO) directly controlled devices based on a centralized optimization. The control was limited to allowing or blocking power consumption by a particular device, and customers received, in return, a reduced constant grid-usage tariff for providing flexibility to the DSO. In the second, indirect load control scheme (strategy 2), the tariff was time-dependent. Here, two different tariff schemes were compared, a pre-planned Time-of-Use (ToU) tariff that extends existing high/low tariff rates and a fully dynamic real-time tariff that adapts to newly developing grid situations. Part of the customers were equipped with a device on which an intelligent local agent could control Electric Water Heaters (EWHs) and Heat Pumps (HPs) based on the current tariff value, while EV charging was controlled via an Application Programming Interface (API) over the internet. Customers could also react manually to price changes to minimize their electricity costs.

OrtsNetz consisted of three key components, which also formed the basis for the different Work Packages (WPs): Firstly, it studied customer acceptance of dynamic tariffs and automated control of devices, as well

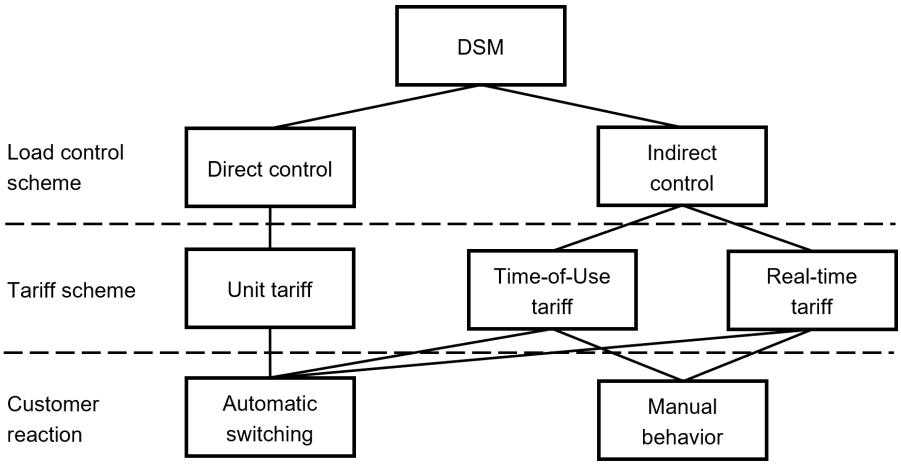


Figure 1: Overview of demand side management schemes studied in the project.

as manual intervention of participants. Secondly, it explored and developed algorithms to determine the tariff values and the switching commands for the automatic load control. Finally, it provided important insights regarding the required infrastructure and hardware for a successful implementation of DSM schemes.

The remaining report is structured as follows. Section 2 provides an overview of the pilot setup. Section 3 describes the methodology and outcomes of each WP and introduces the approach for computing baseline load profiles for the automated load control analyses. Section 4 presents the pilot phase results. Finally, Section 5 concludes the project, while Sections 6–8 detail cooperations, communication, and publications related to the project.

# 2 Overview of the experimental setup

The pilot project was set in the municipality of Winkel, located in the canton of Zurich. Winkel has a population of 5,058 persons (as of 2024) living in 2,213 private households [3]. All inhabitants are supplied by the local electricity supply company EKZ.

The households are equipped with smart electricity meters that measure active and reactive energy consumption (and possibly feed-in) at intervals of 15 minutes. The measurements are communicated once a day to EKZ via Power Line Communication (PLC). In some cases, a household can have more than one Smart Meter (SM) for separately monitoring the consumption of appliances like HPs.

Due to the rapidly increasing share of EV sales, the number of vehicles registered in Winkel has significantly changed in the last three years. According to data by the canton of Zurich, there are 178 privately owned EVs (5.6 % of all registered vehicles) and 357 hybrid vehicles (11.2 %) in Winkel [3], which is a higher share of EVs compared to the rest of Switzerland (4.2 % and 9.6 %, respectively) [4].

Customers' residences are connected to one of 16 Transformer Stations (TSs) with a total power rating of 10 MVA. Three TSs are equipped with fiber networked equipment that allows near real-time monitoring of power and voltage. Each of the DSM schemes described in Section 1.2 was assigned to one of these TSs. A Battery Energy Storage System (BESS) for peak shaving was installed at a fourth TS.

For automatic switching of EWHs and HPs, 64 Load Control Service Agents (LCSAs) and Load Control Devices (LCDs) were installed in households. The LCSA is an intelligent control device that can compute switching commands based on a price signal, while the LCD is a simple device implementing the switching commands computed by the LCSA or the central system. Since the project focused on using existing infrastructure, the LCSAs were not networked and only communicated through PLC with the central system. Furthermore, LCDs acted as simple on/off switches and did not receive any information on the state of the device they control, e.g., the water temperature. LCDs could only block devices from running but not actively turn them on. Furthermore, 42 customers registered their EVs to be used as flexible loads. EV charging was controlled via an API that directly communicated with the vehicles. This allowed retrieving information on a vehicle's current status, e.g., its State of Charge (SoC) and whether it was plugged in. The charging process could be started and stopped via the API, while the vehicle determined the charging power.

Automated load control was used either for direct load control (following a command issued by the central system) or for indirect load control via price signals. Figure 2 depicts the flow of information for the direct control and the real-time tariff setting. In the former case, the DSO communicated a switching profile to the LCDs every 15 minutes for the next 96 15-minute intervals (24 hours) or in case of EVs potentially started or stopped the charging process. In the latter case, the LCD received switching commands from the LCSA, which computed them based on the real-time tariff. The DSO dynamically calculated this price signal and communicated it every 15 minutes to the households. The algorithm determining the EV charging schedules in the real-time tariff setting was implemented centrally but acted in the interest of each individual customer. In the ToU tariff setting, the price profile and corresponding cost-minimizing EWH and HP switching profiles were known in advance. Therefore, real-time communication with LCSAs was less important, and for simplicity, both the LCD switching profiles and the EV charging schedules were computed centrally in the interest of each individual customer.

The existing PLC infrastructure had a direct impact on the kind of data that was available at each location and time. Communication errors could lead to data being available later or not at all. Furthermore, 15-minute interval SM readings and the truly applied switching commands were collected only once a day by the central location, while local LCSAs might have immediate access.

In order to ensure comparability among the different settings that were evaluated, the basis for decision-making was the same in all approaches. Therefore, the assessment of the grid situation (Fig. 2) was based on the same information for both the direct and indirect load control setting (corresponding TS measurement and weather data), and the same flexibility constraints were applied in all schemes.

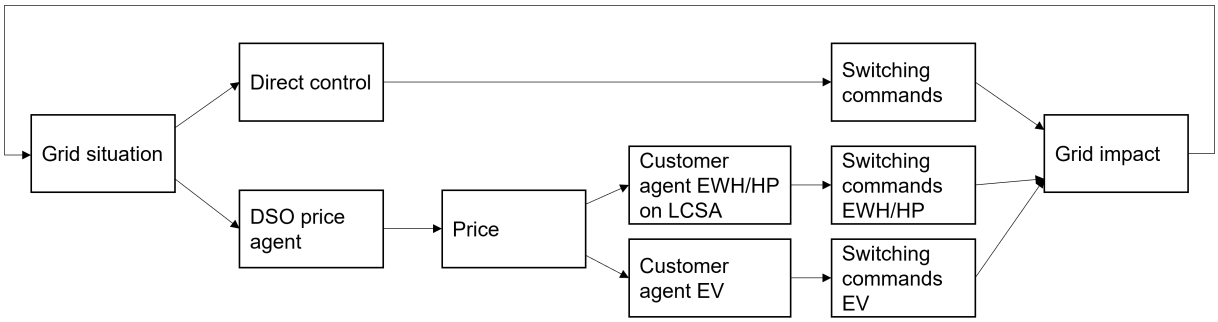


Figure 2: Influence of the grid situation on automatic switching through direct control or a real-time tariff.

The pilot phase ran from October 2023 until the end of 2024. Automated load control was introduced at a later stage, see Section 4.2. For participating customers connected to a TS without automated load control, the OrtsNetz tariff was only applicable until September 2024.

# 3 Approach and methodology

OrtsNetz was a collaboration of two laboratories at ETH Zurich and EKZ, the electricity utility company of the canton of Zurich. OrtsNetz was organized in WPs distributed across the partners, each having distinct milestones. Exchange between partners and collaboration in WPs happened in weekly meetings on a technical level and quarterly steering meetings on an organizational, strategic, and administrative level. The activities conducted in the various WPs and their results are presented in the following sections.

## 3.1 WP 1: Customer interaction and tariff design

Work package WP1 dealt with the design of the tariff schemes as well as the evaluation of customer behavior and overall impact. Over the course of the first two years, the tariff schemes and customer groups of the project were developed in detail and implemented. Letters with tariff sheets were sent to customers in the summer of 2023.

The next section presents the grouping of study participants. This is followed by a detailed explanation of the tariff structure and design decisions in regard to cost recovery and fairness.

### 3.1.1 Study groups

Participation in the OrtsNetz study is differentiated along three dimensions.

**Tariffs** Firstly, OrtsNetz features three distinct grid-usage tariffs (OrtsNetz Tariffs) that are different from the standard tariff (EKZ Tariff):

- Time-of-Use tariff
- Dynamic real-time tariff
- Unit tariff for participants with directly controlled devices

Each tariff was matched to one of the three selected TSs.

**Load control** Secondly, two classes of participants are discerned: Those with automatically controlled devices and those without (Fig. 3). The automatically controlled devices were EWHs, HPs and EVs. As EWHs and HPs were controlled via PLC, they were distributed among the three selected TSs equipped with the required gateways (Section 3.4.2). These participants received an LCD installed in their electrical panel. EVs were distributed across the whole project area as they were controlled via the internet. As detailed in the next section, customers with automatically controlled devices might receive a modified energy tariff in addition to their OrtsNetz grid tariff to provide further compensation. Additionally, customers with EVs could decide for every charging session if they wanted to deactivate the intelligent control and opt out of the associated energy tariff for the following 12 hours.

**Recruiting** Thirdly, participants were either recruited in an Opt-in or an Opt-out scheme. The initial announcement of the project encouraged proactive registrations by the customers. In summer 2023, an additional group of customers was selected and informed by letter about their respective new OrtsNetz tariff, with the possibility to opt out. All participants were subject to the best-accounting policy, such that per day no one would pay more than they would under the normal EKZ Tariff.

This design allowed for three major studies:

- The effect of different DSM approaches by comparing the efficiency of automatic control between direct control, agents reacting to ToU prices, and agents reacting to real-time prices.
- The behavior of participants in response to novel time-varying prices.

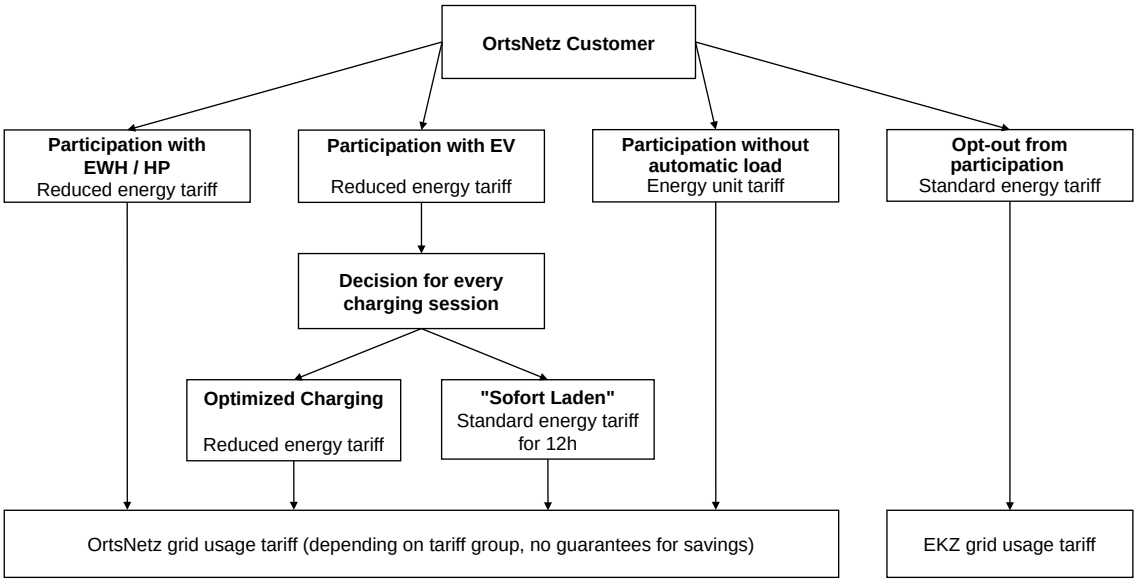


Figure 3: Overview of ways to participate in the OrtsNetz project. When taking part with an EV, participants still had the chance to opt-out of intelligent charging of their vehicle for individual charging sessions.

- The difference in behavior between participants recruited by Opt-in and Opt-out strategies, which can unveil the impact of selection biases on observed participant behavior.

These participation schemes were implemented in the project area of Winkel as described in Section 4.1.1.

### 3.1.2 Tariff design

This section discusses the specific tariffs designed for the participant groups presented above. Apart from the different grid-usage tariffs, participants received a new energy tariff depending on the exact group they belonged to. Due to geopolitical developments, the standard EKZ energy tariff became significantly more expensive in January 2024. To ensure cost-neutrality, this increase was also respected in the OrtsNetz tariffs.

**Automatic devices** Participants with automatic devices were compensated for the inconvenience of having an LCD installed, as well as giving up some flexibility in when they can use their device. This was implemented by billing them a lower energy component of the electricity tariff. Specifically, they received the low-tariff component of the normal EKZ Tariff, which is usually only valid during night times and weekends, for all points in time (10.35 Rp./kWh in 2023 and 17.50 Rp./kWh in 2024[1]). This change in the tariff has the benefit that it is easy to communicate to customers. Assuming the H4 standard profile published by ElCom [5] with additional demand of 2000 kWh/year for an EV, the reduction in the energy component results in savings of 33 CHF over one year. The exact savings for the participants, however, strongly depend on their heating and driving demand and can be far greater. On top of this compensation, participants were subject to the grid-usage OrtsNetz Tariff at their respective TS, which enabled additional savings.

**Time-of-Use tariff** The ToU grid-usage price profile was determined based on a bilevel programming problem that optimizes grid utilization and customer costs simultaneously (Section 3.2.3). While the optimization selects the best times for the price switches, the exact values of the profile need to be scaled for cost recovery and fair distribution of costs.

[1] Unless stated otherwise, all tariff values are without taxes.

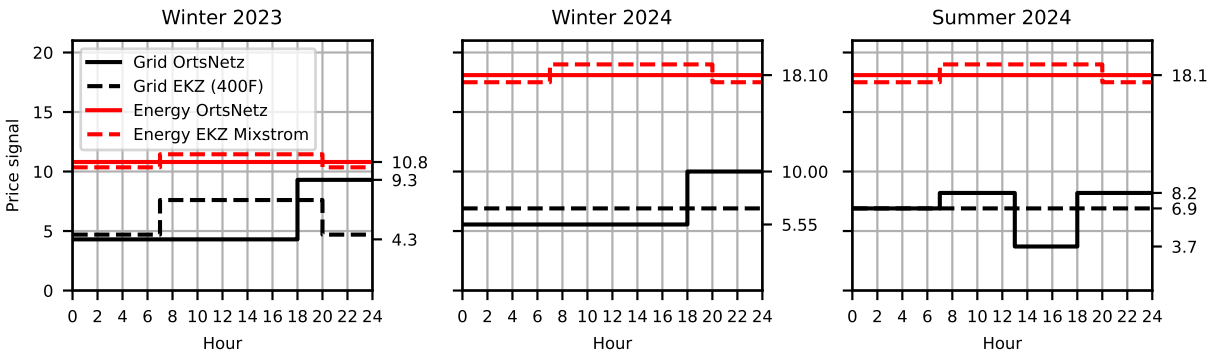


Figure 4: Final ToU tariff profiles selected for the project. Exact values are annotated on the right y-axis of each plot. All price values are in Rp./kWh.

Cost recovery was implemented by calculating the revenue from non-responding customers without flexible loads to the baseline EKZ Tariff. Calculations for a specific season are based on historic demand in the equivalent period from 2022–2023. Specifically, we used the total demand of residential households at a selected TS without devices that could be controlled automatically. For these, we calculated the hypothetical revenue for Winter 2023 (October–December), Winter 2024 (January–April and October–December), and Summer 2024 (May–September) based on the smart meter consumption data of the previous year. This implementation reflects the understanding of fair cost distribution in the project that is also compatible with the best-accounting policy. Customers without the ability to majorly shift demand pay the same, whereas customers with large loads are encouraged to shift their operation to times of cheaper prices, which are the ones with lower grid utilization.

Before selecting the final grid-usage tariff values, we take another consideration into account. The standard 2023 EKZ Tariff already includes a ToU profile, not only for the grid-usage component, but also for the electricity price. The two components have the same profile (high tariff on weekdays from 7:00–20:00), resulting in a price jump between only two levels that is convenient for customers to memorize. However, the ToU profile that is selected by the bilevel optimization (Section 3.2.3) has up to three price levels at different times (Fig. 4). Overlaying this with the existing time profile of the EKZ Tariff energy component would result in an undesirably complicated profile. Instead, we calculate a single energy tariff component from the low and high tariffs. We use the average weighted by the energy demand of the selected subgroup of inflexible load customers to ensure cost recovery.

The preceding considerations allow to determine the specific tariff values for the ToU grid tariff. For a tariff with two price levels, selecting one level determines the other one to achieve cost recovery. For a three component tariff there is another degree of freedom that needs to be decided. As the grid component of the EKZ Tariff 2024 is a unit tariff, we decided to fix the mid value of the summer profile of the OrtsNetz 2024 tariff to the same value. This reduces one degree of freedom and cost recovery enforces a direct relation between the high and low tariff components. To analyze the effect of this relation we developed a tool that allows to dynamically visualize the tariff profiles, ratios, and cost impacts (Fig. 5). The final selection of the tariff values was conducted together with the tariff department of EKZ and aimed to increase the span between high and low tariff components while keeping them at reasonable levels (Fig. 4).

**Real-time tariff** The real-time grid-usage tariff is based on the instantaneous TS load measurements. Both a proportional price and one determined by a Reinforcement Learning (RL) agent were implemented. The price has the same range as the ToU tariff (4.30–9.30 Rp./kWh for 2023 and 3.70–10.00 Rp./kWh for 2024). Cost recovery is based on the revenue of a corresponding cost-neutral unit tariff. The implementation of the real-time tariff and cost recovery is detailed in Section 3.3.2.

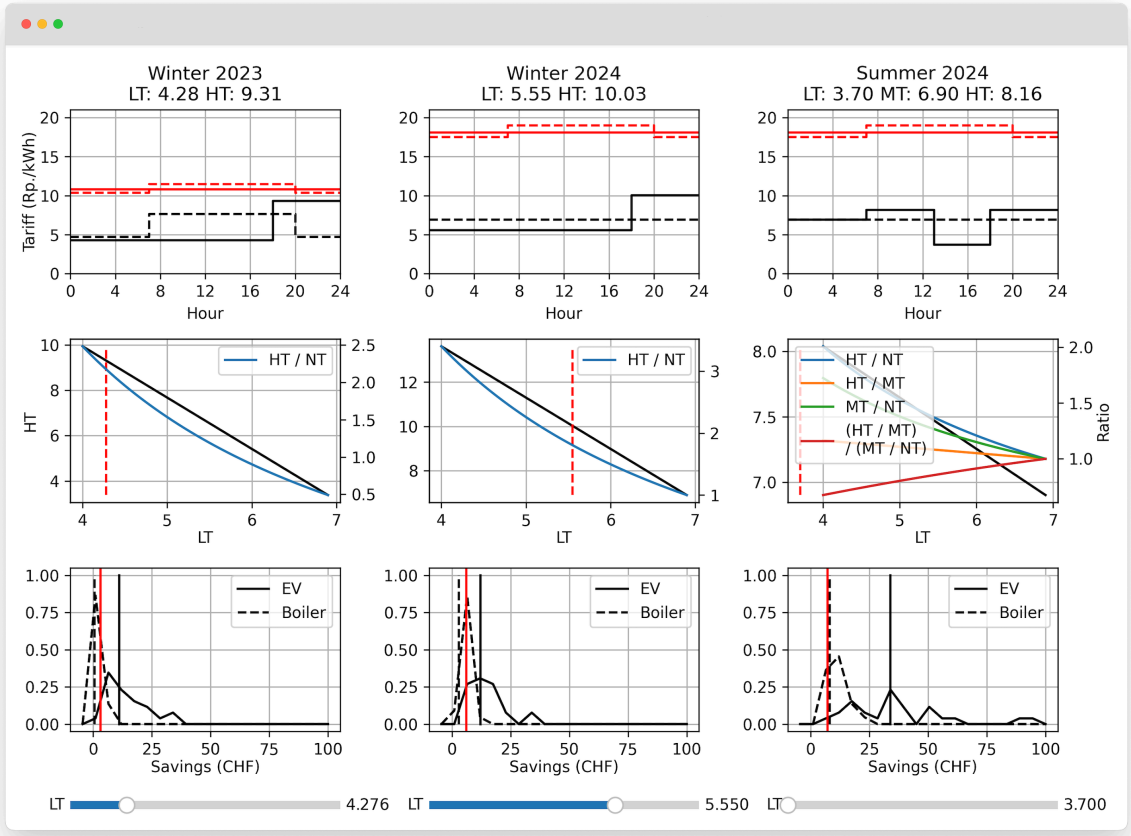


Figure 5: Screenshot of the OrtsNetz tariff tool to analyze the ToU tariff scaling for the three separate time spans (columns). The first row shows the baseline (dashed) and currently selected tariff profiles for the grid-usage component (black) and the energy component (red). The second row shows the linear relation between the high tariff (HT) and low tariff (LT) values (black), their ratio (blue) and the currently selected low tariff (red, dashed). In summer, the mid tariff (MT) and the ratios between all components are shown. The bottom row shows the probability distribution and averages (black vertical lines) of hypothetical annual savings in grid costs incurred by EVs and boilers and serves as reference for deciding the tariff values. Red vertical lines indicate the average additional savings in energy cost for EVs. The sliders at the bottom allow to dynamically select the low tariff. The tool then automatically determines the high tariff based on cost recovery.

**Direct control** Finally, as the direct control setting is not price-based, participants received a unit tariff for grid-usage. This allows the direct control system to optimize based on the grid situation alone, without taking potential cost (dis-)advantages for customers due to time-varying prices into account. The grid component of the 2024 EKZ Tariff is a unit tariff anyways (6.90 Rp./kWh). For 2023 the value was determined based on the same calculations as above, as the demand weighted average of the low and high tariff, using the demand profile of customers without flexibility for costs recovery (5.80 Rp./kWh).

## 3.2 WP 2: Idealized analysis of interactions and tariff design

A key component of the project was determining the tariff values for indirect load control via time-varying grid-usage tariffs. The tariff values influence customer behavior as the customers aim to minimize their electricity costs while meeting their demand needs. On the other hand, the resulting consumption profiles affect the power flows in the grid. Therefore, there is a mutual impact between the tariff values and the consumption behavior. Thus, the DSO must take the customers' reactions into account when computing the tariff values, which results in a problem structure that is rather complex to describe and solve mathematically. As a first step, idealized conditions were assumed in WP 2. It was assumed that

the inflexible consumption and production profiles, as well as the load behavior, are known. Furthermore, the customers behave rationally with respect to the cost minimization. Lastly, there is complete transparency, i.e., the DSO has the same information as the customers.

### 3.2.1 Problem formulation

The above-mentioned interdependency between the DSO's and customers' actions were modeled as a bilevel programming problem. Thereby, the hierarchy between the DSO (upper-level problem) and the customers (lower-level problems) can be represented. As described in [6], the customer problem is a mixed-integer problem when the control is modeled according to the given infrastructure in the project, i.e., blocking a device or not. Several solution approaches for bilevel problems with binary variables in the lower-level problem were evaluated, but none of the investigated approaches showed satisfactory results. Population-based metaheuristics [7] and the branch-and-cut method by Fischetti et al. [8] do not perform well due to the size of the upper-level search space, while the bounding procedure proposed in [9] does not scale for a realistic number of customers. Therefore, the focus of WP 2 in this report is on a simplified problem formulation with continuous variables for the device power. Further, it is limited to the ToU tariff scheme to reduce the upper-level search space, only considers EWHs as flexible loads, and does not take self-consumption optimization into account.

**Customer's perspective (lower level)** Each customer aims to minimize the electricity costs by shifting EWH consumption to low-price periods:

$$\min_{\mathbf{P}_c^{\mathsf{EWH}}} \quad \sum_{d=0}^{N_d-1} \sum_{t=0}^{K-1} \left( \pi_t^{\mathsf{buy}} \cdot \Delta t + \beta_c \cdot t \right) \cdot P_{c,d,t}^{\mathsf{EWH}} \tag{1a}$$

$$\text{s.t.} \quad \sum_{t=0}^{K-1} P_{c,d,t}^{\mathsf{EWH}} \cdot \Delta t = E_{c,d}^{\mathsf{EWH}}, \qquad \forall d \tag{1b}$$

$$0 \leq P_{c,d,t}^{\mathsf{EWH}} \leq P_{c,\mathsf{nom}}^{\mathsf{EWH}}, \qquad \forall d, t \tag{1c}$$

where $N_d$ denotes the number of considered days, $K$ is the number of time steps within one day (96 for 15-minute resolution), $\Delta t$ is the duration of one time step, and $\pi_t^{\mathsf{buy}}$ denotes the electricity price in time step $t$ (the price profile is the same for all days). The variable $P_{c,d,t}^{\mathsf{EWH}}$ describes the EWH demand for customer $c$ in time step $t$ on day $d$ and is limited by the nominal power $P_{c,\mathsf{nom}}^{\mathsf{EWH}}$, while $E_{c,d}^{\mathsf{EWH}}$ is the energy that must be delivered by the EWH on day $d$. Finally, $\beta_c$ specifies the customer preference for running the EWH as early (positive value) or late (negative value) as possible. This preference is included to ensure the uniqueness of the lower-level solution, as explained at the end of this section. $\beta_c$ is set to a small value such that the second summand in (1a) does not shift consumption to a different tariff level, but only shifts consumption among times with the same price.

**DSO's perspective (upper level)** The DSO aims to determine the tariff values for drawing electricity from the grid such that the maximum aggregated active power of all customers $P^{\mathsf{max}}$, i.e., the peak absolute power observed within the analyzed time horizon, is minimized. The constraints of the DSO are the following:

$$P^{\mathsf{max}} \geq P_{d,t}^{\mathsf{inf}} + \sum_{c=1}^{N_{\mathsf{customers}}} P_{c,d,t}^{\mathsf{EWH}}, \qquad \forall d, t \tag{2a}$$

$$P^{\mathsf{max}} \geq -\left( P_{d,t}^{\mathsf{inf}} + \sum_{c=1}^{N_{\mathsf{customers}}} P_{c,d,t}^{\mathsf{EWH}} \right), \qquad \forall d, t \tag{2b}$$

$$\pi^{\mathsf{buy,min}} \leq \pi_t^{\mathsf{buy}} \leq \pi^{\mathsf{buy,max}}, \qquad \forall t \tag{2c}$$

$$\pi_{t+1}^{\mathsf{buy}} = \pi_t^{\mathsf{buy}}, \qquad \forall t \in [t_p^{\mathsf{start}}, t_p^{\mathsf{end}}), \quad \forall p \tag{2d}$$

Constraints (2a) and (2b) define the lower bound for $P^{\text{max}}$, given by the sum of the inflexible load $P^{\text{inf}}_{d,t}$ and the EWH load in each time step. Constraint (2c) puts bounds on the tariff values, while constraint (2d) specifies that the price must be constant within each pre-specified period $p$. If there should not be a change in the tariff value at midnight, this is enforced by an additional constraint $\pi^{\text{buy}}_{K-1} = \pi^{\text{buy}}_{0}$.

**DSO - customer interaction** The interaction between the DSO and the customers is expressed in a bilevel programming problem:

$$\min_{\pi^{\text{buy}}, P^{\text{max}}, \mathbf{P}^{\text{EWH}}} \quad P^{\text{max}} \tag{3a}$$

$$\text{s.t.} \quad \text{(2a)} - \text{(2d)} \tag{3b}$$

$$\text{(1a)} - \text{(1c)}, \quad \forall c \tag{3c}$$

Note that the customer problems can be combined into one problem with the sum of the individual customers' objectives as the overall objective function, subject to all the individual constraints.

**Uniqueness of the lower-level solution** Preliminary analyses without the second term in (1a) showed that the DSO tends to choose a flat tariff profile, thus enabling the direct control of the loads for the optimistic version of bilevel optimization. Under the optimistic assumption, the upper-level agent chooses the solution leading to the lowest upper-level cost if the lower-level solution is non-unique. For two time steps with the same tariff value, for example, the customer cost when withdrawing power from the grid in time step 1 is equal to the cost when withdrawing power in time step 2. Thus, the lower-level solution is not unique and the one leading to the smaller overall peak power is chosen by the DSO. However, it is not ensured that the customer or the corresponding load control algorithm chooses the same solution, and the actual resulting upper-level cost may be unexpectedly high. To avoid such behavior, the preference regarding consuming as early or as late as possible within a given tariff window is explicitly modeled in (1a).

### 3.2.2 Solution approach

The bilevel programming problem presented is a pricing problem with linear upper-level and lower-level constraints, a linear upper-level objective function, and a bilinear lower-level objective function as it contains products of upper- and lower-level variables. However, the lower-level objective function is linear for fixed upper-level variables, and therefore, the lower-level problem can be replaced by its Karush-Kuhn-Tucker (KKT) conditions or by optimality conditions based on the strong duality theorem [10].

We chose the second approach to transform (3) into a single-level problem, i.e., the lower-level problem is replaced by its primal constraints, its dual constraints, and the strong duality condition, which states that the primal and dual objective function values must be equal. The only non-linearities in the resulting problem are the products $\pi^{\text{buy}}_t \cdot P^{\text{EWH}}_{d,t}$ in the primal objective function ($P^{\text{EWH}}_{d,t} = \sum_{c=1}^{N_{\text{customers}}} P^{\text{EWH}}_{c,d,t}$). These bilinear terms are linearized by discretizing $\pi^{\text{buy}}_t$ using a binary expansion, and linearizing the resulting products of a binary and a continuous variable, as proposed, e.g., in [11], and described in the following. The price variable $\pi^{\text{buy}}_t$ is rewritten as $\pi^{\text{buy}}_t = \pi^{\text{buy,min}}_t + \Delta\pi^{\text{buy}} \sum_{w=0}^{W-1} 2^w b_{t,w}$, where $b_{t,w}$ is a binary variable, $\pi^{\text{buy,min}}_t$ is the lower price bound, $\Delta\pi^{\text{buy}}$ describes the discretization interval, and the parameter $W$ determines the number of considered different price values $2^W$. Then, the bilinear terms $\pi^{\text{buy}}_t \cdot P^{\text{EWH}}_{d,t}$ can be replaced by $\pi^{\text{buy,min}}_t P^{\text{EWH}}_{d,t} + \Delta\pi^{\text{buy}} \sum_{w=0}^{W-1} 2^w z_{d,t,w}$, where the continuous variable $z_{d,t,w}$ is defined by the following two constraints:

$$0 \leq z_{d,t,w} \leq G \cdot b_{t,w}, \qquad \forall d, t, w \tag{4a}$$

$$0 \leq P^{\text{EWH}}_{d,t} - z_{d,t,w} \leq G \cdot (1 - b_{t,w}) \qquad \forall d, t, w \tag{4b}$$

$G$ is a sufficiently large positive constant. A valid value for $G$ is given by $\sum_{c=1}^{N_{\text{customers}}} P^{\text{EWH}}_{c,\text{nom}}$. The resulting model is a Mixed Integer Linear Programming (MILP) and is solved using Gurobi [12].

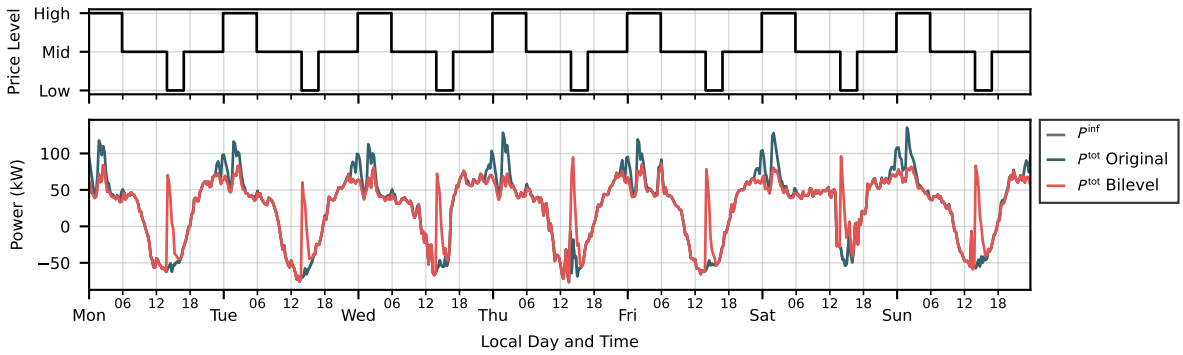


Figure 6: Original TS load and bilevel results for the week from 18.07.2022 to 24.07.2022. The results show that the start of the lowest price period is most relevant as the peak EWH load occurs at this hour. To leverage the EWHs' flexibility for injection peak reduction, the start of the lowest price period should thus be aligned with the time when PV generation is highest.

### 3.2.3 Case study

**Setup** The optimization was applied to one of the TSs in Winkel. According to EKZ's records, 45 households at this TS have an EWH. For each of these households, the energy consumption $E_{c,d}^{\text{EWH}}$ was determined by disaggregating the EWH load from the SM data using the approach described in Section 3.3.1. The nominal device power $P_{c,\text{nom}}^{\text{EWH}}$ is specified according to EKZ's records, and the inflexible load $P_{d,t}^{\text{inf}}$ at the TS was estimated by subtracting the EWH load from the total TS load. Note that HPs and EVs are considered inflexible in this analysis, while they are flexible in the pilot implementation. The constant $\beta_c$ is set to a small positive value, such that all EWHs operate as early as possible, which is reasonable assuming that devices are unblocked for the entire low-price period. The analysis focuses on one week in summer and one week in winter. More specifically, we analyze the week in 2022 for which the grid load in Winkel most closely resembles the average over eight weeks in July and August for summer and January and February for winter [13]. The duration of one time step $\Delta t$ is 15 minutes.

The project partners agreed that the price could change every full hour (enforced by constraint (2d)), but there can be at most three different price levels and four price changes. As the model does not consider price sensitivities, only the shape of the price profile matters and not the actual price values, i.e., the customers' response is the same for any linear transformation of the price profile obtained from the bilevel solution [14]. Therefore, we enforced $\pi_t^{\text{buy}} \in \{1, 2, 3\}, \forall t$ to reduce the search space and transform the profile ex-post to meet the cost neutrality condition. The number of price changes is enforced by adding a binary variable per time step that takes a value of 1 if the price differs from the previous time step and 0 otherwise. The sum of these binaries over the entire day must be smaller than or equal to four.

**Results** Figures 6 and 7 show the results for summer and winter, respectively. From Fig. 6, it is visible that the disaggregation captures a major share of the nightly peaks (original $P^{\text{tot}} - P^{\text{inf}}$), which are caused by the current ripple control of EWHs. However, the remaining peaks in $P^{\text{inf}}$, e.g., at 3:00 on the first day, indicate that the actual EWH load is potentially higher than considered in this analysis. For summer, the optimization chooses a low price value starting from 14:00 and thereby shifts the peak EWH load to this time. It does not operate the EWHs at an earlier hour with excess Photovoltaic (PV) power, e.g., 10:00, because this would lead to a higher maximum load $P^{\text{max}}$. Note that several other tariff profiles lead to the same customer response. What is most relevant is the start of the lowest price period. In winter, the overall consumption is higher and there is no excess PV power. A main contributor to the high load during the night is electric storage heaters, which are unblocked from 23:00 to 7:00. The dip in original demand before noon stems from HP blocking during weekdays. The optimization chooses a low price value starting from 11:00. The resulting load peaks are comparable to the original peaks. If HPs and electric storage heaters were also considered flexible, this would further increase the peaks in total load. This indicates that synchronized operation of devices is not desirable in winter.

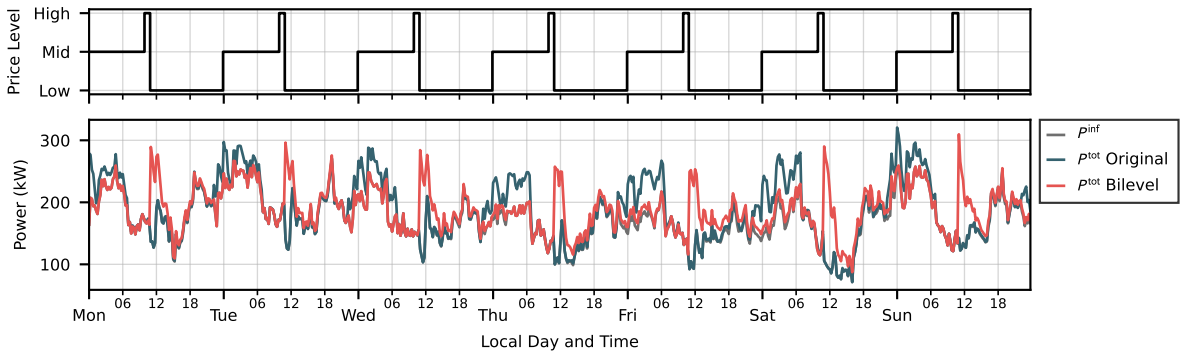


Figure 7: Original TS load and bilevel results for the week from 31.01.2022 to 06.02.2022. The results indicate that the synchronized operation of devices may lead to new peaks as the spread between the minimum and maximum inflexible load is not high enough to schedule power rebounds effectively.

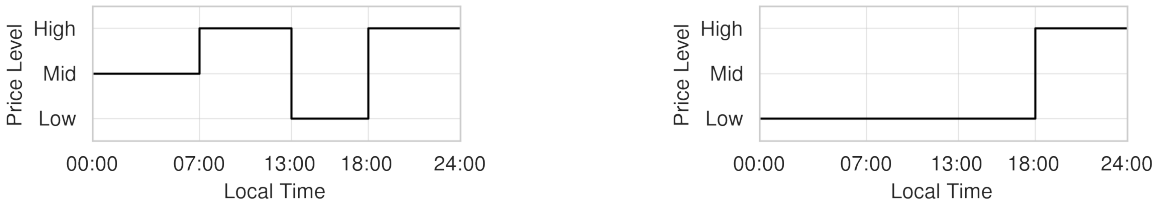


(a) Summer

(b) Winter

Figure 8: Tariff profiles for OrtsNetz participants with a ToU tariff.

### 3.2.4 Discussion and pilot Time-of-Use tariff

Two limitations of the above analysis are that only EWHs are considered as flexible loads, and that the disaggregation could potentially be improved, which impacts the shiftable energy and inflexible load. Even though these could be addressed in future work, the results already give important insights into the tariff design and were leveraged for determining the ToU tariffs in the OrtsNetz pilot. As discussed by many studies in the literature and observed above, time-variable prices can cause power rebounds. In summer, the DSO can exploit these rebounds to reduce injection peaks. For this, it is important to "schedule" the flexible devices to run during the hours with the highest PV power. Solar noon in Zurich in summer occurs around 13:30 local time, so we chose 13:00 as the start of the low-price period. Most EVs are only connected to the charging station from evening to morning. To reduce the coincidence between EV charging and inflexible load peaks in the morning and the evening, a mid-price period is applied from midnight to 7:00, which incentivizes shifting charging to these hours. Note that we intentionally chose the medium price for this period and not the low price, such that EWHs, which are always available, do not shift to the same time. In winter, the results show that synchronized operation of devices should be avoided, as there is less PV power and the spread between the minimum and the maximum inflexible load is not high enough to schedule a power rebound effectively. To increase randomness in EWH operation, the price was chosen to be low for most of the day, with a high-price period applied only from 18:00 to midnight to reduce the coincidence between the evening inflexible load peak and EV charging. The resulting price profiles are visualized in Fig. 8 and were scaled according to Section 3.1 before they were communicated to the customers. The summer tariff was applied from the beginning of May until the end of September, and the winter tariff was applied in the remaining months.

## 3.3 WP 3: Automated load management and tariff design

WP 3 focused on developing the algorithms for computing the dynamic real-time price signal and for automated load control. The following sections will introduce an approach for forecasting the inflexible load at a TS level, the algorithms related to the dynamic tariff setting, the control logic in the ToU tariff setting, the central optimization for direct load control, a verification module, as well as the control approach for the BESS.

### 3.3.1 Inflexible load forecast

**Overview** Forecasting the inflexible load is required for direct load control and the proportional pricing scheme, which is one of the two proposed approaches for determining the dynamic real-time tariff. The most similar historical day to the one being forecasted is identified to forecast this load. Then, the estimated inflexible load for that historical day is used as a forecast. The method is split into two steps:

1. Load disaggregation: This step disaggregates past SM data to create a database of historical flexible demand.
2. Most similar day matching: This step involves leveraging weather data to match the day to be forecasted to a similar historical day. Then, the inflexible load for that historical day is computed using the historical TS load measurements and flexible demand.

In the following paragraphs, these two steps are described in detail.

**Load disaggregation** Disaggregating the total TS load into its flexible and inflexible components is the first step toward forecasting the inflexible load. The flexible load at a TS level is the sum of the load of every EWH, HP, and EV managed through a control scheme. While the demand of EVs is known via the API, EWHs and HPs are not measured separately. Therefore, this paragraph describes how the load profiles of EWHs and HPs can be estimated given the SM data at a household level, i.e., the active and reactive energy withdrawn from the grid in each 15-minute interval. First, the SM data is converted from energy to power. Then, the load disaggregation is split into two sub-components:

1. HP load detection: this component estimates the average active power of the HP given measurements of active and reactive power withdrawn from the grid at a household level (with a 15-minute resolution) minus the EV consumption (if present), the nominal power of the HP installed, and a list of switching commands. Each switching command $u_t^{\mathsf{HP}} \in \{0,1\}$ determines whether the HP can run in time step $t$ for a specific customer/household.
2. EWH load detection: this component estimates the active power of the EWH given the active power measurements at a household level where the HP and EV consumption (if present) has been already extracted, the nominal power of the EWH installed, and a list of switching commands. Each switching command $u_t^{\mathsf{EWH}} \in \{0,1\}$ determines whether the EWH can run in time step $t$.

The HP load detection component uses the SM measurements converted to power values (without the EV consumption) to estimate the time steps when the HP is running. The heuristic algorithm defines a variable $hp_t^{\mathsf{ON}} \in \{0,1\}$ that represents whether the HP is running at time step $t$ or not ($hp_t^{\mathsf{ON}} = 1$ represents a running HP at time step $t$). At every time step $t$, $hp_t^{\mathsf{ON}}$ is computed as follow:

$$hp_t^{\mathsf{ON}} = \mathbf{1}_{\{P_t > \gamma \cdot P_{\mathsf{nom}}^{\mathsf{HP}}\}} \cdot \mathbf{1}_{\{Q_t > Q_{\mathsf{AVG24h}}\}} \cdot u_t^{\mathsf{HP}} \tag{5}$$

The first indicator function $\mathbf{1}_{\{P_t > \gamma \cdot P_{\mathsf{nom}}^{\mathsf{HP}}\}}$ is 1 if the active power measurement from the SM data is greater than the discounted nominal power of the HP: $\gamma \cdot P_{\mathsf{nom}}^{\mathsf{HP}}$. The discount factor $\gamma$ is heuristically determined to be 0.3. The second indicator function evaluates to 1 if the reactive power measurement is greater than the average reactive power of the measurements in the 24-hour window that is being disaggregated. If both indicator functions evaluate to 1 and the switching command ($u_t^{\mathsf{HP}}$) is 1, the HP is considered to be running. In the second step, the heuristic algorithm computes an approximation of the magnitude of the HP demand. To that end, the average active power when the HP cannot run $P_{\mathsf{AVG24h}}^{\mathsf{noHP}}$ (i.e., during

Table 1: Assessment of load disaggregation accuracy. AP refers to active power.

| Test Case | TECA | MAE AP (kW) | Mean AP (kW) | Std. AP (kW) |
|---|---|---|---|---|
| 1 | 0.88 | 0.49 | 1.44 | 2.43 |
| 2 | 0.94 | 0.07 | 0.84 | 1.76 |

the time steps in the 24-hour window when the switching command is 0) is computed based on the SM measurement. Then the HP active power at time step $t$ is estimated as follow:

$$P_t^{\text{HP}} = \mathbf{1}_{\{hp_t^{\text{ON}}=1\}} \cdot \max(\min(P_t - P_{\text{AVG24h}}^{\text{noHP}}, P_{\text{nom}}^{\text{HP}}), 0) \tag{6}$$

If the HP is estimated to be running ($hp_t^{\text{ON}} = 1$), its active power is obtained by subtracting $P_{\text{AVG24h}}^{\text{noHP}}$ from the active power measured via the SM ($P_t$) and taking the minimum between the result and the nominal power of the HP ($P_{\text{nom}}^{\text{HP}}$). The outer $\max$ operator ensures that the HP active power is non-negative.

The EWH load detection component leverages the active power $P_t^{\text{noHP}}$ from the SM measurements where the HP load (and if present, the EV load) has already been subtracted. The heuristic algorithm defines a variable $ewh_t^{\text{ON}} \in \{0, 1\}$ that represents whether the EWH is running at time step $t$. At every time step $t$, $ewh_t^{\text{ON}}$ is computed as follows:

$$ewh_t^{\text{ON}} = \mathbf{1}_{\{P_t^{\text{noHP}} > \zeta(P_{\text{nom}}^{\text{EWH}}) \cdot P_{\text{AVG24h}}^{\text{noHPnoEWH}}\}} \tag{7}$$

The EWH is estimated to be running if the active power measured without the HP load exceeds the average active power without the HP when the EWH cannot run, i.e. $P_{\text{AVG24h}}^{\text{noHPnoEWH}}$, by $\zeta(P_{\text{nom}}^{\text{EWH}})$ times. $\zeta(P_{\text{nom}}^{\text{EWH}})$ is heuristically determined as follow:

$$\zeta(P_{\text{nom}}^{\text{EWH}}) = \begin{cases} 2 & \text{if} \quad P_{\text{nom}}^{\text{EWH}} < 3 \\ 3 & \text{if} \quad 3 \leq P_{\text{nom}}^{\text{EWH}} \leq 7 \\ 4 & \text{otherwise} \end{cases} \tag{8}$$

Once $ewh_t^{\text{ON}}$ has been computed for the entire 24-hour window, all the groups of 1s that are not fully included in an unblocked window (i.e., where the switching commands allow the EWH to run) are discarded. The new obtained variable is called $\overline{ewh_t}^{\text{ON}}$. Finally, the EWH active power at time step $t$ is estimated as follow:

$$P_t^{\text{EWH}} = \mathbf{1}_{\{\overline{ewh_t}^{\text{ON}}=1\}} \cdot \max(P_t^{\text{noHP}} - P_{\text{AVG24h}}^{\text{noHPnoEWH}}, 0) \tag{9}$$

If the EWH is estimated to be running, its active power is obtained by subtracting $P_{\text{AVG24h}}^{\text{noHPnoEWH}}$ from the active power measured via the SM $P_t^{\text{noHP}}$ without the HP (and if present, without the EV). The outer $\max$ operator ensures that the EWH active power is non-negative. In this case, the power is not capped at the nominal value because the records of the nominal EWH power are not always accurate.

To assess the accuracy of the disaggregation approach, the algorithm is applied to two households in Winkel for which the EWH and HP consumptions are measured with a separate meter. More specifically, one meter measures both the EWH and the HP load, and one meter measures the remaining household load. For testing purposes, the sum of these two measurements, i.e., the total power, serves as input to the algorithm. Table 1 presents the results for applying the algorithm to the two households for the one-year period from June 2022 to May 2023. The table shows the Total Energy Correctly Assigned (TECA), the Mean Absolute Error (MAE) in the EWH and HP load estimate, the mean EWH and HP active power demand, and its standard deviation. TECA is introduced in [15] and is a dimensionless metric evaluating the degree to which energy is correctly assigned (and not assigned) in relation to the total energy. The

analytical formulation of TECA is given by:[2]

$$TECA = 1 - \frac{\sum_{t=1}^{\tau} |y_t - \hat{y}_t|}{\sum_{t=1}^{\tau} P_t} \tag{10}$$

In the above equation, $y_t$ is the ground truth EWH and HP active power at time step $t$, $\hat{y}_t$ is the corresponding estimated value, and $P_t$ is the total active power. Interpreting the results for test cases 1 and 2, it is noticed that in both cases, TECA is high (above 0.8). In test case 2, the metric even exceeds the 0.9 mark. To further understand the accuracy of the disaggregation algorithm, a few results for both test cases are plotted.

The results displayed in Figs. 9, 10, and 11 show that the heuristic algorithm can estimate fairly accurately the HP and EWH loads. The major challenge for the algorithm lies in identifying the correct magnitude of the loads. In particular, it can be seen in Fig. 10 that the algorithm underestimates the HP load. This is because the estimation of the HP load is capped at its reported nominal power. However, in some instances, the HP shows a higher load than this value.

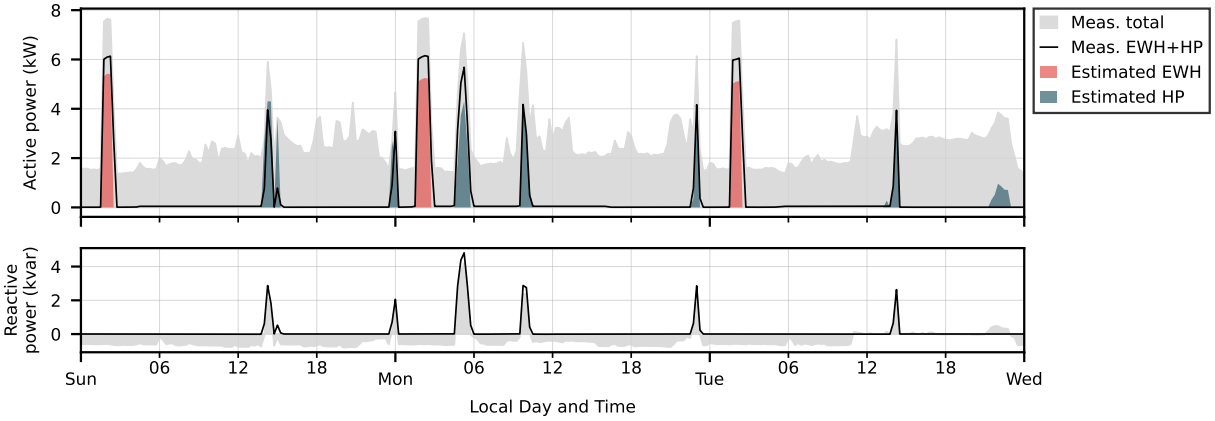


Figure 9: Load disaggregation results versus ground truth for test case 1 from 10.07.2022 to 12.07.2022. The results illustrate that the EWH and HP load estimate is aligned with the measurements.

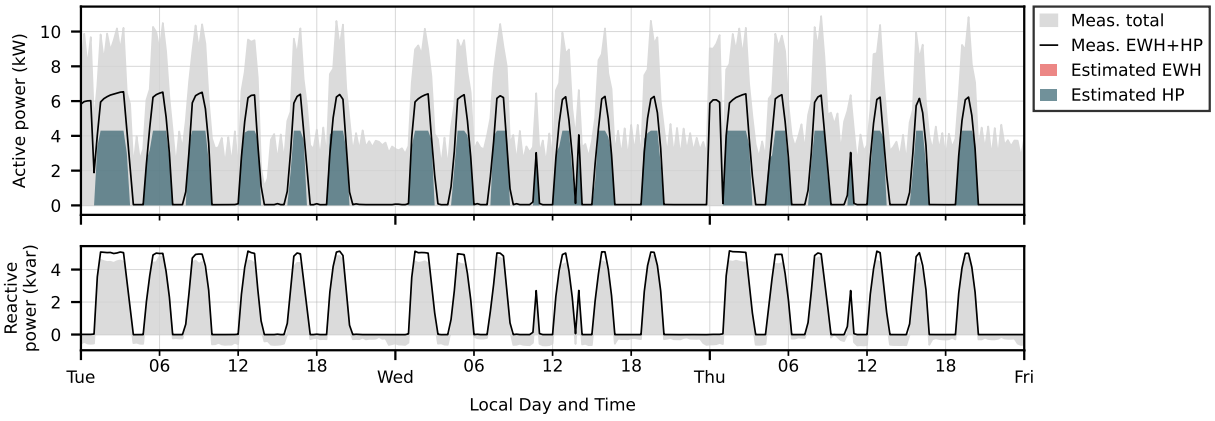


Figure 10: Load disaggregation results versus ground truth for test case 1 from 10.01.2023 to 12.01.2023. The shape of the estimated HP load is aligned with the measurements, while it is challenging to identify the correct power value.

[2] In [15], the metric is defined for components/devices $i \in \{1, \ldots, n\}$, and a factor $2$ appears in the denominator to account for counting every error twice. In the given case, there are only two components, namely (i) the EWH and HP load and (ii) the remaining household load. Therefore, the equation is simplified to (10).

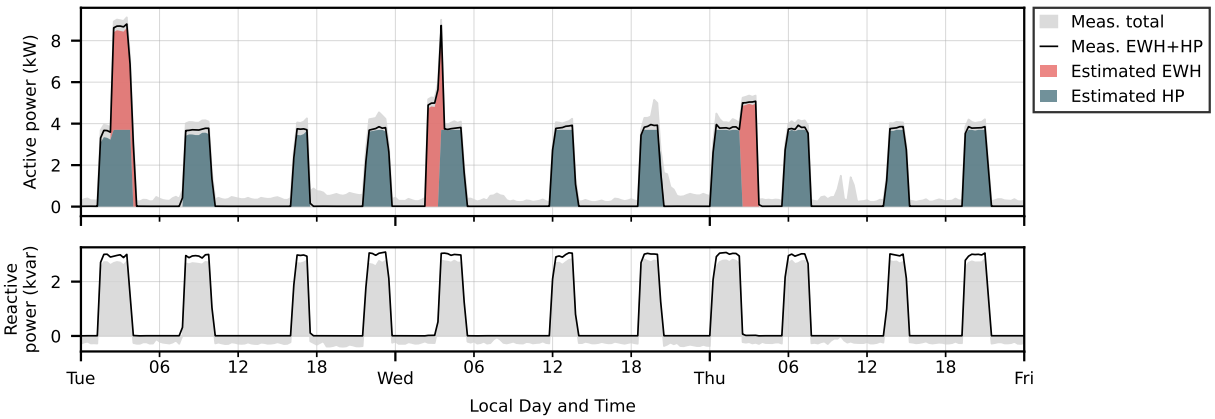


Figure 11: Load disaggregation results versus ground truth for test case 2 from 10.01.2023 to 12.01.2023. The results illustrate that the EWH and HP load estimate is aligned with the measurements.

**Most similar day matching** After having populated a database with the demand of EWHs and HPs for every household, there is the need to identify the most similar day to the one being forecasted. Similarity between days is measured by leveraging weather data. In particular, temperature ($T$) and global radiation ($S$) are considered.

Given two different days $d1$ and $d2$ and two lists for each day $T^{di}, S^{di}, i \in \{1, 2\}$ with measurements (or forecasts) of temperature and global radiation at a fixed frequency, a dissimilarity score is defined:

$$DIS^{d1,d2} = \frac{\sqrt{\sum_{t=1}^{\tau}(T_t^{d1} - T_t^{d2})^2} + \sqrt{\sum_{t=1}^{\tau}(S_t^{d1} - S_t^{d2})^2}}{2} \tag{11}$$

This equation computes the dissimilarity between $d1$ and $d2$ as a simple average of the Euclidean distance between the temperature lists and the global radiation lists. The lower the score, the higher the similarity between the days. In practice, before computing the Euclidean distance, the lists are normalized from 0 to 1 to ensure comparability.

To forecast the inflexible load, the following approach is used:

1. For each day in the database where historical flexible load profiles are present, the dissimilarity score is computed based on the available weather data.
2. The day with the lowest dissimilarity score is identified.
3. The inflexible load estimate for this day is calculated by subtracting the flexible load profiles (EWH, HP, and EV, the latter obtained through direct measurement) from the total TS load.

It is important to note that days are clustered in types (weekdays, Saturdays, Sundays and holidays), and the dissimilarity score is computed only between days of the same type. In the actual implementation of the component, the temperature and global radiation measurements and forecasts have a 15-minute frequency.

### 3.3.2 Real-time tariff setting

**Overview** This section presents the algorithms that were developed for the indirect load control scheme with real-time prices. Figure 12 provides an overview of the different components.

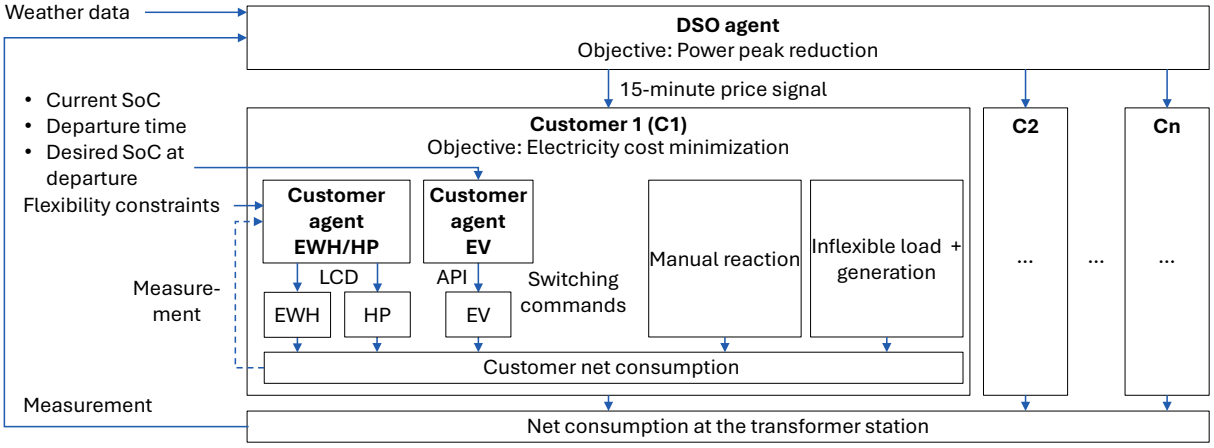


Figure 12: Interactions of the DSO agent and the customer agents.

On the DSO level (DSO agent), the price values need to be determined taking the uncertainties in customer behavior and consumption and generation forecasts into account. However, the DSO's knowledge of the customers' load models and device states, such as temperatures and charging states, is limited. On the one hand, this is due to technical limits. On the other hand, customers might also have privacy concerns when sharing their data with the DSO. Additionally, WP 2 showed that already under the assumption of idealized conditions, the bilevel problem is hard to solve. This is especially the case for the real-time tariff, which can take a different price value in each time step. Modeling the uncertainty in the bilevel programming problem would increase the computational complexity further. Therefore, we applied a proportional pricing scheme in the first phase of the pilot (October 2023 until end of June 2024) and an RL-based approach starting from July 2024.

On the customer level, the optimal commands for the EWH, HP, and EV charging need to be determined. For the EWH and the HP (Customer agent EWH/HP), the LCSA receives a new price value via PLC every 15 minutes and takes the blocking decision locally at the household. A key challenge is the limited information on the devices and customer behavior. Besides the current electricity price, only the SM measurements and the rated power of the devices are known. To overcome this challenge, again an RL-based solution approach was applied in the project. The arrow for the measurement in Fig. 12 is dashed because this information was not used in the final implementation. For the EV (Customer agent EV), information on the current SoC and whether the EV is plugged in at home is available via the API. Additionally, customers specify their desired SoC and a departure time. The commands are determined by solving an optimization problem that chooses the time intervals with the lowest price while ensuring that all the constraints are met. The following subsections provide more details on the formulation for the different agents.

**DSO agent** In the initial pilot phase, the real-time price was proportional to the estimated inflexible load. Shortly before midnight on each day, the inflexible load for the next day is forecasted using the approach explained in Section 3.3.1. The resulting profile is scaled to meet the cost neutrality condition defined in Section 3.1. For this, the following equation is solved to compute $\pi^{\text{buy,max}}$ given $\pi^{\text{buy,min}}$:

$$\sum_{t=0}^{K-1} \left( \pi_t^{\text{buy}} \cdot P_t^{\text{inf,cons}} \right) = \sum_{t=0}^{K-1} \left( \pi_t^{\text{buy,ref}} \cdot P_t^{\text{inf,cons}} \right), \tag{12}$$

where the price in time step $t$ is defined as:

$$\pi_t^{\text{buy}} = \pi^{\text{buy,min}} + \frac{P_t^{\text{inf}} - P^{\text{inf,min}}}{P^{\text{inf,max}} - P^{\text{inf,min}}} \cdot \left(\pi^{\text{buy,max}} - \pi^{\text{buy,min}}\right). \tag{13}$$

$K$ denotes the number of time steps within one day, and $P_t^{\text{inf,cons}}$ describes the mean demand of inflexible consumers for the given type of day (weekday, Saturday, Sunday or holiday) and month, while $P_t^{\text{inf}}$ is the forecasted inflexible net load at the TS, with minimum and maximum values $P^{\text{inf,min}}$ and $P^{\text{inf,max}}$. The reference price $\pi_t^{\text{buy,ref}}$ is a flat tariff, which is cost-neutral with respect to the monthly demand of inflexible consumers and the EKZ standard tariff. The EKZ standard tariff in 2023 had a high-price window from 7:00 to 20:00 on weekdays and low prices at all other times [16]. Therefore, directly using it as $\pi_t^{\text{buy,ref}}$ in (12) would have led to considerably lower prices on weekends. To ensure comparable savings for flexible loads, $\pi^{\text{buy,min}}$ was set to the lowest price of the ToU tariff in the corresponding year. If a price $\pi_t^{\text{buy}}$ exceeded the maximum price specified in the dynamic tariff sheet, it was replaced by the corresponding value.

The proportional pricing scheme can shift flexible loads to times when the inflexible load is low. However, it cannot leverage specific device characteristics, e.g., that EWHs are always connected while EVs are not or that the EWH load is highest at the start of an unblocked period. Moreover, in reality, the DSO would not know the EV load and at which time steps an EWH or HP was blocked, which is leveraged for the disaggregation. Therefore, we developed a RL-based approach for determining the dynamic real-time price signal [17][3], which was applied in the pilot starting from July 2024.

The inputs to the agent in each time step $t$ are information on the current time (quarter-hour of the day, day of the week, holiday or not), the 100 latest TS load measurements, price signals, outside temperature, and global radiation values in 15-minute resolution, as well as a 24-hour forecast for outside temperature and global radiation in 15-minute resolution. The agent's action $a_t$ is defined as the price change compared to the previous price signal, i.e., $\pi_{t+1}^{\text{buy}} = \pi_t^{\text{buy}} + a_t$. If the resulting price lies outside of the predefined price range, the price is clipped to the minimum or maximum value. The overall objective of reducing peaks in the absolute TS power is represented by the reward function

$$r_{t+1} = -\left(\max\left(0, (|P_{t+1}^{\text{tot}}| - P^{\text{th}})/P^{\text{th}}\right)\right)^2 \tag{14}$$

which penalizes the agent every time the absolute load exceeds a threshold value $P^{\text{th}}$. The deviation is squared such that higher power values result in a higher penalty. Based on this formulation, the Double DQN algorithm [18] was used to learn a policy that maps a given observation to action $a_t$. The Q-network is extended by a Long Short-Term Memory (LSTM) layer to account for limited information.

Two separate DSO agents were trained on a simulation environment emulating the load of the TS with the dynamic real-time tariff scheme (see Appendix 10.1). Different from the household-level decision-making described in [17], the trained household-level agents were integrated to control EWHs and HPs, and EV charging could only be controlled after reaching a given minimum SoC. The first agent was trained and evaluated using TS, SM, and weather data from May to August 2022, adding 50 kWp PV generation to account for new installations visible as of April 2024 (time of training). For EV charging, measurement data from March 2023 to April 2024 was used and shifted to cover the same period as the remaining data while keeping calendar weeks intact. The second agent, which was applied as soon as the three-day temperature mean dropped below 15 °C, was trained and evaluated using data from February 2022 to April 2023, skipping the summer months June to August. The additional PV generation was increased to 130 kWp as PV infeeds further increased in summer 2024. Cost neutrality was addressed by applying the DSO agents in the simulation environment for June to August and September to December, respectively (i.e., the relevant months in the pilot). Using the resulting normalized price profile in the range $[0, 1]$, denoted as $\lambda_t$, and a given minimum price value $\pi^{\text{buy,min}}$, (12) is extended to the entire considered time

[3] The code and data are available on: `https://github.com/ka-kai/price_agent`

period to determine the maximum value $\pi^{\text{buy,max}}$:

$$\sum_{t=0}^{N_d \cdot K-1} \left( \pi_t^{\text{buy}} \cdot P_t^{\text{inf,cons}} \right) = \sum_{t=0}^{N_d \cdot K-1} \left( \pi_t^{\text{buy,ref}} \cdot P_t^{\text{inf,cons}} \right), \tag{15}$$

where $N_d$ is the number of considered days and the price in time step $t$ is:

$$\pi_t^{\text{buy}} = \pi^{\text{buy,min}} + \lambda_t \cdot \left( \pi^{\text{buy,max}} - \pi^{\text{buy,min}} \right). \tag{16}$$

In real-time, the agent's price signal for a given 15-minute interval was then mapped to the determined range $[\pi^{\text{buy,min}}, \pi^{\text{buy,max}}]$ in Rp./kWh.

**Customer agent EWH/HP** The customer agents were implemented according to the second approach described in [19], i.e., using a hypothetical energy consumption instead of the actual SM measurement as feedback to the agent. Key differences between [19] and the final implementation are that (i) EV charging is not considered anymore, as the control of EVs is implemented via the API and not, as initially planned, via the LCSA and the charging station, (ii) PV generation is not considered as self-consumption optimization is out of the scope of the project, and (iii) the agent is trained not to violate the constraints concerning the maximum number of blocked time intervals in each 24-hour window instead of per calendar day. Thus, in the final version, the agent's observation includes information on the time step for which the action is taken (quarter-hour of the day, day of the month, weekday or weekend/holiday, month), the electricity price for the given 15-minute interval, as well as the 95 latest price values and the 95 latest applied blocking actions. Given this input, the agent determines whether the EWH and/or HP should be blocked in the next 15-minute interval. If the household has both an EWH and HP, there are four possible actions, encoding all possible combinations of $(u_t^{\text{EWH}}, u_t^{\text{HP}})$. If $u_t \in \{0, 1\}$ is 1, the device may operate or not depending on the internal device controller. If it is 0, the device is blocked and cannot consume energy. The reward function is defined as a combination of the hypothetical electricity cost and penalties for constraint violations:

$$r_t = -w_1 \cdot \left( \hat{u}_t^{\text{EWH}} + \hat{u}_t^{\text{HP}} \right) \cdot \pi_t^{\text{buy}} - w_2 \cdot \xi_t^{\text{EWH}} - w_3 \cdot \xi_t^{\text{HP}} \tag{17}$$

where $w_1$ - $w_3$ are non-negative weight values, $\hat{u}_t$ describes the potentially corrected action which meets all the flexibility constraints detailed in Section 3.3.4, and $\xi_t$ represents whether the agent's action for the device was valid ($\xi_t$ is 0 if the action is valid and 1 if it would lead to a constraint violation). The agent should thus learn to reduce the electricity cost while meeting the flexibility constraints. It assumes that a device operates whenever it is unblocked. If only one of the devices is present, the number of possible actions reduces to 2, and the reward function is adjusted accordingly. The customer agents for the pilot were trained using the Soft Actor-Critic algorithm [20], modified for discrete action spaces, and using the corresponding TS load measurement in 2022, scaled to $[0, 1]$ on a daily basis, as price input. The settings for the flexibility constraints for each household were based on the previous ripple control scheme.

**Customer agent EV** This agent computes the switching (blocking/unblocking) commands to the EV by solving a MILP. The optimization model was coded in Python, and the problem was solved by Gurobi [12]. As depicted in Fig. 12, the customer agent EV uses as input the electricity price signal, the current SoC and the desired SoC at the departure time (in $t_{goal}$ time steps), as defined by the EV owner. Only the price for the next time step is known. For the remaining time steps in the 24-hour optimization horizon, the price values are predicted using the most similar day matching approach described in Section 3.3.1. We expect that different customers or service providers would use different forecasting approaches and input data, e.g., weather data, potentially leading to different price forecasts. To integrate such variations in price forecasts, the vehicles are split into 3 groups, which use the price data of the most similar day (group 1) up to the third most similar day (group 3) within the previous 8 weeks as their respective

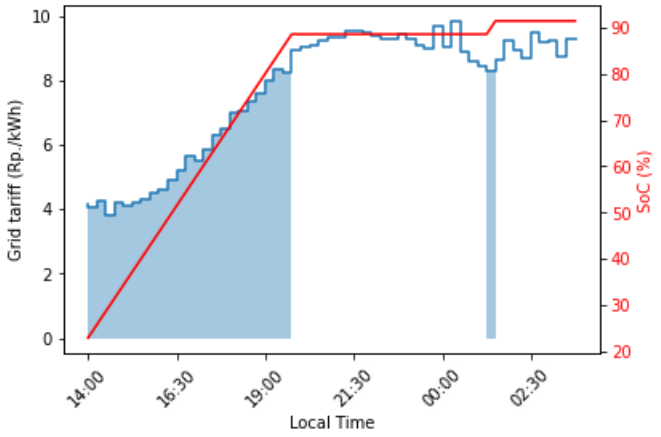


Figure 13: Optimal EV charging based on the price forecast.

prediction. The following is the optimization problem solved for customer $c$:

$$\min_{\mathbf{u}_c^{\mathsf{EV}},\mathbf{s}_c^{\mathsf{EV}},\mathbf{SoC}_c^{\mathsf{EV}}} \quad \sum_{t=0}^{t_{goal}-1} (\pi_t^{\mathsf{buy}} + \beta_c \cdot t) \cdot u_{c,t}^{\mathsf{EV}} \tag{18a}$$

$$\text{s.t.} \quad \mathsf{SoC}_{c,t}^{\mathsf{EV}} = \mathsf{SoC}_{c,t-1}^{\mathsf{EV}} + u_{c,t}^{\mathsf{EV}} \frac{P_{c,\mathsf{nom}}^{\mathsf{EV}} \Delta t}{E_{c,\mathsf{EV}}^{\mathsf{max}}} 100, \ \forall t \tag{18b}$$

$$\sum_{t=0}^{K_{c,\mathsf{EV}}^{\mathsf{min}}-1} (1 - u_{c,t}^{\mathsf{EV}}) = 0 \tag{18c}$$

$$\mathsf{SoC}_{c,t_{goal}-1}^{\mathsf{EV}} \geq \mathsf{SoC}_{c,\mathsf{EV}}^{\mathsf{goal}} \tag{18d}$$

$$\sum_{i=0}^{t} s_{c,i}^{\mathsf{EV}} + \sum_{i=1}^{K-1-t} s_{c,-i}^{\mathsf{EV}} \leq N_{c,\mathsf{EV}}^{\mathsf{max,24h}}, \ \forall t \tag{18e}$$

$$s_{c,t}^{\mathsf{EV}} \geq u_{c,t}^{\mathsf{EV}} - u_{c,t-1}^{\mathsf{EV}}, \ \ \forall t \tag{18f}$$

$$u_{c,t}^{\mathsf{EV}} \in \{0,1\}, \ \ s_{c,t}^{\mathsf{EV}} \in \{0,1\} \ \forall t \tag{18g}$$

The objective is to minimize the cost of EV charging. The second summand in (18a) is used to incentivize early EV chargings in case of time instants with the same price, and $\beta_c$ is set to a very small value. In addition, $u_{c,t}^{\mathsf{EV}}$ is the switching (0 blocked and 1 unblocked) command to be sent to the EV, $s_{c,t}^{\mathsf{EV}}$, is an auxiliary variable used to model the OFF-to-ON switchings, and $\mathsf{SoC}_{c,t}^{\mathsf{EV}}$ is the EV battery's SoC in percentage, at time $t$. These are the decision variables in the optimization problem.

Constraint (18b) models the evolution of the EV's SoC, for the nominal EV charger power $P_{c,\mathsf{nom}}^{\mathsf{EV}}$ and the capacity of the EV battery $E_{c,\mathsf{EV}}^{\mathsf{max}}$. Constraint (18c) guarantees the EV reaches a minimum SoC value in $K_{c,\mathsf{EV}}^{\mathsf{min}}$ time steps without blockings. Constraint (18d) ensures that the desired SoC, namely $\mathsf{SoC}_{c,\mathsf{EV}}^{\mathsf{goal}}$, is reached at the departure time, i.e. in $t_{goal}$ time steps. Finally, constraints (18e)-(18f) does not allow more than $N_{c,\mathsf{EV}}^{\mathsf{max,24h}}$ OFF-to-ON switchings in any 24-hour window.

Figure 13 illustrates an optimal EV charging based on the problem in (18) for the predicted electricity price shown in the plot. It was assumed that the EV owner wants to charge the battery to $\mathsf{SoC}_{c,\mathsf{EV}}^{\mathsf{goal}} = 90$ %. In this case, the owner did not define any departure time, but $N_{c,\mathsf{EV}}^{\mathsf{max,24h}}$ was set to 3. The charging session started at 14:00 hours and was interrupted at about 19:45 when the electricity prices were high. The charging was restarted after 01:00 and continued until the desired SoC was reached.

### 3.3.3 Automated load management in the Time-of-Use tariff setting

The same optimization as in the real-time tariff setting (cf. Section 3.3.2) was applied for the EVs in the ToU tariff setting. The difference is that the optimization takes the price values of the ToU tariff for the next 24 hours as an input instead of a price prediction. Figure 14 presents the optimal charging for a second EV based on the formulation in (18) for the price values of the ToU tariff. In this case, the EV owner defines that the SoC should be 90 % before 04:00 (departure time). The charging session starts at 14:00 hours and is interrupted at 18:00 when the electricity prices for the ToU tariff are higher. The charging is restarted at midnight until the desired SoC is reached.

EWHs are unblocked for the entire low-price period. Additionally, if the minimum number of hours for which the device must be unblocked in each 24-hour window exceeds five hours (duration of low-price period in summer), the earliest hours of the mid-price period are unblocked, as shown in Fig. 15.

HPs can be blocked for up to four hours in each 24-hour window and up to two hours per blocking instance. Therefore, they are blocked for two hours at the end of each high-price period, such that the rebound falls into the following lower-price period.

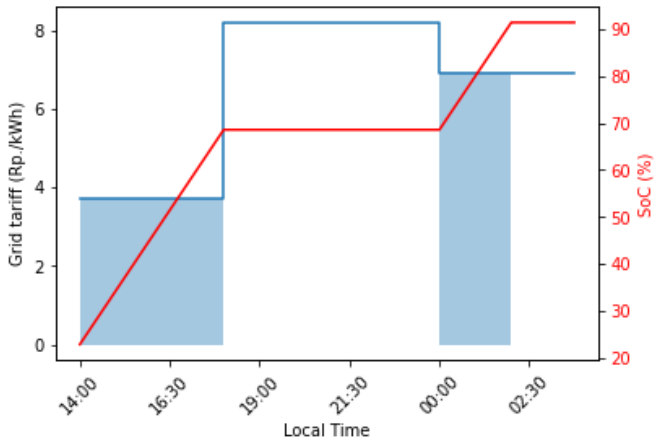


Figure 14: Optimal EV charging based on ToU-price signal in summer.

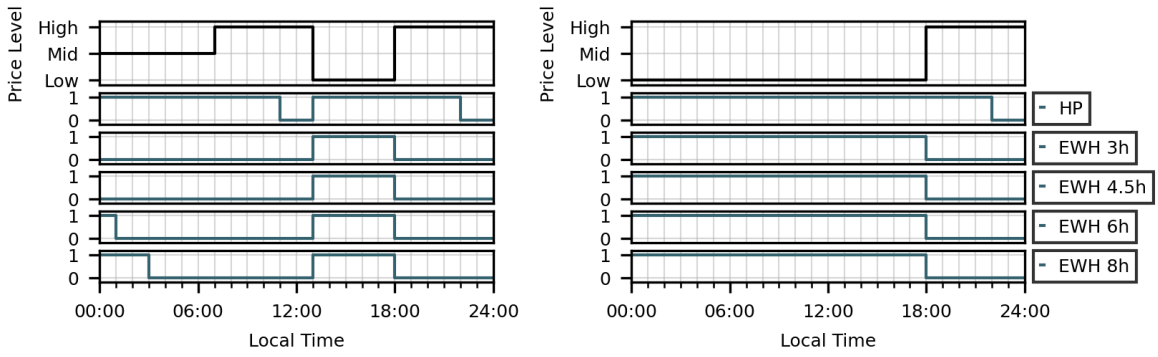


(a) Summer (b) Winter

Figure 15: EWH and HP control based on ToU-price signal; 1 means a device can operate, while 0 means it is blocked; the number of hours indicates how long an EWH needs to be unblocked according to the previous ripple control scheme.

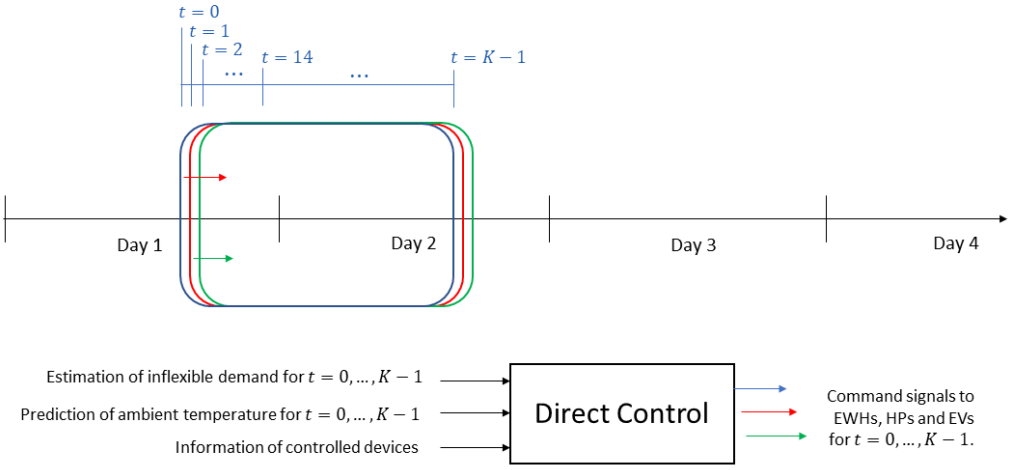


Figure 16: Rolling horizon for DLC with inputs and outputs.

### 3.3.4 Direct load control

The proposed Direct Load Controller (DLC) consists of a centralized optimization-based scheme that sends optimal switching commands every 15 minutes to EWHs, HPs, and EVs to flatten the total demand curve of the TS. The optimization is a Mixed Integer Quadratic Programming (MIQP) problem coded in Python and solved by Gurobi [12].

This controller uses a 24-hour rolling horizon ($K = 96$ time steps of 15 minutes each) to compute the switching commands ($u_{c,t}^{\text{EWH}}$, $u_{c,t}^{\text{HP}}$, $u_{c,t}^{\text{EV}}$) sent to the flexible loads of each customer $c$ for $0 \leq t \leq K-1$, see Fig. 16. The DLC inputs are the estimation of the inflexible load, the prediction of the ambient temperature, and the information of the controlled devices, for example, the nominal powers ($P_{c,\text{nom}}^{\text{EWH}}$, $P_{c,\text{nom}}^{\text{HP}}$, $P_{c,\text{nom}}^{\text{EV}}$), the switching commands in the previous 24 hours, the maximum number of blocking intervals in any 24 hours ($K_{c,\text{EWH}}^{\text{block,24h}}$ and $K_{c,\text{HP}}^{\text{block,24h}}$), the minimum ($K_{c,\text{EWH}}^{\text{min,block}}$ and $K_{c,\text{HP}}^{\text{min,block}}$) and maximum ($K_{c,\text{EWH}}^{\text{block,instance}}$ and $K_{c,\text{HP}}^{\text{block,instance}}$) consecutive blocking intervals, and the minimum consecutive unblocking intervals ($K_{c,\text{EWH}}^{\text{min,unblock}}$ and $K_{c,\text{HP}}^{\text{min,unblock}}$) for all EWHs and HPs. For each EV, the DLC receives information of the current SoC and the desired $\text{SoC}_{c,\text{EV}}^{\text{goal}}$ at the departure time step $t_{goal}$, the charger's power $P_{c,\text{nom}}^{\text{EV}}$, the battery capacity $E_{c,\text{EV}}^{\text{max}}$, the maximum OFF-to-ON switches allowed in any 24-hours $N_{c,\text{EV}}^{\text{max,24h}}$, and the OFF-to-ON switching events in the last 24 hours.

**Objective function** The objective of the DLC is to flatten the total 24-hour demand curve by managing the times when the available flexible loads are allowed to operate. For this, we penalize the deviations from a reference value $P^{\text{ref}}$ of the total demand $P^{\text{tot}}$ at any time $t$ of the 24-hour horizon.

$$\min_{\mathbf{u},\mathbf{s}^{\text{EV}},\mathbf{SoC}^{\text{EV}}} \quad \sum_{t=0}^{K-1} (P_t^{\text{tot}} - P^{\text{ref}})^2 \tag{19}$$

where $P_t^{\text{tot}} = P_t^{\text{inf}} + P_t^{\text{flx}}$, and the flexible load is estimated as:

$$P_t^{\text{flx}} = \sum_{c=1}^{N_{\text{customers}}} u_{c,t}^{\text{EWH}} \cdot P_{c,\text{nom}}^{\text{EWH}} + \sum_{c=1}^{N_{\text{customers}}} u_{c,t}^{\text{HP}} \cdot \rho_t^{\text{HP}} \cdot P_{c,\text{nom}}^{\text{HP}} + \sum_{c=1}^{N_{\text{customers}}} u_{c,t}^{\text{EV}} \cdot P_{c,\text{nom}}^{\text{EV}} \quad \forall t \tag{20}$$

The variable $0 \leq \rho_t^{\text{HP}} \leq 1$ represents the variation of HPs power demand with ambient temperature. It is computed from a regression model extracted from two years of historical data of the power demand of dozens of HPs in Zurich. The objective function in (19) is subject to the following constraints:

### EWH flexibility constraints

$$\sum_{i=0}^{t} u_{c,i}^{\text{EWH}} + \sum_{i=1}^{K-1-t} u_{c,-i}^{\text{EWH}} \geq K - K_{c,\text{EWH}}^{\text{block,24h}}, \quad 0 \leq t \leq K-2 \tag{21}$$

$$\sum_{t=0}^{K-1} u_{c,t}^{\text{EWH}} \geq K - K_{c,\text{EWH}}^{\text{block,24h}} \tag{22}$$

$$\sum_{i=0}^{K_{c,\text{EWH}}^{\text{block,instance}} - N_{c,\text{EWH}}^{\text{blocked}}} u_{c,i}^{\text{EWH}} \geq 1, \quad \text{if } u_{c,-1}^{\text{EWH}} = 0 \text{ and } t = 0 \tag{23}$$

$$\sum_{i=t}^{t+K_{c,\text{EWH}}^{\text{block,instance}}} u_{c,i}^{\text{EWH}} \geq 1, \quad 1 \leq t \leq K - 1 - K_{c,\text{EWH}}^{\text{block,instance}} \tag{24}$$

$$\sum_{i=0}^{K_{c,\text{EWH}}^{\text{min,block}} - N_{c,\text{EWH}}^{\text{blocked}} - 1} u_{c,i}^{\text{EWH}} \leq 0, \quad \text{if } u_{c,-1}^{\text{EWH}} = 0 \text{ and } t = 0 \tag{25}$$

$$\sum_{i=t}^{t+K_{c,\text{EWH}}^{\text{min,block}}-1} (1 - u_{c,i}^{\text{EWH}}) \geq K_{c,\text{EWH}}^{\text{min,block}} \cdot (u_{c,t-1}^{\text{EWH}} - u_{c,t}^{\text{EWH}}), \quad 0 \leq t \leq K - K_{c,\text{EWH}}^{\text{min,block}} \tag{26}$$

$$\sum_{i=t}^{K-1} (1 - u_{c,i}^{\text{EWH}}) \geq (K-t) \cdot (u_{c,t-1}^{\text{EWH}} - u_{c,t}^{\text{EWH}}), \quad K - K_{\text{min,block}}^{\text{EWH}} + 1 \leq t \leq K-2 \tag{27}$$

$$\sum_{i=0}^{K_{c,\text{EWH}}^{\text{min,unblock}} - N_{c,\text{EWH}}^{\text{unblocked}} - 1} u_{c,i}^{\text{EWH}} \geq K_{c,\text{EWH}}^{\text{min,unblock}} - N_{c,\text{EWH}}^{\text{unblocked}}, \quad \text{if } u_{c,-1}^{\text{EWH}} = 1 \text{ and } t = 0 \tag{28}$$

$$\sum_{i=t}^{t+K_{c,\text{EWH}}^{\text{min,unblock}}-1} u_{c,i}^{\text{EWH}} \geq K_{c,\text{EWH}}^{\text{min,unblock}} \cdot (u_{c,t}^{\text{EWH}} - u_{c,t-1}^{\text{EWH}}), \quad 0 \leq t \leq K - K_{c,\text{EWH}}^{\text{min,unblock}} \tag{29}$$

$$\sum_{i=t}^{K-1} u_{c,i}^{\text{EWH}} \geq (K-t) \cdot (u_{c,t}^{\text{EWH}} - u_{c,t-1}^{\text{EWH}}), \quad K - K_{\text{min,unblock}}^{\text{EWH}} + 1 \leq t \leq K-2 \tag{30}$$

$$K_{c,\text{EWH}}^{\text{min,block}} > N_{c,\text{EWH}}^{\text{blocked}}, \quad K_{c,\text{EWH}}^{\text{min,unblock}} > N_{c,\text{EWH}}^{\text{unblocked}}, \quad u_{c,t}^{\text{EWH}} \in \{0,1\} \; \forall t. \tag{31}$$

where $N_{c,\text{EWH}}^{\text{blocked}}$ (resp. $N_{c,\text{EWH}}^{\text{unblocked}}$) is the number of previous consecutive blocking (resp. unblocking) intervals for the EWH of customer $c$ at $t = 0$. The constraints (21)-(22) ensure that a maximum number of blocking intervals is not exceeded in any 24-hour window. These are the only flexibility constraints imposed to the DLC for EWHs. However, the constraints (23)-(30) were added to reduce the uncertainty related to the time instants the EWHs are ON when unblocked. More specifically, constraints (23)-(24) ensure that the maximum number of consecutive blocking intervals is not exceeded. The constraints (25)-(27) specify a minimum duration of a blocking instance. Similarly, the constraints (28) - (30) ensure that the EWHs remain unblocked for the specified number of time steps between two blocking events.

### HP flexibility constraints

$$\sum_{i=0}^{t} u_{c,i}^{\text{HP}} + \sum_{i=1}^{K-1-t} u_{c,-i}^{\text{HP}} \geq K - K_{c,\text{HP}}^{\text{block,24h}}, \quad 0 \leq t \leq K-2 \tag{32}$$

$$\sum_{t=0}^{K-1} u_{c,t}^{\text{HP}} \geq K - K_{c,\text{HP}}^{\text{block,24h}} \tag{33}$$

$$\sum_{i=0}^{K_{c,\text{HP}}^{\text{block,instance}} - N_{c,\text{HP}}^{\text{blocked}}} u_{c,i}^{\text{HP}} \geq 1, \quad \text{if } u_{c,-1}^{\text{HP}} = 0 \text{ and } t = 0 \tag{34}$$

$$\sum_{i=t}^{t+K_{c,\text{HP}}^{\text{block,instance}}} u_{c,i}^{\text{HP}} \geq 1, \quad 1 \leq t \leq K - 1 - K_{c,\text{HP}}^{\text{block,instance}} \tag{35}$$

$$\sum_{i=0}^{K_{c,\text{HP}}^{\text{min,block}} - N_{c,\text{HP}}^{\text{blocked}} - 1} u_{c,i}^{\text{HP}} \leq 0, \quad \text{if } u_{c,-1}^{\text{HP}} = 0 \text{ and } t = 0 \tag{36}$$

$$\sum_{i=t}^{t+K_{c,\text{HP}}^{\text{min,block}}-1} (1 - u_{c,i}^{\text{HP}}) \geq K_{c,\text{HP}}^{\text{min,block}} \cdot (u_{c,t-1}^{\text{HP}} - u_{c,t}^{\text{HP}}), \quad 0 \leq t \leq K - K_{c,\text{HP}}^{\text{min,block}} \tag{37}$$

$$\sum_{i=t}^{K-1} (1 - u_{c,i}^{\text{HP}}) \geq (K-t) \cdot (u_{c,t-1}^{\text{HP}} - u_{c,t}^{\text{HP}}), \quad K - K_{\text{min,block}}^{\text{HP}} + 1 \leq t \leq K-2 \tag{38}$$

$$\sum_{i=0}^{K_{c,\text{HP}}^{\text{min,unblock}} - N_{c,\text{HP}}^{\text{unblocked}} - 1} u_{c,i}^{\text{HP}} \geq K_{c,\text{HP}}^{\text{min,unblock}} - N_{c,\text{HP}}^{\text{unblocked}}, \quad \text{if } u_{c,-1}^{\text{HP}} = 1 \text{ and } t = 0 \tag{39}$$

$$\sum_{i=t}^{t+K_{c,\text{HP}}^{\text{min,unblock}}-1} u_{c,i}^{\text{HP}} \geq K_{c,\text{HP}}^{\text{min,unblock}} \cdot (u_{c,t}^{\text{HP}} - u_{c,t-1}^{\text{HP}}), \quad 0 \leq t \leq K - K_{c,\text{HP}}^{\text{min,unblock}} \tag{40}$$

$$\sum_{i=t}^{K-1} u_{c,i}^{\text{HP}} \geq (K-t) \cdot (u_{c,t}^{\text{HP}} - u_{c,t-1}^{\text{HP}}), \quad K - K_{\text{min,unblock}}^{\text{HP}} + 1 \leq t \leq K-2 \tag{41}$$

$$K_{c,\text{HP}}^{\text{min,block}} > N_{c,\text{HP}}^{\text{blocked}}, \quad K_{c,\text{HP}}^{\text{min,unblock}} > N_{c,\text{HP}}^{\text{unblocked}}, \quad u_{c,t}^{\text{HP}} \in \{0,1\}\ \forall t \tag{42}$$

where $N_{c,\text{HP}}^{\text{blocked}}$ (resp. $N_{c,\text{HP}}^{\text{unblocked}}$) is the number of previous consecutive blocking (resp. unblocking) intervals for the HP of customer $c$ at $t = 0$. The constraints (32)-(33) ensure that the maximum number of blocking intervals is not exceeded in any 24-hour window. Constraints (34)-(35) ensure that the maximum number of consecutive blocking intervals is not exceeded. The constraints (36)-(38) specify a minimum duration of a blocking instance. Similarly, the constraints (39) and (41) ensure that the HPs remain unblocked for the specified number of time steps between two blocking events.

**EV flexibility constraints**

$$\mathrm{SoC}^{\mathrm{EV}}_{c,t} = \mathrm{SoC}^{\mathrm{EV}}_{c,t-1} + u^{\mathrm{EV}}_{c,t} \frac{P^{\mathrm{EV}}_{c,\mathrm{nom}} \Delta t}{E^{\mathrm{max}}_{c,\mathrm{EV}}} 100, \ \forall t \tag{43}$$

$$\sum_{i=0}^{K^{\mathrm{min}}_{c,\mathrm{EV}}-1} (1 - u^{\mathrm{EV}}_{c,i}) = 0 \tag{44}$$

$$\mathrm{SoC}^{\mathrm{EV}}_{c,t_{goal}-1} \geq \mathrm{SoC}^{\mathrm{goal}}_{c,\mathrm{EV}} \tag{45}$$

$$\mathrm{SoC}^{\mathrm{EV}}_{c,t} \leq (1 + \gamma^{\mathrm{EV}}) \cdot \mathrm{SoC}^{\mathrm{goal}}_{c,\mathrm{EV}}, \ \forall t \tag{46}$$

$$\sum_{i=0}^{t} s^{\mathrm{EV}}_{c,i} + \sum_{i=1}^{K-1-t} s^{\mathrm{EV}}_{c,-i} \leq N^{\mathrm{max,24h}}_{c,\mathrm{EV}}, \ \ 0 \leq t \leq K-2 \tag{47}$$

$$\sum_{t=0}^{K-1} s^{\mathrm{EV}}_{c,t} \leq N^{\mathrm{max,24h}}_{c,\mathrm{EV}} \tag{48}$$

$$s^{\mathrm{EV}}_{c,t} \geq u^{\mathrm{EV}}_{c,t} - u^{\mathrm{EV}}_{c,t-1}, \ \forall t \tag{49}$$

$$u^{\mathrm{EV}}_{c,t} \in \{0,1\}, \ \ s^{\mathrm{EV}}_{c,t} \in \{0,1\} \ \forall t \tag{50}$$

Constraint (43) models the evolution of the EV's SoC, whereas constraint (44) guarantees the EVs reach a minimum SoC value in $K^{\mathrm{min}}_{c,\mathrm{EV}}$ time steps. Constraints (45) and (46) ensure that the desired SoC are reached at the departure time, but the EVs are allowed to charge slightly higher than $\mathrm{SoC}^{\mathrm{goal}}_{c,\mathrm{EV}}$, according to parameter $\gamma^{\mathrm{EV}} > 0$, which avoids infeasible solutions. Finally, constraints (47)-(49) does not allow more than $N^{\mathrm{max,24h}}_{c,\mathrm{EV}}$ OFF-to-ON switchings for any 24-hour window.

### 3.3.5 Local verification module

All switching commands for EWHs and HPs were locally verified and corrected before they were passed to the LCD, such that communication issues or invalid actions by the DLC and RL agent did not lead to a violation of the flexibility constraints. At every time step, the verification module checked if the 24-hour switching command schedule to be saved in the LCD (i) satisfies the flexibility constraints with respect to the previously applied blocking actions and (ii) satisfies the flexibility constraints if it is played in a loop. The first requirement ensures that the system meets the flexibility constraints during normal operation, while the second requirement ensures that the system meets the constraints if communication to the LCD fails for a longer period and the schedule is repeated.

### 3.3.6 Control approach for the Battery Energy Storage System

Besides the described DSM schemes, a BESS was installed at a separate TS. It followed a threshold-based control approach. This means that the control signal to the BESS is a threshold value, and the power results from the difference between the currently measured load and this threshold value. Compared to a schedule-based control, which specifies the BESS power for each time step, the threshold control is less sensitive to errors in the predicted peak time [21]. Figure 17 illustrates the difference between the two approaches.

The threshold value is computed using an optimization problem with a 12-hour rolling horizon (48 time steps of 15 minutes each). The optimization aims to minimize the peak power $P^{\mathrm{max}}$ in the considered time horizon. Compared to the DLC, the computational complexity is low, which allows for considering multiple scenarios to capture the uncertainty in the future load profile. The control follows a robust formulation,

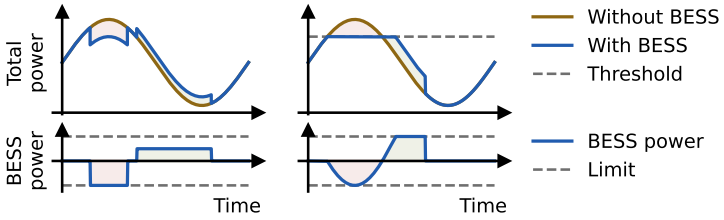


Figure 17: Illustrative comparison between the schedule-based control (left) and the threshold control (right).

which minimizes the maximum $P^{\text{max}}$ over all scenarios, as defined by constraint (51b):

$$\min_{P^{\text{max}},\mathbf{P}^{\text{B},+},\mathbf{P}^{\text{B},-},\mathbf{x}^{+},\mathbf{SoC}} \quad P^{\text{max}} \tag{51a}$$

$$\text{s.t.} \quad P^{\text{max}} \geq P_{t,s} + P_{t,s}^{\text{B,+}} - P_{t,s}^{\text{B,-}}, \qquad \forall t, \forall s \tag{51b}$$

$$0 \leq P_{t,s}^{\text{B,+}} \leq x_{t,s}^{+} \cdot P^{\text{B,+,rated}}, \qquad \forall t, \forall s \tag{51c}$$

$$0 \leq P_{t,s}^{\text{B,-}} \leq (1 - x_{t,s}^{+}) \cdot P^{\text{B,-,rated}}, \qquad \forall t, \forall s \tag{51d}$$

$$\text{SoC}_{t,s} = \text{SoC}_{t-1,s} + \left(\eta \cdot P_{t,s}^{\text{B,+}} - \frac{1}{\eta} \cdot P_{t,s}^{\text{B,-}}\right) \cdot \frac{\Delta t}{E} \cdot 100, \qquad \forall t, \forall s \tag{51e}$$

$$\text{SoC}^{\text{min}} \leq \text{SoC}_{t,s} \leq \text{SoC}^{\text{max}}, \qquad \forall t, \forall s \tag{51f}$$

The given TS does not show injection peaks, so the formulation focuses on consumption peaks for clarity. However, it can be easily adjusted to address injection peaks. The parameter $P_{t,s}$ is the load without BESS in time step $t$ and scenario $s$ (there are no flexible loads at this TS; thus, there is no differentiation between the inflexible and flexible load), while the variables $P_{t,s}^{\text{B,+}}$ and $P_{t,s}^{\text{B,-}}$ denote the charging and discharging power. Constraints (51c) and (51d) specify the corresponding limits, where the binary variable $x_{t,s}^{+}$ avoids simultaneous charging and discharging. The variable $\text{SoC}_{t,s}$ represents the SoC at the end of time step $t$ in percentage. It evolves as given in (51e) and is bounded by $\text{SoC}^{\text{min}}$ and $\text{SoC}^{\text{max}}$ in (51f). The symbol $\eta$ describes the charging and discharging efficiency, and $E$ is the BESS capacity.

Historical TS load profiles are used as scenarios. Similar to the inflexible load estimate in the DLC, the load profiles are selected by choosing the most similar days in terms of weather data. Unlike the procedure described in Section 3.3.1, the selection is solely based on temperature data (considering 24 hours before and after the current quarter-hour of the day) and does not depend on global radiation data and the day type. The given changes were performed based on a preliminary data analysis. The number of scenarios was selected based on simulation results and was set to 5.

After solving (51), the resulting objective function value can be used as the threshold value $P^{\text{th}}$. To avoid shaving lower intermediate peaks, the highest load (including the BESS power) observed on the current day or other period of interest serves as an additional lower bound on the threshold value, i.e., the threshold communicated to the BESS is $\hat{P}^{\text{th}} = \max\left(P^{\text{th}}, \max_{j \in \mathcal{T}}\left(P_j + P_j^{\text{B,+}} - P_j^{\text{B,-}}\right)\right)$ where $\mathcal{T}$ represents the relevant past time steps.

## 3.4 WP 4: Hardware and infrastructure

### 3.4.1 Customer platform

The OrtsNetz platform was the main channel to communicate with participants in the pilot project. Its central functions were the following:

1. Providing functionalities for the Peer-to-Peer (P2P) trading of certificates of origin
2. Displaying individual and aggregate energy information

3. Displaying electricity cost information
4. Displaying tariff information
5. Computing costs according to the pilot tariffs
6. Providing an interface for customers to enter their preferences regarding load control
7. Providing notification functions
8. Providing an interface for ETH Zurich to access pseudonymized data

Functionalities 1, 2, and 8 were made available during the first year of this project. The trading of certificates of origin was an additional offer independent of the new grid tariffs. Customers with PV could sign up to sell their excess electricity to the neighborhood. In turn, interested customers could voluntarily set a bidding price (price per kWh and a monthly limit) that they would be willing to pay on top of the normal tariffs to receive some of the locally produced electricity. Functionality 4 was made available so that the customers could see their tariffs at the time tariffs were introduced (October 2023). The customers could see the current and historic energy and grid prices depending on their corresponding tariff. For the customers getting a dynamic tariff, the grid tariff price was updated every 15 minutes. The prices were sent from the Load Control Master Agent (LCMA) running in the cloud (Microsoft Azure) to the customer platform.

Functionalities 3 and 5 were implemented in the last year of the project. Furthermore, functionalities 6 and 7 were successfully implemented by EKZ and ETH Zurich.

### 3.4.2 Transformer station active components

Figure 18 provides an overview of the communication and hardware infrastructure in OrtsNetz. In the three TSs, at which the LCSAs were installed, G3-PLC gateways were installed. These gateways communicated via PLC with the LCSAs that were installed in customer houses within the TS network. Furthermore, the gateways were connected to the EKZ internal network. The prices and switching tables were sent to the LCSA devices through the gateways. The LCSAs could also be monitored via the gateways. Furthermore, the gateways read consumption data from the SMs and sent these to the Head End System (HES). This data could then be accessed by the LCMA. The gateways were connected to a router connected to the EKZ internal fiber network. However, only a mobile connection was used, since the fibers were not completely installed in the area.

### 3.4.3 Control devices

The LCDs are the devices that receive the switching tables from the LCSAs and then switch the EWHs and the HPs. The LCDs were provided by Swistec. The LCSA devices were developed in collaboration with Neuron. Neuron provided the basis for communication via PLC and an environment where the agents' codes ran. ETH Zurich provided the software of the agents and the verification module. The verification module ensured that the EWHs and HPs were operating sufficiently long per day. Furthermore, it prevented the HPs from too many switching operations which could result in equipment damage. In addition to the load control, the LCSA also read the electricity consumption from the customer's SM via an MBUS connection. This data was not used by the agent running on the LCSA throughout the project. EKZ provided the software infrastructure that handled the data management, the connection to the LCD, and the agents' operation. The setup was extensively tested on a test setup, see Fig. 19. Subsequently, 64 LCSAs were installed in the project.

For controlling the EVs, the consortium decided not to control the vehicles via the charging stations. Instead, the EVs were controlled via the internet through an API platform. The API platform was provided by enode and provided a unified interface to the EVs independently of the car manufacturer. This allowed to see the current SoC of the EVs as well as more convenient monitoring and control via the internet.

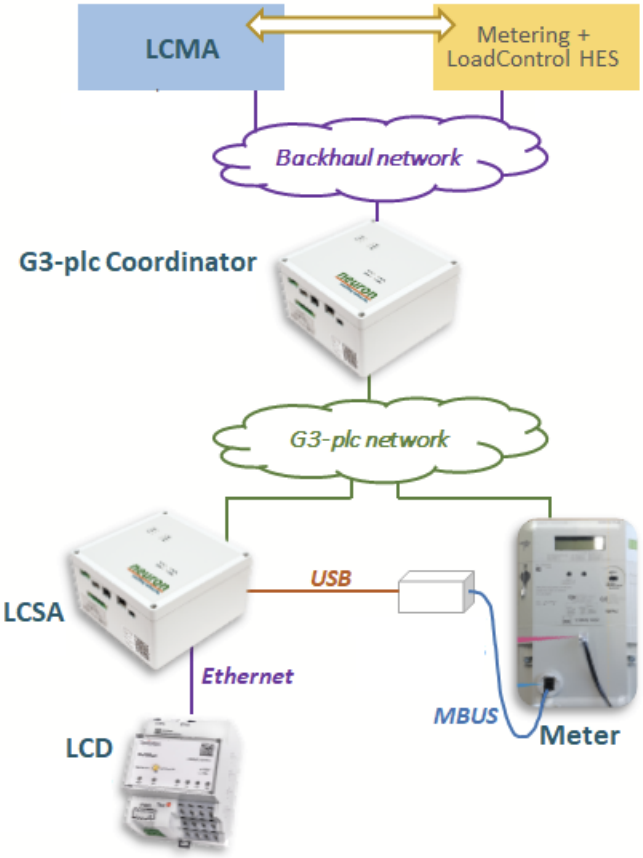


Figure 18: Overview of the system in OrtsNetz. The G3-plc coordinator is the gateway installed in the TSs. This device connects the G3-plc network with the internet and finally with the cloud, where the LCMA runs and sets the prices and switching commands.

### 3.4.4 Community electricity storage

The community BESS was installed by the end of November 2023. The installed BESS is a Pixii PowerShaper 2. The battery has a capacity of 48 kW h with a power of 50 kW.

### 3.4.5 Algorithms in the field

The cloud infrastructure was set up to control and monitor the EVs. Furthermore, the infrastructure for the price setting agent, the DLC optimization problem, the ToU algorithm, and the BESS algorithm were set up.

On the LCSAs, the algorithms were extensively tested on a test setup at EKZ and then deployed to the customers. The software includes a trained model for each combination of EWH size and HP. During the project, individual scripts could be updated via remote connection. However, remote updates proved to be challenging whenever the data volume to be transferred via PLC was large.

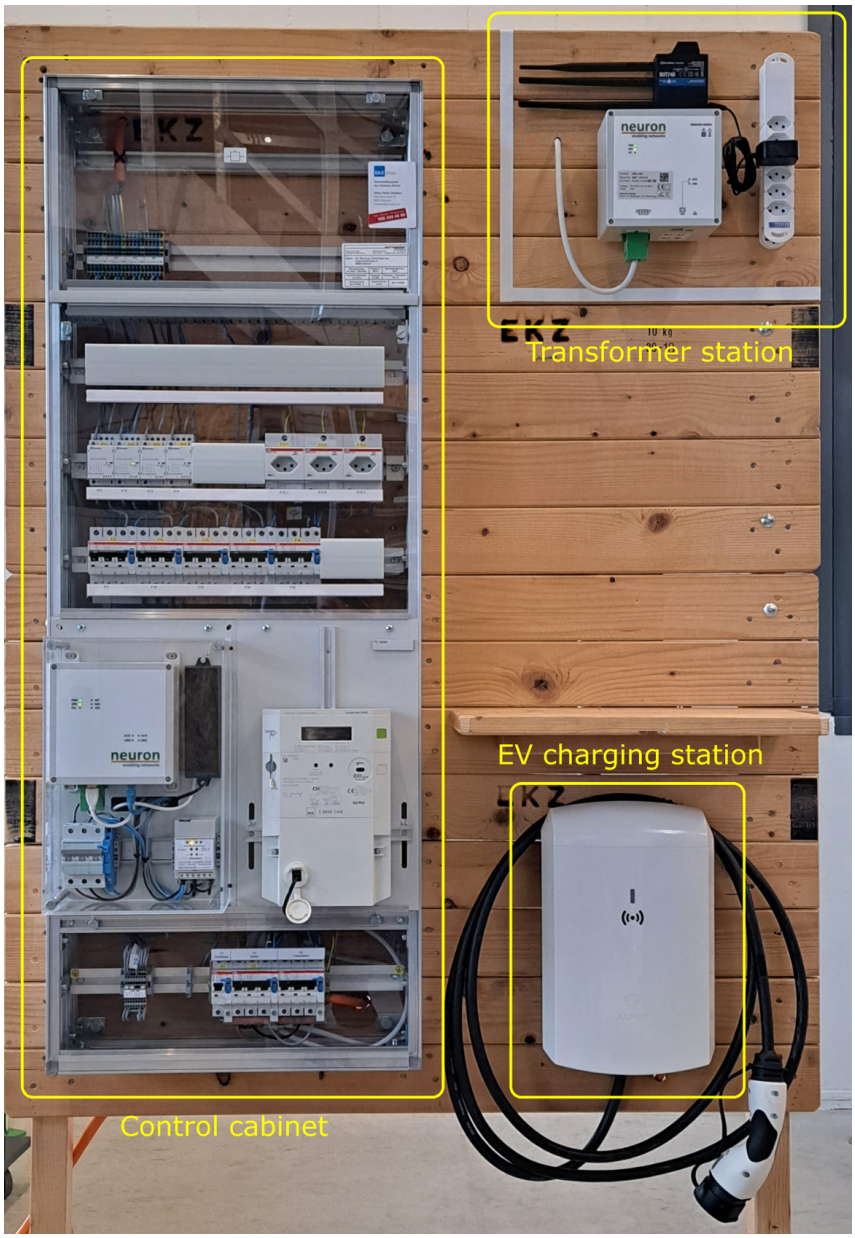


Figure 19: Test setup at EKZ. The EV charging station is not controlled via the LCSA. In the control cabinet, the LCSA is on the lower left side and the SM on the lower right side.

## 3.5 Baseline load estimation in automated load control

In OrtsNetz, we aimed to reduce injection and consumption peaks seen at the TS level. Therefore, the evaluation should focus on how much the proposed schemes help to flatten the total TS demand. However, the acquisition of new devices, replacement of technologies, adoptions of EVs, and new PV installations indicate that we cannot simply compare the TS demand before and during the pilot. Such a comparison is inadequate because changes in the TS demand exogenous to the project would affect our analyses and conclusions.

To evaluate the performance of the proposed schemes in the pilot phase, we must first estimate a baseline load, i.e., the TS demand profiles if the OrtsNetz project was not implemented. For this, we leverage historical data of weather and SM load profiles to a) identify first the most similar days to those of the pilot

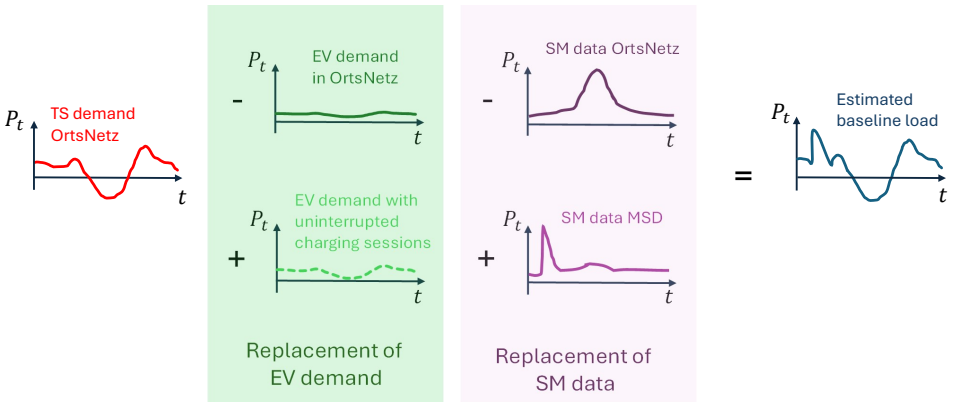


Figure 20: Procedure for estimating the baseline load for a given pilot day.

phase and then b) adjust the actual TS load profile during the pilot day with load profile replacements.

### 3.5.1 Identification of Most Similar Days

For any given day in the pilot phase, we identify the Most Similar Day (MSD) before OrtsNetz using two approaches:

**Weather** Using historical 15-minute weather data of temperature and global radiation, we use the score defined in (11) to identify the most similar day to that of the pilot phase. The day with the lowest dissimilarity is considered the MSD.

**Control group** For the automated load control, the control group consists of the customers in Winkel who did not participate in the project, i.e., did not receive a new tariff. Only Single Family Homes (SFHs) with an EWH or HP and without electric storage heating or EVs are considered. To identify the MSD to that of the pilot phase, we compare the total load profiles of the control group before and during OrtsNetz. For a given day in the pilot phase, the corresponding MSD is the one with the most similar load profile, based on the Euclidean distance.

### 3.5.2 Replacement of load profiles

Figure 20 depicts the procedure to estimate the baseline load profile for a given pilot day. This procedure is applied per TS. The baseline load is estimated as the actual TS load profile, minus the load profile of the EVs during the pilot[4], plus the load profiles of those EVs assuming uninterrupted charging, minus the load profiles of participants[5] on the pilot day, plus the load profiles of those customers on the corresponding MSD. The replacements in Fig. 20 aim to estimate the total TS demand without OrtsNetz running.

The following customers are excluded from the replacement of SM data:

- Customers with a change in energy consumption higher than 30 %. This prevents large demand changes of customers from distorting the baseline load profile, e.g., due to the installation of a new HP.
- Customers with storage heating. This exclusion is only applicable when estimating the baseline load for a winter day. It prevents storage heaters from adding large demand mismatches between the pilot day and the MSD to the baseline load.
- Customers with PV systems. This avoids distortions of the baseline load due to mismatches of PV power injections caused by unequal irradiation conditions between the pilot day and the MSD.

[4] In the TS corresponding to the DLC, only the EV charging sessions that took part in the DLC are considered.
[5] These are customers with an OrtsNetz load control device that participate in the corresponding OrtsNetz scheme: ToU tariff, Dynamic tariff, or DLC.

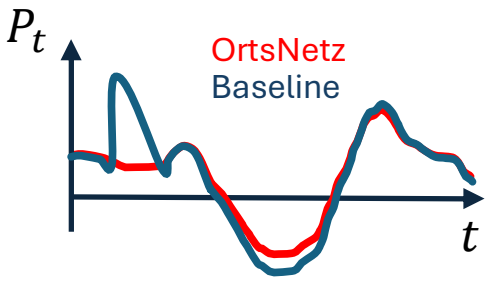


Figure 21: Comparison of TS demand and corresponding baseline load.

This exclusion is only applicable when estimating the baseline load for a summer day, i.e., when the focus is on injection peaks. In winter, these customers are also considered in the load profile replacement. However, for PV installations that were not present on the MSD yet, a PV profile from Winkel is scaled to match the observed peak power and added to the baseline load profile.

After this procedure, the TS demand profile during OrtsNetz can be compared with the corresponding baseline load, see Fig. 21. The comparisons in Section 4.2.4 follow this procedure for reporting the peak reductions during the pilot.

# 4 Pilot phase results

This section summarizes the pilot results, including the customer behavior analysis and the evaluation of the automated load control schemes. Key takeaways are highlighted throughout by blue vertical bars.

## 4.1 Customer behavior

In this section, we present the customer sign-up and participation behavior observed throughout the project.

### 4.1.1 Customer recruiting and sign-up

The OrtsNetz tariffs described in Section 3.1.1 were offered to a total of 646 participants in Winkel, of which 31 chose to opt out. The three automatic control settings were distributed across three selected TSs. Table 2 lists the number of customers that received an LCD, as well as the additional customers with an EV or without automatic control. The latter are part of the same control scheme and tariff, but are not necessarily located at the same TS. The table counts all customers with an EV that showed interest in the project. As will be discussed in Section 4.1.6, not all of the vehicles ended up being optimized.

Table 2: Number of participants by tariff.

| | LCD | EV | No automatic device | |
|---|---|---|---|---|
| | | | Opt-in | Not opt-out |
| Direct control | 22 | 19 | 20 | 32 |
| Time-of-Use | 13 | 2 | 103 | 141 |
| Real-time | 29 | 21 | 112 | 138 |

**Opt-in vs opt-out recruiting** OrtsNetz featured a dual recruiting strategy. Initial customers were reached by opt-in, while later a share of participants was recruited by an opt-out strategy.

The project was announced in summer of 2021 by letters sent to 1993 customers of EKZ in Winkel. Over the course of the following two years, a total of 258 (12.9 %) signed up to the project by opt-in through a web form or by signing up on the web platform. Apart from the letters, the project was also repeatedly featured in the local newspaper and on various community events (cf. Section 7). This way, also customers who did not receive an initial letter might have been reached for opt-in participation.

In the summer of 2023, the opt-out recruiting strategy was introduced. A selected group of 368 customers that had not signed up yet were informed by letter that they would receive a new tariff by default, with the possibility to decline. Out of these, only 11 (3.0 %) opted out, indicating a generally high participation rate. Here, the best-accounting policy must be kept in mind, which ensures that participants can only save costs with the project. This may significantly impact the willingness of customers to participate in the project.

Combining these recruiting strategies leads to different kinds of participant groups. In the following we distinguish the groups “Opt-in”, “Not opt-out” and “Non-participant” (as a control group), which are characterized in Fig. 22 and 23. The average yearly energy is calculated based on smart meter data for the year 2022 (before project start). The installation type and operand information is based on metadata available to EKZ for each household. Each installation is separately metered, but a customer can have multiple installations. For example, heat pumps can be listed as a separate installations if they are metered separately from the rest of the household. Operands are any larger appliances present at an installation that need to be registered with the utility. Therefore, heat pumps can alternatively appear as operands if they are connected to the same meter as the rest of the household. Since customers have to inform the utility about changes in operands, this data may not be fully up to date or complete.

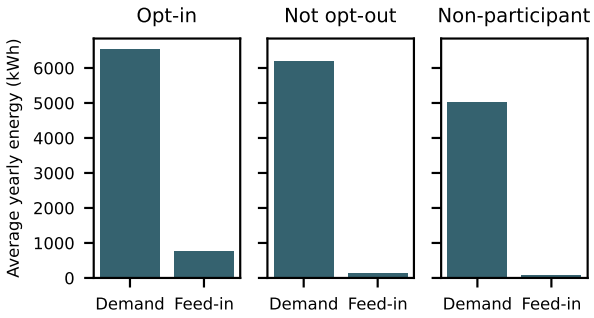


Figure 22: Average yearly energy demand and feed-in among the different customer groups before the project start (2022). Opt-in participants have substantially more PV feed-in. This aligns with the extra incentive for selling excess PV power to the neighborhood. Both participant groups have higher annual consumption on average. This is caused by the targeting of specific TSs with a particularly high share of SFHs.

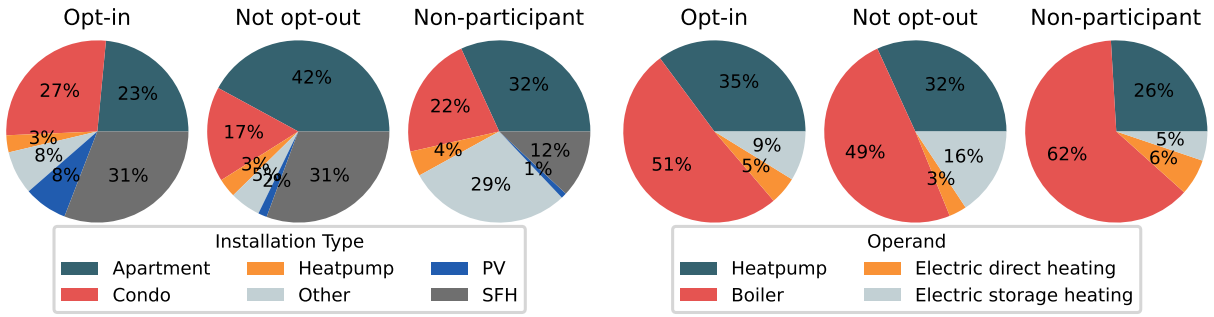


(a) Share of different installation types among each group. A customer can have multiple installations (e.g., SFH and PV).

(b) Share of operands among all installations in each group.

Figure 23: Characteristics of the customer groups. Participants have a disproportionally high share of SFHs and HPs as these were targeted for the installation of LCDs. Opt-in participants have a particularity high share of PV.

We observe that Opt-in participants have generally higher consumption and substantially more feed-in (Fig. 22). This is to be expected due to the special incentive for participants with PV, who could sell their excess production to neighboring households for an extra bonus (cf. Section 3.4.1). This observation also aligns with the much higher share of SFHs in the Opt-in group (Fig. 23(a)) compared to the Non-participants. Furthermore, in the operands (Fig. 23(b)) this manifests in an above average share of HPs, which are more common among SFHs, and a correspondingly lower share of EWHs.

The Not opt-out participants also feature above average energy consumption, higher share of SFHs and HPs (compared to Non-participants). This is caused by the way in which participants for the opt-out study were selected. The selection targeted all customers at the three TSs chosen for automatic control, plus one additional TS. In turn, these TSs were originally chosen because of their above average share of SFHs with the goal of reaching as many customers eligible for an LCD as possible.

- 12.9 % customers targeted by opt-in actively signed up for participation. Disproportionally many of these have a SFH, HP and PV with accordingly high electricity consumption and feed-in.
- 97 % of customers targeted by opt-out passively participated by not opting out.
- A large difference in participation rate is expected between the two recruitment groups. Accordingly, the recruiting strategy has to be taken into account when interpreting study results.

**Installation of LCDs** The LCDs were installed in fall of 2023. Of the 117 households applicable for automatic load control, 14 opted-out (12 %). Installers visited the remaining 103 customers. However,

only 64 devices (62 % of attempts) could be installed due to space constraints in the electrical panel or other technical reasons. Therefore, we conclude that customers are generally open to automatic load control, but the sizing and technical characteristics of the LCDs are more decisive for successful installation. While the prototype device employed in the project could not be installed in many cases, a fully developed commercial product should be more compact and fit in the standard space available.

**EV recruiting** Recruiting of EV participants started in March 2023. The Federal Roads Office (FEDRO) provided a list of all plugin vehicles (battery electric vehicles and plugin hybrid electric vehicles) registered by inhabitants of Winkel. Out of a total of 206 vehicles, 143 were fully supported by the provider of the API interface that allows to control the charging process (exactly 100 of which are battery electric vehicles). Recruiting was done by letter, which provided project information and a link to the EV sign-up platform through which vehicles could be connected to the OrtsNetz system. To incentivize participation, the letter advertised savings of around 100 CHF/year on average. This amount corresponds to average driving demand and shifting of all charging to the lowest tariff times. Naturally, the exact savings highly depend on real driving demand and general household electricity consumption. To protect residents' privacy, the letter was sent by FEDRO in the name of EKZ to all inhabitants of Winkel that own a plugin vehicle.

Overall interest in the EV study has been high. Within the first two weeks, 221 page visits were registered and 50 unique email addresses were entered into the system. Over the course of the year a total of 76 unique customers registered on the portal. However, out of these only 42 ended up actually linking a vehicle. This can in part be explained by the lack of support for specific vehicle vendors (we received messages from multiple customers asking about their vehicle). Furthermore, throughout the project some customers had to deregister their vehicles (e.g., not charging at home, not residing in Winkel, sold vehicle).

> Initial interest in EV smart charging was high (over 30 % of targeted vehicles), but participation was limited by technical support of vehicles.

### 4.1.2 Manual reaction to new tariff signals

In this section we explore the changes in energy consumption observed from households without any automatic load control. These can be seen as manual load shifting or energy savings caused by participants directly changing their energy usage behavior. We specifically focus on the differences in changes observed for the Opt-in and Not opt-out participants and compare them to the Non-participant group.

For these manual reactions we exclusively analyze apartments and condominiums without large appliances like electrical heating or EV charging stations. Such large appliances typically overshadow the remaining energy consumption of a household, while their change is more related to weather condition and changes in driving demand. Instead, in this analysis we are interested in the changes in electricity demand behavior directly caused by customers.

Figures 24 and 46 (in the Appendix) show the changes in the household power profiles from before to during the project. Specifically, for each household the average power profile is calculated for the winter (October to April) and summer (May to September) seasons before and after project start. The difference is then calculated for each household separately and the graphs show the median (solid line) and quartiles (shaded area) across households. The shaded background indicates the value of the ToU tariff at the respective time, the darker the shading, the higher the tariff. The figures furthermore show box plots of the distribution of the profiles averaged over the time dimension. The "Total" box corresponds to the change in average daily consumption, while the "Critical" box only accounts for the average across specific hours of the day. These are the hours with the highest (winter) respectively lowest (summer) tariff (cf. shading in the power profile plots).

We start with discussing the results for the ToU tariff in the winter period (Fig. 24(a)) where the price signals are the most simple and clear. While the control group does show changes in consumption for some households, these are symmetric around zero and the median falls very close to zero throughout the day. In contrast, the profile for the Opt-in participants shows a clear decrease in power consumption

towards the afternoon and evening hours, especially dominated by certain households (cf. shaded quartiles), but also visible in the median. This is confirmed by the box plots for the total, and especially for the critical power consumption. Note that these changes are generally small on the order of tens of Watts per household, corresponding to a few percent. While normalization with the baseline consumption can lead to strong outliers in the percentage changes, for completeness we include the graphs in Fig. 46 in the Appendix.

To quantify these findings, we perform a one-tailed Mann–Whitney U test which shows that the change is significantly larger in the Opt-in group compared to the Non-participants ($p = 0.06$ for the total change and $p = 0.01$ during the critical period). Thus, we can conclude that Opt-in participants not only significantly reduced their power demand during the high tariff period compared to Non-participants, but even outright saved energy throughout the day. The latter effect may be attributed to an increased awareness of energy consumption due to the project.

In summer we observe a slight reverse of the effect during the low tariff period (Fig. 24(b)). Opt-in participants increase their power consumption, making use of the cheaper electricity. This effect is however much smaller and not significant compared to the Non-participants, who also increase their consumption compared to the previous year, especially toward the evening. The latter observation might be related to a difference in air conditioning demand, which is generally on the rise [22].

The Not Opt-out group shows a less clear trend. While the power profile does show a slight dip during the high tariff period in winter, this effect is not significant compared to the Non-participants. On the contrary, the effect of the Opt-in participants compared to the Not Opt-out participants is (slightly) significant ($p = 0.07$ for total and $p = 0.09$ for critical power). This shows that the main effect in manual response to the tariffs is caused by Opt-in participation and not by the tariffs themselves. This has major implications for the applicability of time-varying tariffs. While pilot projects and Opt-in offers may find a substantial response to new tariffs, based on our findings, we expect a much lower impact on the power consumption in the broader public.

Conducting the same analysis for participants with the dynamic tariff (cf. Fig. 47 and 48 in the Appendix) reveals a similar trend. Especially in summer it is however less clear and the increase in power is not significant. This can be attributed to the more difficult and less predictable price signal. In contrast, for the ToU tariff it is easy to remember that the price always goes up/down at a certain time.

- Average changes in energy consumption are generally low, in the range of a few percent.
- Opt-in participants reduced their energy consumption significantly more than Non-participants and Not Opt-out participants, both during high tariff periods and throughout the day.
- In consequence, the recruiting strategy has a bigger influence on the change in consumption behavior than the new tariff.
- While pilot projects and Opt-in offers may find a substantial response to new tariffs, based on our findings, we expect a much lower impact on the power consumption in the broader public.

### 4.1.3 Costs and savings

In this section we analyze the financial savings incurred by the participants. As mentioned, the project featured a best-accounting policy that allowed participants to reduce their electricity bill, if their costs were lower under the new tariff compared to the normal EKZ tariff. However, if their costs were higher, this was not billed to them. The policy was applied on a per day basis and independently for the grid and energy components of the tariffs. A customer might have incurred additional costs under the new energy tariff by increasing their demand during what used to be a low tariff period (e.g., late at night in winter, cf. Fig. 4). Simultaneously, they may have made savings due to the lower grid tariff at that time. In this case, the extra costs were ignored, and only the savings were accounted on their bill. Similarly, additional costs on one day did not cancel savings on another day.

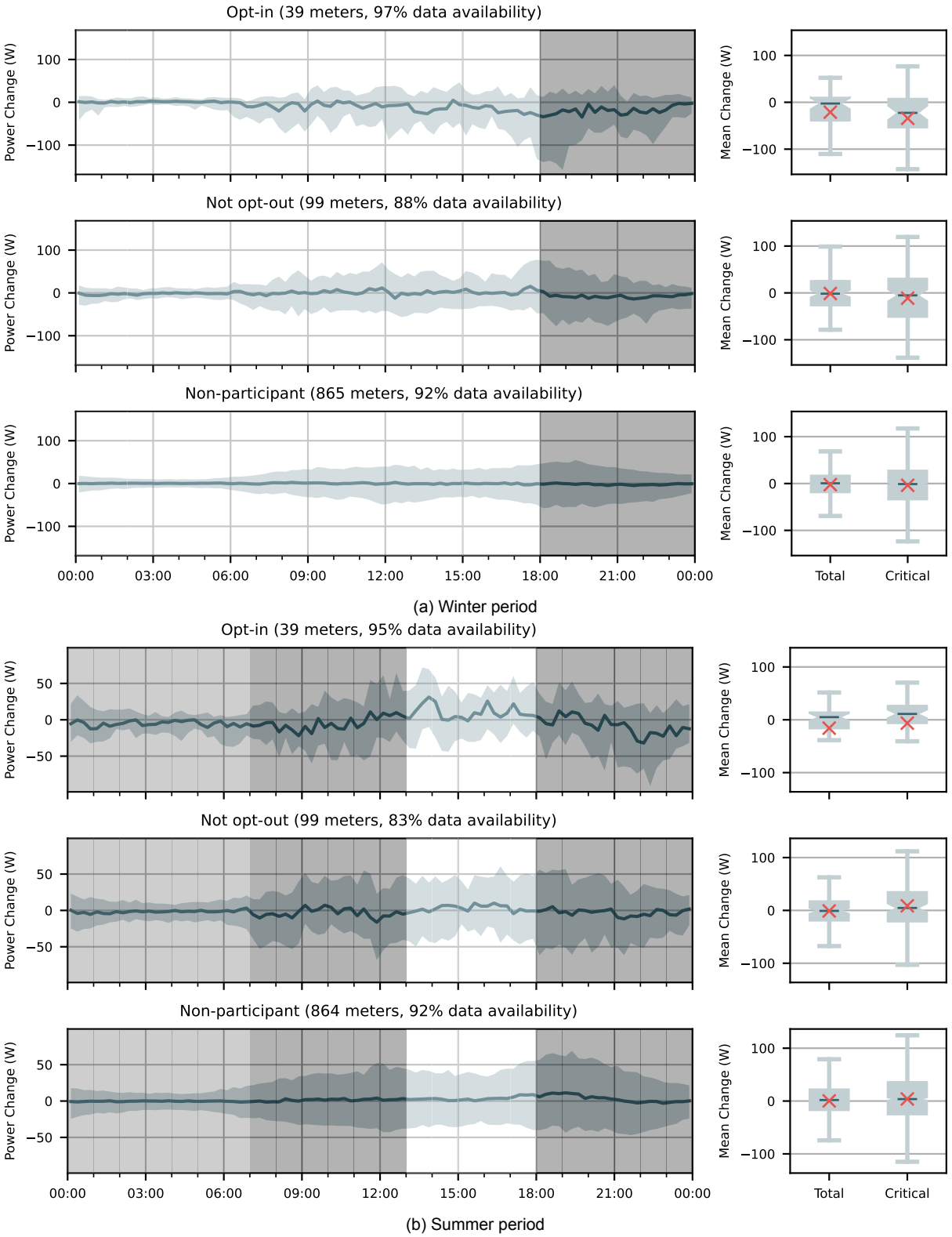


Figure 24: Manual response in power consumption of customers with the Time-of-Use tariff. The change in the average power profile is calculated from before to after the project start within the winter (a) and summer (b) tariff period. Solid lines show the median across households and shaded areas the quartiles. The box plot labeled “Total” represents the average across the whole day, the one labeled “Critical” the average across the hours with the highest/lowest (winter/summer) tariff. Crosses represent the mean, lines the median.

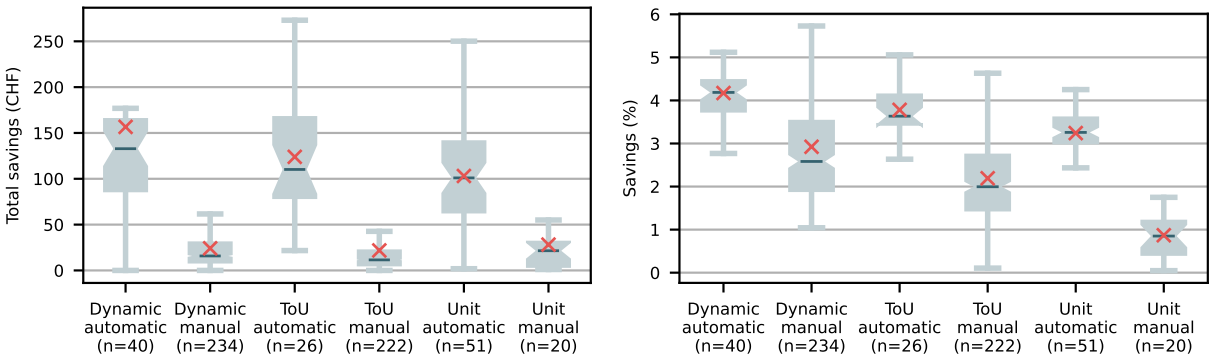


(a) Total savings

(b) Relative savings

Figure 25: Total and relative savings of customers in the different participant groups. Crosses represent the mean, lines the median. n indicates the number of participants in the respective group. Absolute savings are substantially higher for customers with automatic loads, as these have a higher energy consumption. Relative savings account for this and are comparable between groups, while still showing a significant spread between customers within a group.

The distribution of the resulting total savings per customer is shown in Fig. 25(a) for the different participant groups. Generally, savings spread quite a lot between different participants even within the same tariff group.

On average, customers with automatic loads incurred substantially higher savings. Looking at the relative savings (Fig. 25(b)) shows that this effect is mostly caused by the overall higher demand of participants with automatic loads. Furthermore, another factor increases this effect. The project duration was extended by three months for those customers connected to a TS with automatic load control. Therefore, all of the customers with automatic load control accumulated savings for longer, while only a small number of customers without automatic loads (only those physically connected to the three TSs) had this opportunity. In the relative savings this effect is corrected for.

Savings are particularly low for customers with the unit tariff and no automatic loads (average below 1 %). These customers received the standard EKZ grid and a new unit tariff for the energy component that was specifically designed for cost recovery (cf. Sec. 3.1.2). This group only existed because not all customers at the TS were eligible for automatic load control, but all customers within the same TS should receive the same price signal, such that the TS load measurement reflects the response to one specific price. On average, these customers should not incur any savings. Savings on one day should be canceled by extra costs on another. Thus, the small savings observed in reality can be attributed to the effect of the best-accounting policy.

- Average savings are substantially higher among participants with a Load Control Device.
- Relative savings vary widely between participants but are comparable across different tariffs. This implies that monetary incentives, while implemented differently, were similar for the three control schemes.

### 4.1.4 Survey responses

In the following we present the findings from the final participant survey conducted at the end of the project. For participants at the three TSs with automatic control, the project was extended and ended in December 2024. For all other participants the project already ended in September 2024. Correspondingly, participants were contacted by letter (that included a personalized link and QR code for the survey) in October and December respectively. Non-respondents were reminded by email with a personalized link about four weeks later.

Figure 26 shows the cumulative responses over time colored by communication medium. The results demonstrate the effectiveness of the email reminder compared to the letter. In total, the survey received 95 responses.

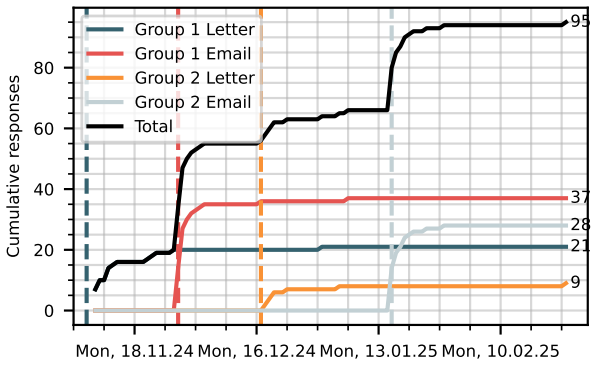


Figure 26: Cumulative responses to the final participant survey by communication medium.

Figure 27(a) presents the responses to the questions asked on a 5-point Likert scale. The majority of respondents were satisfied or very satisfied with the project as a whole (57 %). Furthermore, most respondents agree or strongly agree that a utility should offer novel tariffs comparable to the ones in OrtsNetz (75 %). About half found the OrtsNetz tariffs to be comprehensible or very comprehensible (49 %). Happiness and comprehensibility were slightly higher among respondents with the dynamic tariff compared to the ToU tariff. However, a Mann–Whitney U test for the difference in Likert score shows no clear significance ($p = 0.16$). A point of discontent among participants is the amount of savings during the project, with only 35 % agreeing that the the amount was appropriate, versus 39 % disagreeing.

Of the respondent with a time-varying tariff, 57 % say they attempted to shift demand to times with a lower tariff. Most state to have shifted the use of the dishwasher and washing machine, followed by lighting (Fig. 27(b)). Less than 20 % say they have shifted the consumption of heating and hot water production.

To conclude this section, we discuss the differences in responses between Opt-in and Not Opt-out participants. Unsurprisingly, significantly more Opt-in participants responded to the survey (22.1 % vs. 6.2 %, $\chi^2$ test: p<0.001). Furthermore, according to a Mann–Whitney U test, a significantly higher share of Opt-in respondents states to have shifted consumption ($p = 0.04$). Lastly, the survey included the standard catalog of ten questions for the System Usability Scale (SUS) [23]. A Mann–Whitney U test shows a significantly higher usability score $S$ for Opt-in ($S = 71$, $n = 33$) than for Not opt-out ($S = 51$, $n = 14$) respondents ($p < 0.001$).

- Survey respondents support the introduction of novel tariffs, but expect substantial savings.
- Opt-in participants are more engaged with the project in terms of survey responses (22.1 % vs 6.2 %) and stated load shifting.
- This finding is expected since Opt-in customers actively signed up for the project and were likely more interested in participation.

### 4.1.5 Platform logins and solar market bidding

As a final data source for participant behavior we analyze the login behavior on the OrtsNetz platform. The platform was already available in 2022 for voluntary trading of certificates of origin (cf. Section 3.4.1). As an indicator for the engagement with the new tariffs, we calculate the share of participants who logged into the platform at least once during the tariff phase, i.e., since October 2023. This fraction is much larger among Opt-in participants (34.5 %) compared to Not Opt-out ones (5.6 %). Furthermore, among those who did log in, the average number of logins during 2024 is higher for Opt-in than Not Opt-out participants (4.4 vs. 3.8 ).

This increased engagement can also be seen from the bidding behavior for the voluntary purchase of certificates of origin. Among the Opt-in participants 44 % set at least one bidding price and 33 % made

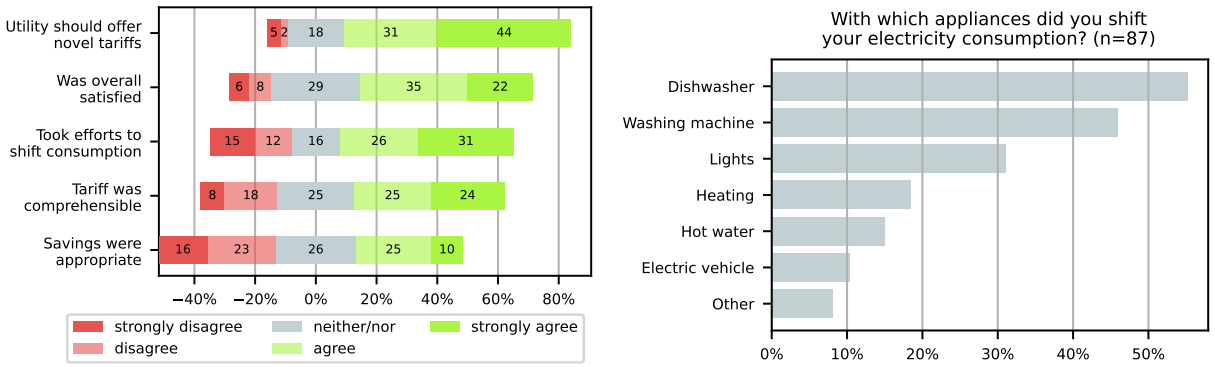


(a) Results for the questions asked on a 5-point Likert scale. The exact wording of questions is listed in the Appendix 10.4.

(b) Share of respondents that state to have shifted the electricity consumption of a specific appliance.

Figure 27: Results for the final participant survey.

at least one adjustment. This compares to only 4 % with one bidding setting and 0.3 % with at least one adjustment for the Not Opt-out participants. Among the bidding participants, those from the Opt-in group made an average of 5.1 adjustments and set an average monthly bidding budget of 20.4 CHF compared to only 1.0 adjustment and an average budget of just 0.99 CHF. Thus, we can conclude that Opt-in customers not only showed much higher engagement with the project in terms of platform interactions, but were also willing to spend substantially more on local PV energy.

> Opt-in participants are significantly more active on the web platform and the voluntary market for certificates of origin.

### 4.1.6 EV charging and customer engagement

In this section we describe the behavior of customers with EVs participating in smart charging. We analyze both their interaction with the EV platform as well as their general vehicle plugin and charging behavior.

**EV platform** As described in Section 4.1.1, initial interest in the EV smart charging offer was very high. After registration and linking of a vehicle, the OrtsNetz system received status updates including charging information that will be analyzed in the following section. Once the EV platform and optimization algorithms were finalized, users with vehicles were prompted to activate the system by setting a desired departure time at which they require their EV to be fully charged (cf. Fig. 28).

Compared to the initial interest, final participation in smart charging was rather low. A total of 31 customers (41 % of initial sign-ups) set a departure time at least once. Many customers were not reachable by email, letter, or an in-person visit. Figure 29 visualizes the activity among those customers who did log in at least once. The histograms show the average count of days per week on which one of the three main actions on the EV platform was taken. We focus on the days with actions instead of the number of actions, because customers tended to perform multiple actions in rapid successions (e.g., change the departure time a few times within a minute). Most customers logged in less then once a week. A substantial share of customers only logged in once at the beginning of the project. Similarly, customers updated the next departure time less than once a week, with many setting the value only once. The platform also featured an “Instant charge” button that allowed to override any smart charging and ensure that the vehicle charges directly as soon as it is plugged in. This feature was used very scarcely, with only 10 customers using it more than once. The button could be pressed at any time, even if the vehicle was not plugged in, and would disable the smart charging system for the next 12 h. In total, only 13 actual charging sessions were affected by instant charging.

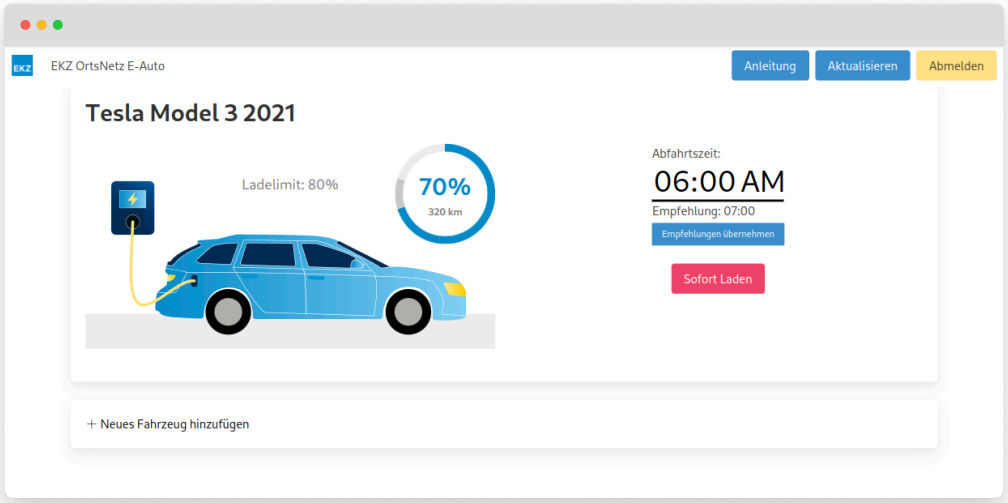


Figure 28: Screenshot of the EV platform for linking of vehicles and setting the departure time.

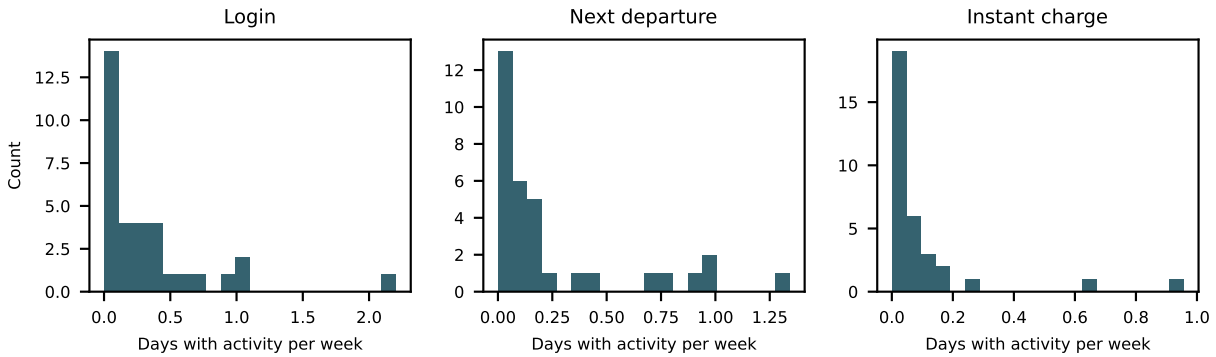


Figure 29: Distributions of days per week with one of the three major actions — login, setting of next departure, and instant charging — available on the EV platform across vehicles.

**EV charging** In the following, we present findings from the general charging behavior observed during the project. The impact of smart charging with one of the automatic load control schemes is discussed in Section 4.2.4.

EV data is available in the form of regular events received from the web API and includes information on the SoC, charging status, and location. From these events, we derive a dataset of plugin and charging sessions, characterized by the time of plugin and plugout, respectively, charging start and stop. The full dataset includes all vehicles that were linked to the system, even those that were not optimized during the project. We exclude sessions with a duration of less than 10 minutes or more than 14 days, as these are not relevant for typical charging behavior. Furthermore, we mostly focus on sessions for which the vehicle was known to be located at the home charging station, as we are interested in residential charging behavior. We classify the remaining sessions as “Other”, however this does not necessarily mean they were not at home. For some vehicles, no location information is available, but they may still have been at home. The final dataset includes sessions from 55 unique vehicles in the range from March 2023 to December 2024.

Firstly, we study the average charging behavior. The per vehicle probability of being plugged in at home (Fig. 30(a)) shows a clear plateau of 25 % at night that lasts into the morning hours (blue). Here the profile is averaged over vehicles, where vehicles with less than 10 days of data are excluded. Compared to the plugins, the charging probability peaks earlier in the evening at below 10 % and drops throughout the night (red). In contrast, the “Other” sessions peak throughout the day and are lower at night. The steady value at night is likely due to missing location information of vehicles that are actually at home. The ratio of charging time to plugged in time (Fig. 31(a)) gives further insight into the potential of postponing charging and thus shifting grid load. Vehicles are plugged in much longer than they charge. Only for 17 % of sessions the vehicle charges for the whole time it is plugged in (“hot-unplug”). In half of the sessions, vehicles are plugged in at least three times longer than they charge.

From a session’s average charged energy, the mean charging power can be calculated, which allows to determine the average per vehicle power demand at a given time of day (Fig. 30(b)). These profiles demonstrate the significantly lower average charge rate for residential charging (blue) compared to away-from-home (public) charging (red). The steady power demand of “Other” charging at night is most likely caused by missing information on the home location and not by vehicles actually charging away from home at night.

To further understand plugin behavior, we investigate the relation between the times of day of vehicle plugin and plugout (Fig. 32). The dependency shows clearly distinct clusters. Most sessions start in the evening between 16:00 and 20:00 and end in the morning between 6:00 and 9:00 (top and right insets with marginal distributions). The joint distribution reveals that these sessions typically last over night from one day to the next (red). Additionally, there is a smaller subset of sessions that start some time throughout the day and mostly last into the early evening around 17:00 to 18:00 (blue). Finally, only very few sessions last for more than two days (orange). These observations suggest two types of charging requirements, long over night sessions and shorter daytime sessions where the vehicles are required on the same day they are plugged in.

Finally, we focus on only those sessions for which a user has set a desired departure time (during the smart charging phase) and observe the delay between configured time and plugout (Fig. 31(b)). In most of the cases, the vehicles was unplugged within one or two hours of the configured departure time. This indicates that users were quite good at stating when they require their vehicle, but leave a small safety margin. Only in few cases was a vehicle unplugged before the set departure time.[6]

[6] No case can exist for unplugging more than 24 h before the departure, because each specific departure was determined for a specific day. If a vehicle was unplugged 24 h before, it would have needed to be plugged in more than 24 h before, thus the departure would have been calculated for the previous day.

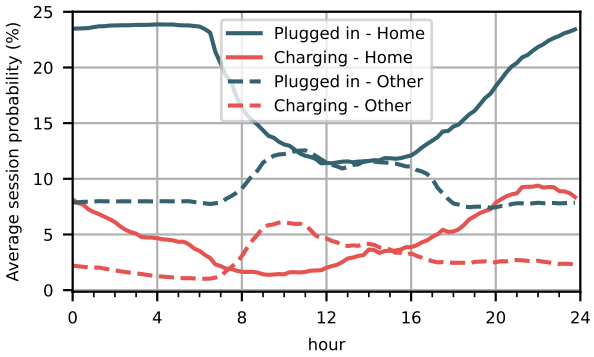


(a) Plugged in and charging probability profiles averaged across vehicles.

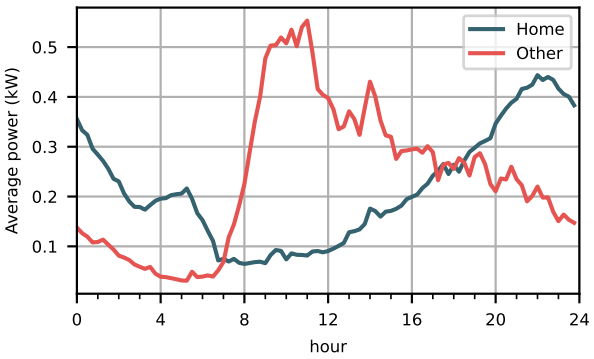


(b) Average per vehicle power demand profile for sessions with and without at-home location information.

Figure 30: EV plugin and charging profiles. Vehicles are more likely to be plugged in than actually charging (a). Especially during night at home, vehicles remain plugged in until the morning while few are still charging. The average at-home charging power per vehicle is rather small below 0.5 kW, compared to a much higher power during day times for not-at-home charging.

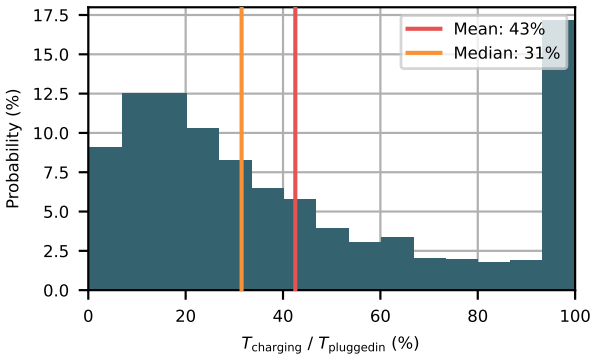


(a) Distribution of the fraction of time a vehicle is charging $T_{\text{charging}}$ to the time it is plugged in $T_{\text{pluggedin}}$ across all sessions.

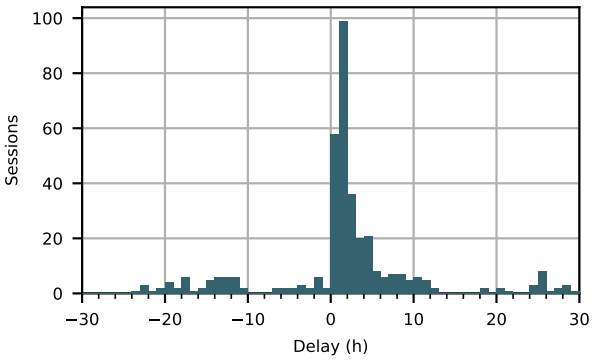


(b) Distribution of the difference of user defined departure time and vehicle unplugging time. The figure is cut at ±30 h as most data falls in this range.

Figure 31: Statistics on the duration of charging, plugin, and user configured departure of EVs.

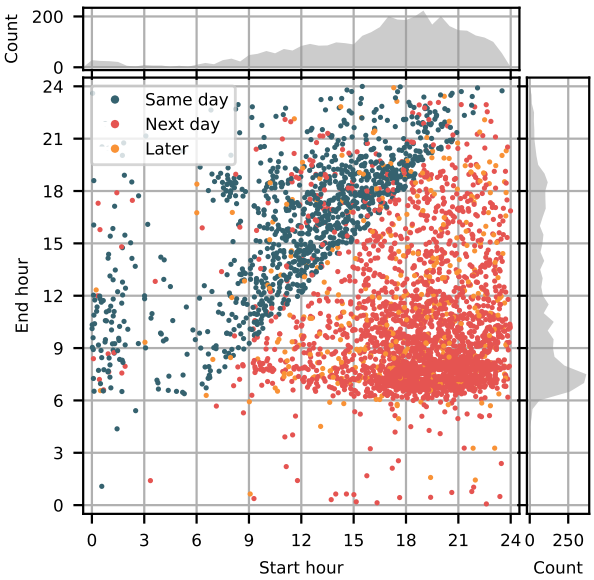


Figure 32: Dependency between vehicles plugin and plugout times. The insets show marginal distributions of plugin and plugout throughout the day. Two distinct clusters are visible. Most vehicles are plugged in during the evening and unplugged the next morning (red). Another set of sessions last for a few hours within the same day (blue). Few vehicles are plugged in more than a day (orange).

- EVs are typically plugged in much more than they are charging (peak of 25 % plugged in vs. 10 % charging). Especially in the early morning hours, vehicles remain plugged in at home while few are charging. In half of the cases, vehicles charge less than a third of the time they are plugged in (median 31 %, mean 43 %).
- EV smart charging participants scarcely used the platform to check or adjust their departure time (less than once a week).
- As long as it technically functions, smart charging rarely affects participants and vehicles remain available for driving needs. Only 13 charging sessions were affected by customers overriding the smart charging system.

## 4.2 Automated load control

In this section, we present the pilot results regarding automated control of EWHs, HPs, and EVs and provide further insights based on simulations. The results for the BESS are presented separately in Section 4.3.

### 4.2.1 ToU tariff

The ToU tariff was applied in the Angel TS. In this scheme, 10 EWHs and 8 HPs with nominal powers from 2.2 to 8.1 kW and 2.4 to 9 kW, respectively, were controlled according to the profiles presented in Section 3.3.3. The control was active from 14 November to 13 December 2023 and from 18 January to 19 December 2024, excluding May 2024. A technical issue on 5 out of 13 LCSAs was fixed on 17 July 2024. Additionally, 2 EVs were controlled according to the ToU tariff scheme. The highest net consumption at the TS in 2024 was 328 kW on 20 January, while the highest injection peak was 207 kW on 17 July 2024.

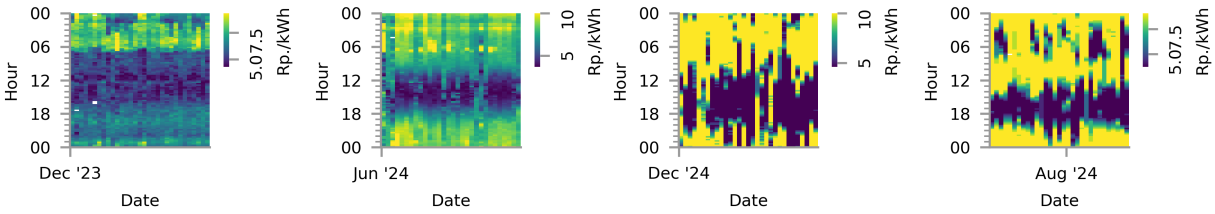


(a) Winter, proportional. (b) Summer, proportional. (c) Winter, RL agent. (d) Summer, RL agent.

Figure 33: Dynamic real-time prices. Each heatmap shows the grid tariff values for one month.

### 4.2.2 Dynamic tariff

The algorithms for the real-time tariff setting presented in Section 3.3.2 were deployed at the Geeren TS. In 2024, the peak demand at this TS was 316 kW on 20 December and the highest injection peak was 201 kW on 18 September. The price was proportional to the estimated inflexible load from October 2023 to June 2024, and the DSO RL agent was deployed starting from 2 July 2024. Figure 33 shows the price signals for a winter and a summer month and each approach. The high prices during the night in Fig. 33(a) are due to storage heating in the inflexible load estimate. Comparing the two summer months, it is visible that the RL agent reduces the price value at a later time, which is in line with the observation in Section 3.2.3. The customer agents on the LCSAs were functional starting from 27 May 2024. A technical issue on 7 out of 28 LCSAs was resolved on 17 July 2024.[7] In total, 17 EWHs with nominal powers from 1.8 to 8 kW and 26 HPs with nominal electrical powers from 2.4 to 9 kW were controlled. Additionally, 31 EVs were assigned to the real-time tariff scheme, while the number of considered and controlled EVs varied over time. Analyzing the time window from 4 December 2024 to 19 December 2024 for 25 LCSAs, the price values used as input by the local customer agents aligned with the actual value in 99.7 % of the cases (time steps and LCSAs). The verification module changed the EWH and HP commands determined by the local customer agents 5.7 % and 2.9 % of the time, respectively. The following analyses focus on the period with the DSO RL agent.

### 4.2.3 Direct load control

The control scheme introduced in Section 3.3.4 was deployed in Hofacher TS and was fully functional from 29 August 2024 to 19 December 2024. In 2024, the winter's peak demand was 239 kW on 20 January. In summer, the peak injections reached 202 kW on 22 July due to PV power injections. Depending on the date and time of day, up to 19 EWHs with nominal powers from 1.8 to 10 kW, 14 HPs with powers from 2.04 to 7.5 kW, and 2 EVs were considered in the optimization of the DLC. Furthermore, the Gurobi solver was set to return the best available solution within five minutes by limiting the maximum runtime to five minutes.

As explained in Section 3.3.5, the switching commands that resulted from the optimization solutions were verified before being applied to the EWHs and HPs. This was done to filter out invalid DLC commands or communication failures that could result in violations of the EWH and HP flexibility constraints. During the deployment of the DLC, 89.7 % (resp. 90.1 %) of the commands sent to the EWHs (resp. HPs) successfully arrived at the LCSAs. Additionally, the verification changed the EWH and HP commands 16.5 % and 7.2 % of the time, respectively.

### 4.2.4 Comparison of schemes in pilot phase

This section summarizes the results of the project's deployment. A separate analysis is performed for injection peaks in summer and consumption peaks in winter.

**Injection peaks in summer** Table 3 presents the selected dates for evaluating the OrtsNetz schemes in summer. The Before column specifies the range of dates available for selecting the MSDs according to the procedure explained in Section 3.5.1. On these dates, EWHs and HPs were controlled by the ripple

[7] One additional LCSA was deactivated in June 2024. It is not considered in the following analyses.

control. For the ToU and Dynamic schemes, minor changes in the EV charging control were performed during the selected time window. Due to the limited flexibility from EVs in the pilot, the impact is expected to be small.

Table 3: Selected dates in summer for scheme evaluations.

| | Before | | OrtsNetz | |
|---|---|---|---|---|
| TS | Scheme | Dates | Scheme | Dates |
| Angel | Ripple control | 01.06.23 - 14.09.23 | ToU | 18.07.24 - 04.09.24 |
| Geeren | Ripple control | 01.06.23 - 14.09.23 | Dynamic | 18.07.24 - 04.09.24[8] |
| Hofacher | Ripple control | 01.06.23 - 14.09.23 | Direct | 29.08.24 - 04.09.24 |

Figures 34 - 36 present the evaluation of the OrtsNetz schemes for summer days. The demand of HPs is almost negligible during these days, while PV injections largely influence the TS load profile. The upper-left box plots compare the distribution of daily injection peaks in OrtsNetz and the corresponding baseline load profiles with ripple control, according to the weather and control group matching approaches. The upper-right box plots show the daily injection peak reductions with respect to the baseline load profiles. For both types of box plots, the x-axis limits are fixed to the same values across all schemes. In the injection peak box plot, outliers with lower values are cut off to increase readability. The plots on the lower left compare the average TS demand $P^{\text{tot}}$ with OrtsNetz and the ripple control. We also compare the aggregated SM profiles[9] $P^{\text{SM}}$ in OrtsNetz and ripple control. The lower-right plots show the electricity prices, the share of unblocked EWHs, and the TS load comparison on 29 August 2024.

Figures 34(a) and 34(b) show that in the ToU tariff setting, the injection peaks on a TS level were reduced by 2 kW on average. However, the highest injection peak observed in the considered time window (198 kW on 22 July 2024 at 13:45) is comparable to the highest peak in the baseline load profiles. This is visible from Fig. 34(a), where the orange vertical line on the right end represents the OrtsNetz maximum peak across all the considered days. Figure 34(c) illustrates the effect of the OrtsNetz control compared to ripple control. The peaks from 01:30 to 04:00 in the ripple control curve are caused by EWHs. With the OrtsNetz control, this EWH load is shifted from the night hours to the start of the low-price period, creating a peak in the mean daily load profile $P^{\text{SM}}$ of the considered SMs at 13:00. This additional load can reduce the injection peak on a TS level, but may fail to reduce it if the highest peak occurs at a different hour. This is, for example, the case for the day depicted in Fig. 34(d), where the highest net injection in the baseline load estimate occurs at 12:45. Furthermore, both Fig. 34(c) and Fig. 34(d) show that the EWHs primarily operate at the start of an unblocked period, a characteristic that is relevant for all three OrtsNetz schemes.

In the dynamic real-time tariff setting, the injection peaks are, on average, reduced by 4 or 5 kW depending on the chosen matching approach, as shown in Figs. 35(a) and 35(b). In this setting, also the highest peak values were reduced. The lower subplot in Fig. 35(c) shows that the EWH load is again shifted to the afternoon hours, but is more spread out compared to the ToU setting. This appearance in the mean daily curves results from two different effects. First, as the price signal can change from day to day, it can adapt to different load profiles and can incentivize flexible devices to operate at different hours. Second, due to different customer agent models and potential communication issues leading to different inputs, not all EWHs are unblocked at the same time. Figure 35(d) illustrates how the unblocking of EWHs follows the dynamic price signal and that EWHs are unblocked gradually, leading to a more spread out load increase.

The box plots in Figs. 36(a) and 36(b) indicate that the DLC reduced the injection peaks in summer by an average of 4 or 5 kW depending on the matching approach. A closer look at the comparison of $P^{\text{SM}}$ in Fig. 36(c) suggests that greater reductions could have been achieved if the EWHs had consumed more power during the peak PV injection hours. As shown in Fig. 36(d), although most EWHs were unblocked from 9:00 to 17:00, they primarily demanded power in the initial hours after the unblocking

[8] excluding 20.-28.08.24 due to missing TS data.
[9] corresponding to the replaced SMs, as explained in Section 3.5.2.

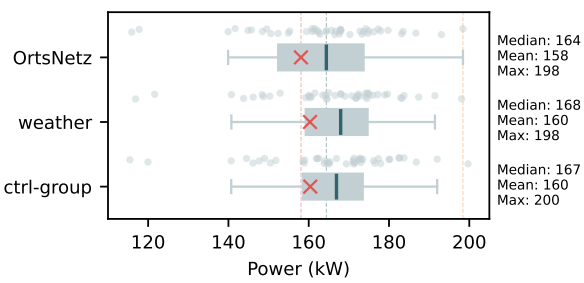


(a) Injection peaks.

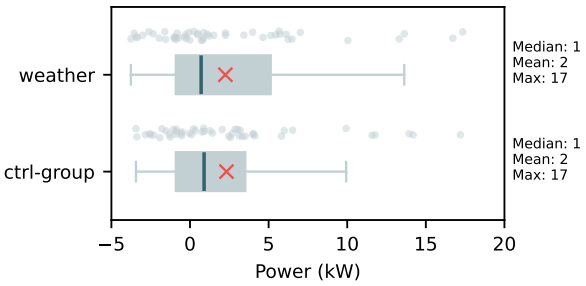


(b) Injection peak reduction.

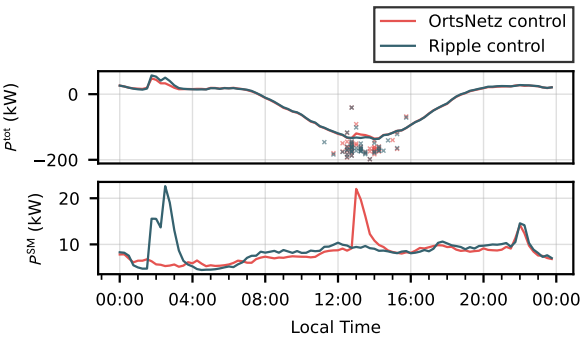


(c) Mean daily profiles and daily peak values (“x”) using the MSD based on weather data.

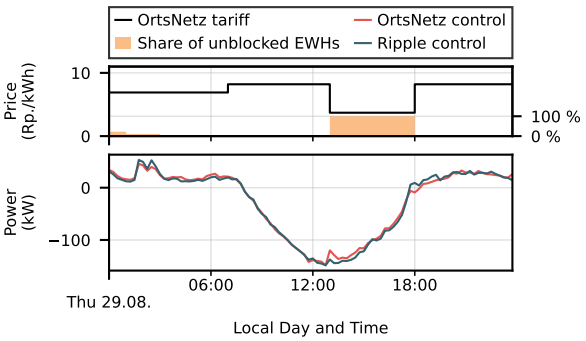


(d) Electricity price, device blocking, and TS load profiles for a single day using the MSD based on weather data.

Figure 34: Pilot results for the ToU tariff in summer. The EWH load shifts from the night hours to the start of the low-price period. Daily injection peaks were, on average, reduced by 2 kW, while the highest injection peak observed was not reduced.

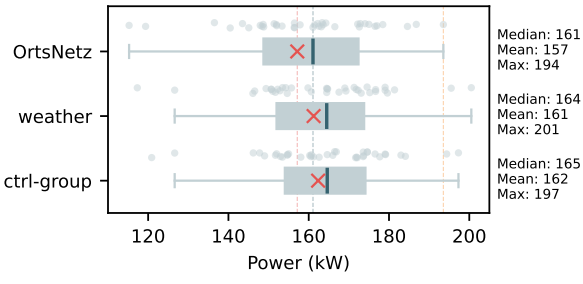


(a) Injection peaks.

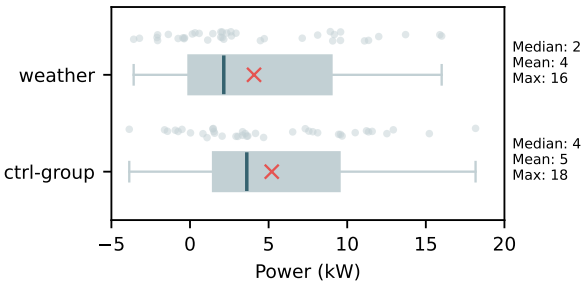


(b) Injection peak reduction.

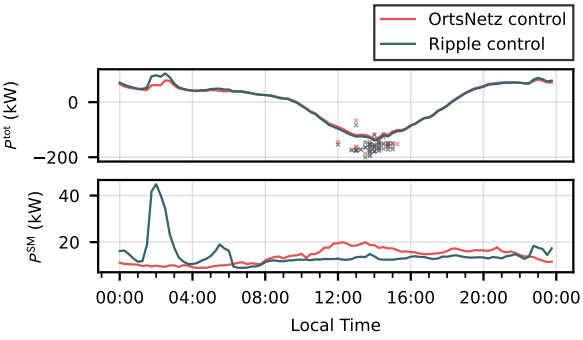


(c) Mean daily profiles and daily peak values (“x”) using the MSD based on weather data.

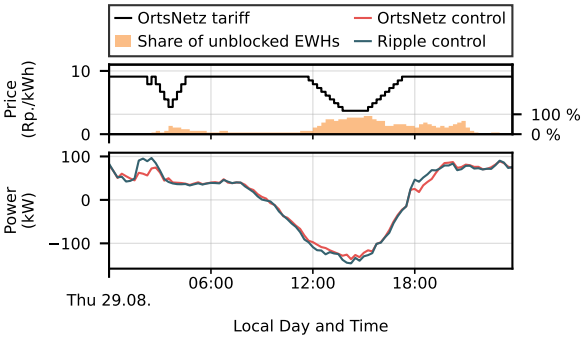


(d) Electricity price, device blocking, and TS load profiles for a single day using the MSD based on weather data.

Figure 35: Pilot results for the dynamic tariff in summer. The EWH load is more spread out over the afternoon compared to the ToU setting. This results in greater peak reductions, including the highest peaks.

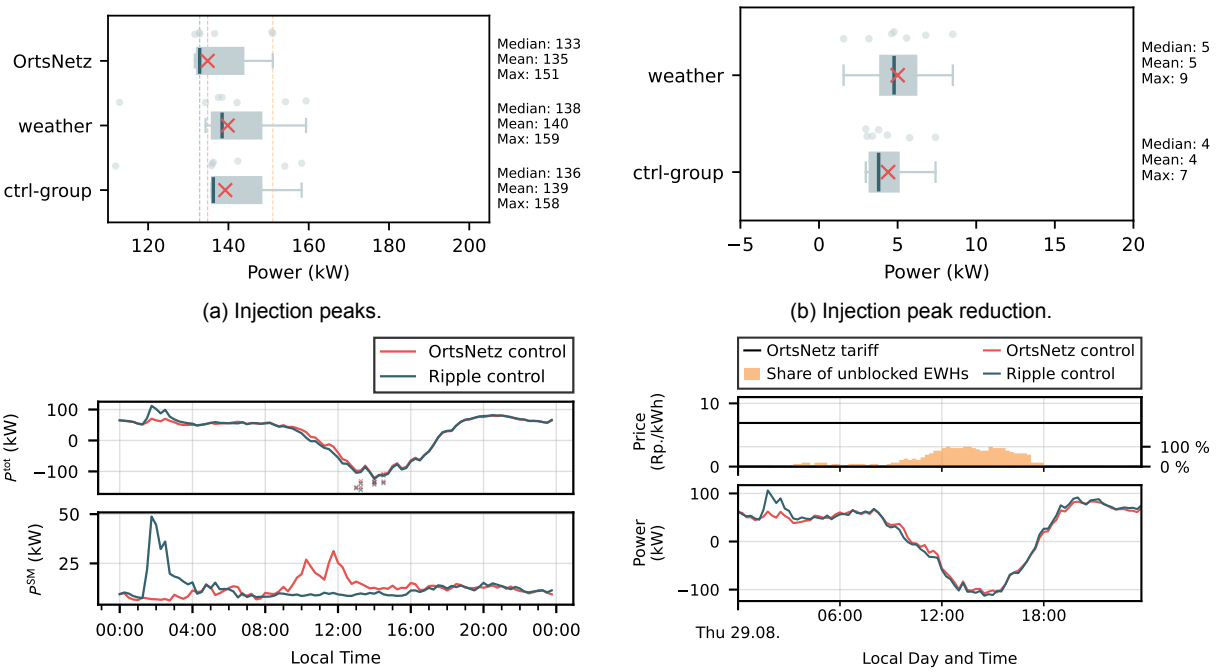


(a) Injection peaks.

(b) Injection peak reduction.

(c) Mean daily profiles and daily peak values ("x") using the MSD based on weather data.

(d) Electricity price, device blocking, and TS load profiles for a single day using the MSD based on weather data.

Figure 36: Pilot results for the direct control in summer. Daily injection peaks were, on average, reduced by 4 or 5 kW depending on the matching approach. Also the highest peak was reduced. The daily profiles indicate that EWHs mostly operated before the peak PV injection hours. An improved optimization formulation could achieve higher reductions, as illustrated in Section 4.2.5.

signals, i.e., consumed power before the injection peaks. A different treatment of the EWH constraints would suffice to overcome this deficiency. Appendix 10.2 introduces an alternative version of the DLC with the proposed change of EWH constraints and Section 4.2.5 presents its performance in a simulation platform.

Table 4 summarizes the pilot results on summer days. $N_d$ is the number of evaluated days, $N^{\text{EWH}}$ is the number of considered EWHs[10], $P^{\text{EWH}}$ is the sum of the EWHs' nominal power values, $E^{\text{EV,flx}}$ is the average flexible EV energy consumption per day, and $\overline{\Delta P_d^{\max}}$ is the average of the peak reductions on the evaluated days. The last column $\overline{\Delta P_d^{\max}/P_d^{\max,b}}$ presents the average of the relative daily peak reduction, i.e., the peak reduction divided by the peak value of the baseline load estimate on day $d$. The amount of installed PV and the number of flexible devices in the system significantly influence these values. As these factors vary among the investigated TSs, we additionally present the results for the ratio $\overline{\Delta P_d^{\max}}/P^{\text{EWH}}$ to enable a comparison between the OrtsNetz schemes. The results indicate that, on average, the dynamic tariff scheme achieved the largest peak reductions (7.9 % and 10.1 %), followed by the DLC (5.6 % and 5.1 %) and the ToU (4.6 % and 5.2 %) schemes.

Table 4: Overview pilot results summer.

| Scheme | MSD approach | $N_d$ | $N^{\text{EWH}}$ | $P^{\text{EWH}}$ (kW) | $E^{\text{EV,flx}}$ (kWh/day) | $\overline{\Delta P_d^{\max}}$ (kW) | $\overline{\Delta P_d^{\max}}/P^{\text{EWH}}$ (%) | $\overline{\Delta P_d^{\max}/P_d^{\max,b}}$ (%) |
|---|---|---|---|---|---|---|---|---|
| TOU | weather | 49 | 9 | 48.6 | 1.0 | 2.25 | 4.6 | 1.5 |
| TOU | ctrl-group | 49 | 8 | 44.6 | 1.0 | 2.32 | 5.2 | 1.5 |
| Dynamic | weather | 39 | 12 | 51.5 | 10.0 | 4.07 | 7.9 | 2.7 |
| Dynamic | ctrl-group | 39 | 12 | 51.5 | 10.0 | 5.20 | 10.1 | 3.4 |
| Direct | weather | 7 | 15 | 89.8 | 5.2 | 5.00 | 5.6 | 3.6 |
| Direct | ctrl-group | 7 | 15 | 86.3 | 5.2 | 4.39 | 5.1 | 3.1 |

[10] corresponding to the replaced SMs, as explained in Section 3.5.2.

- In summer, the ToU tariff setting reduced the injection peaks by 2 kW on average. However, it did not prevent the high peaks outside the periods to which the EWH load was shifted.
- In the dynamic real-time tariff setting, the EWH load was more spread out along the day resulting in greater peak reductions.
- Although the DLC unblocked the EWHs during daylight hours, they mostly operated at the beginning of the unblocking period, preventing greater peak reductions.
- On average, the dynamic real-time tariff achieved the largest injection peak reductions (normalized by the rated power of controlled EWHs) followed by the DLC scheme and the ToU tariff. Per kW EWH rated power, injection peaks could be reduced between 0.05 and 0.1 kW.

**Consumption peaks in winter** Table 5 presents the selected dates for evaluating the schemes in winter. The dates before OrtsNetz, used to select the MSDs, include days when no control scheme and the ripple control were functioning. In the no control setting, all devices connected to an OrtsNetz LCD were unblocked for the entire day and could, therefore, operate freely according to the internal device controller. Figures 37 - 39 present the evaluation of the OrtsNetz schemes for winter days. HPs and other heating systems dominate the TS demand. Thus, the attention is paid to the consumption peaks.

Table 5: Selected dates in winter for scheme evaluations.

| | Before | | OrtsNetz | |
|---|---|---|---|---|
| TS | Scheme | Dates | Scheme | Dates |
| Angel | No control | 20.12.23 - 16.01.24 | ToU | For all schemes: 19.11.24 - 19.12.24[11] |
| | Ripple control | 01.01.23 - 31.03.23 | ToU | |
| Geeren | No control | 20.12.23 - 22.01.24 | Dynamic | |
| | Ripple control | 01.01.23 - 31.03.23 | Dynamic | |
| Hofacher | No control | 20.12.23 - 27.02.24 | Direct | |
| | Ripple control | 01.01.23 - 31.03.23 | Direct | |

Figures 37(a) and 37(b) show that the OrtsNetz control in the ToU setting did not lead to positive mean values regarding the peak reductions, both in the comparison to the no control case and ripple control. Figure 37(c) indicates minor load reductions between 18:00 and 22:00, when only EWHs were blocked, and a more significant load reduction between 22:00 and 00:00, when also HPs were blocked. Right after the high-price period, at 00:00, a load increase is observable. As shown in the upper subplot of Fig. 37(c), most of the daily peaks at this TS were observed around 06:00. The proposed ToU tariff did not target these morning peaks. Figure 37(d) shows the electricity price profile, the OrtsNetz load curve, the baseline load estimates, and the share of (un)blocked devices for 22 November 2024. This is the day with the highest total energy consumption in the considered date range across all three TSs.

Similarly, peaks were not consistently reduced in the dynamic tariff setting and the obtained mean reduction values vary between -4 and 3 kW, as shown in Figs. 38(a) and 38(b). The mean daily profiles in Fig. 38(c) show that load is shifted from the night hours to the time between 07:00 and 19:00 when comparing the OrtsNetz control with ripple control. The highest peak values with OrtsNetz control occur in the early evening hours. One potential reason for this behavior is that the underlying inflexible load curves used for training the DSO RL agent (data from 2022/23, see Section 3.3.2) included a significantly higher amount of storage heating from 23:00 to 07:00. Thus, the learned policy may have targeted reducing

[11] excluding 01.-03.12.24 for the Dynamic and Direct schemes. The devices could not be reached on these days. In general, communication breaks must be considered in the design of the control schemes to ensure customer satisfaction (see, e.g., verification module in Section 3.3.5). The impact of longer communication breaks on the total load depends on the fallback strategy. In OrtsNetz, EVs charged immediately after plug-in per default, and for EWHs and HPs, the latest received signal was applied repeatedly. Repeating schedules may cause new peaks if a synchronized operation of flexible devices is beneficial on one day, e.g., due to a high PV production, but not on the next day.

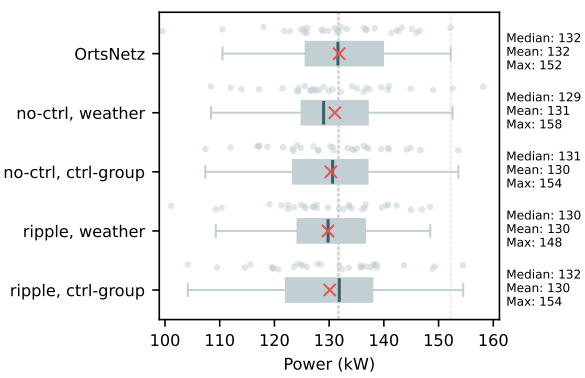


(a) Consumption peaks.

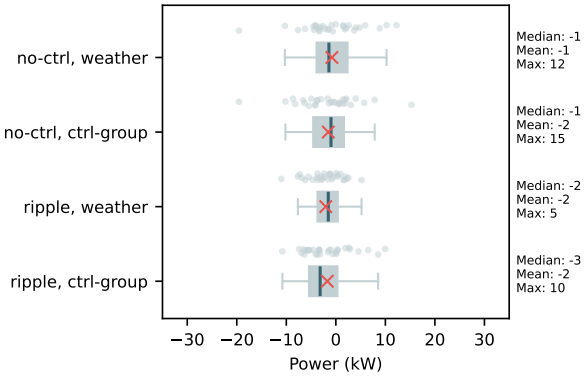


(b) Consumption peak reduction.

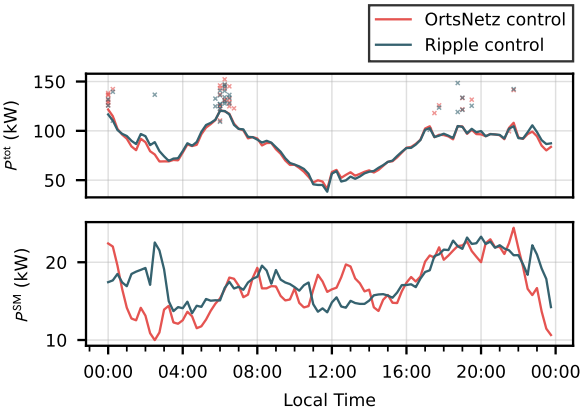


(c) Mean daily profiles and daily peak values (“x”) using the MSD based on weather data.

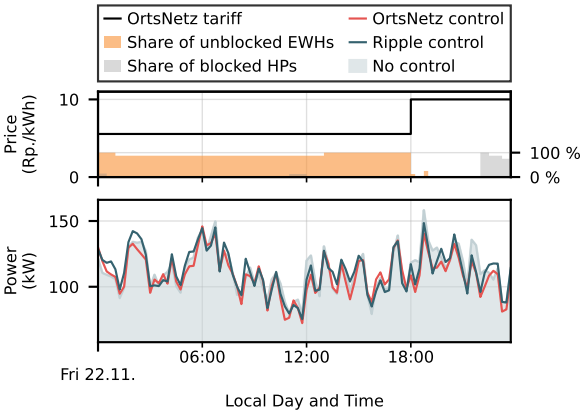


(d) Electricity price, device blocking, and TS load profiles for a single day using the MSD based on weather data.

Figure 37: Pilot results for the ToU tariff in winter. The proposed ToU tariff did not target the morning peaks observed at this TS and led to negative mean values regarding the consumption peak reductions, both in the comparison to the no control case and ripple control. The blocking of devices during the high-price period resulted in a slight power rebound at midnight.

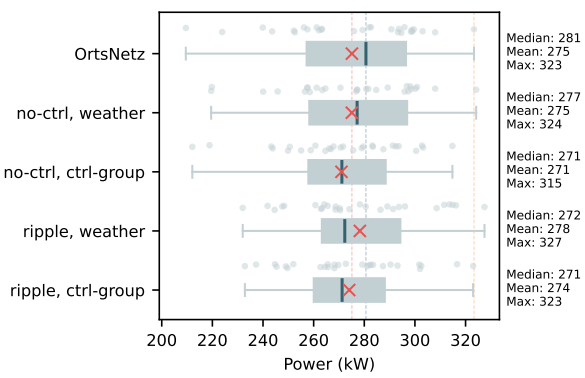


(a) Consumption peaks.

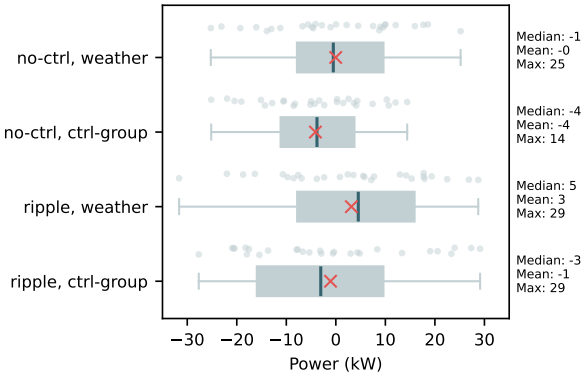


(b) Consumption peak reduction.

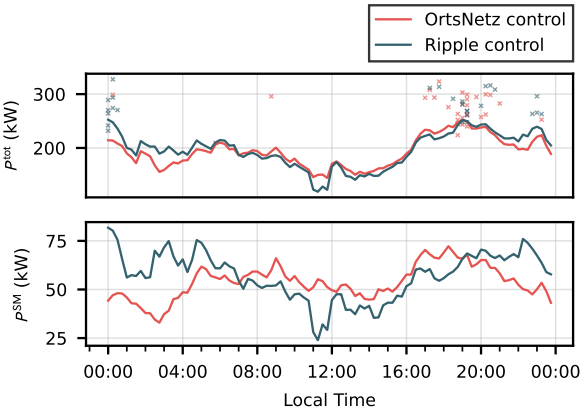


(c) Mean daily profiles and daily peak values (“x”) using the MSD based on weather data.

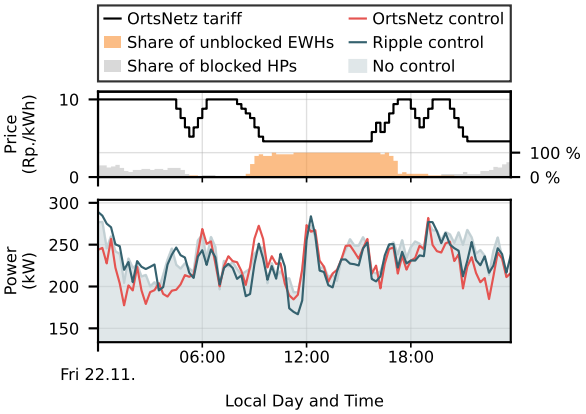


(d) Electricity price, device blocking, and TS load profiles for a single day using the MSD based on weather data.

Figure 38: Pilot results for the dynamic tariff in winter. Subfigure (c) indicates a load shift to the time between 07:00 and 19:00 and high peak values in the early evening hours. The comparison with no control and ripple control suggests that the OrtsNetz control did not consistently reduce the consumption peaks.

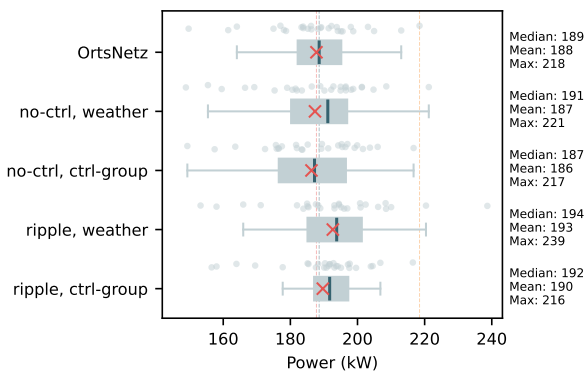


(a) Consumption peaks.

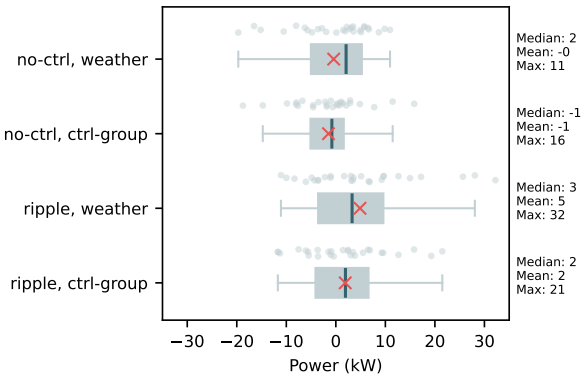


(b) Consumption peak reduction.

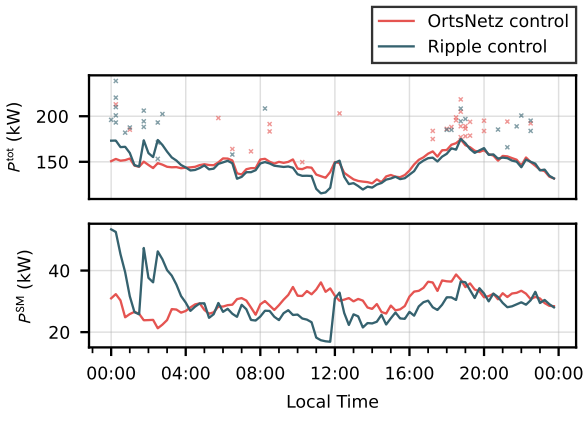


(c) Mean daily profiles and daily peak values (“x”) using the MSD based on weather data.

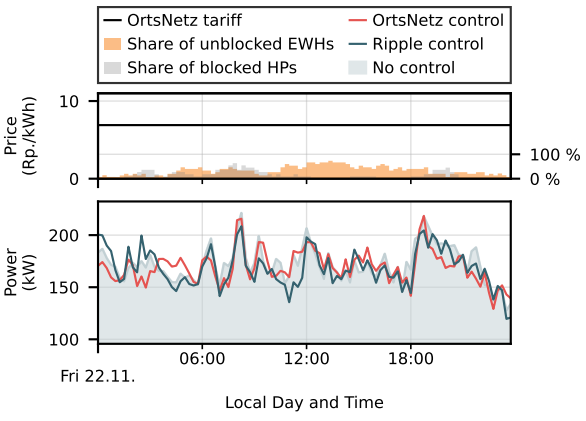


(d) Electricity price, device blocking, and TS load profiles for a single day using the MSD based on weather data.

Figure 39: Pilot results for the direct control in winter. The daily profiles show that the direct control distributed the flexible load throughout the day. It could reduce consumption peaks compared to ripple control, but not compared to the no control case.

the flexible EWH and HP load during the night instead of the evening. This highlights the importance of up-to-date training data or accounting for different scenarios. On the day depicted in Fig. 38(d), the OrtsNetz scheme could reduce the peak compared to ripple control, but not compared to no control.

As shown in the box plots of Figs. 39(a) and 39(b), the DLC reduced the consumption peaks by an average of 2 to 5 kW with respect to the ripple control. However, no peak reductions were seen with respect to no control. The comparison of $P^{\text{SM}}$ in Fig. 36(c) shows that the DLC distributed more evenly the flexible demand throughout the day with some demand concentration between 9:00 and 14:00 hours, and then between 16:00 and 19:00 hours. To understand this better on one specific day, Fig. 39(d) presents the share of unblocked EWHs and blocked HPs on 22 November 2024. At the two consumption peaks of the TS, several HPs and EWHs were blocked, yet insufficient to prevent the peaks. As reported in the load profiles comparison of Fig. 39(d), the DLC reduced the consumption peak experienced in the early hours, but there was no clear advantage when compared to the no-control case for other hours. During the consumption peaks, the DLC reached almost the same demand values as those without control.

Table 6 summarizes the pilot results in winter. $N^{\text{HP}}$ and $P^{\text{HP}}$ stand for the number and aggregated nominal electrical power of considered HPs, respectively. The direct control performed better than the tariff schemes to reduce the consumption peaks seen during ripple control. However, none of the OrtsNetz schemes resulted in peak reductions with respect to no control.

Table 6: Overview pilot results winter. The second column indicates whether flexible devices could operate freely without blocking (no-ctrl) or whether ripple control was active on the MSD. The third column indicates the type of data used to determine the MSD.

| Scheme | Control on MSD | MSD approach | $N_d$ | $N^{\text{EWH}}$ | $P^{\text{EWH}}$ (kW) | $N^{\text{HP}}$ | $P^{\text{HP}}$ (kW) | $E^{\text{EV,flx}}$ (kWh/day) | $\overline{\Delta P_d^{\text{max}}}$ (kW) | $\overline{\Delta P_d^{\text{max}}}/P^{\text{EWH}}$ (%) | $\overline{\Delta P_d^{\text{max}}/P_d^{\text{max,b}}}$ (%) |
|---|---|---|---|---|---|---|---|---|---|---|---|
| TOU | no-ctrl | weather | 31 | 9 | 48.3 | 8 | 51.2 | 1.1 | -0.80 | -1.6 | -0.7 |
| TOU | no-ctrl | ctrl-group | 31 | 9 | 48.3 | 8 | 51.2 | 1.1 | -1.52 | -3.2 | -1.3 |
| TOU | ripple | weather | 31 | 8 | 44.3 | 8 | 51.2 | 1.1 | -2.04 | -4.6 | -1.6 |
| TOU | ripple | ctrl-group | 31 | 8 | 44.3 | 7 | 46.2 | 1.1 | -1.72 | -3.9 | -1.4 |
| Dynamic | no-ctrl | weather | 28 | 15 | 64.4 | 22 | 119.5 | 20.0 | -0.02 | -0.0 | -0.1 |
| Dynamic | no-ctrl | ctrl-group | 28 | 15 | 64.4 | 21 | 115.0 | 20.0 | -4.12 | -6.4 | -1.5 |
| Dynamic | ripple | weather | 28 | 15 | 64.4 | 24 | 129.0 | 20.0 | 3.14 | 4.9 | 1.1 |
| Dynamic | ripple | ctrl-group | 28 | 15 | 64.4 | 23 | 121.9 | 20.0 | -1.07 | -1.7 | -0.4 |
| Direct | no-ctrl | weather | 28 | 16 | 85.7 | 13 | 70.6 | 12.7 | -0.44 | -0.5 | -0.4 |
| Direct | no-ctrl | ctrl-group | 28 | 16 | 86.0 | 12 | 63.2 | 12.7 | -1.48 | -1.7 | -0.9 |
| Direct | ripple | weather | 28 | 15 | 83.9 | 11 | 53.2 | 12.7 | 4.88 | 5.8 | 2.3 |
| Direct | ripple | ctrl-group | 28 | 15 | 83.9 | 11 | 53.2 | 12.7 | 1.90 | 2.3 | 0.9 |

- In winter, the ToU tariff and dynamic tariff did not lead to peak reductions when compared to the no-control case and the ripple control.
- The DLC scheme reduced the consumption peaks with respect to the ripple control only.
- None of the OrtsNetz schemes showed clear advantages for reducing the consumption peaks when compared to the no-control case.

### 4.2.5 Simulation platform results

This section complements the pilot results with simulation results to improve the comparability between the proposed schemes and to illustrate that an alternative formulation of the EWH constraints in the DLC could reduce injection peaks more effectively. The simulation environment represents the Geeren TS and is similar to the one used for the DSO agent training. A high-level description of the simulation environment is included in Appendix 10.1. As visualized in Figs. 40 and 41, the simulated TS load is generally aligned with the real-world measurements. In this comparison, EWHs and HPs were simulated using the blocking commands applied during the pilot, and the EV load represents immediate charging.

In the following, the blocking/charging decisions were determined by five different control approaches. Besides the previously discussed schemes, an adjusted version of the DLC is included. Appendix 10.2

details the alternative formulation, which targets to model the EWH operation more realistically. This new version is referred to as “Direct adjusted”, while “Direct pilot” denotes the version applied during the pilot. Additionally, the fifth approach, denoted as “Direct perfect knowledge”, considers an ideal centralized optimization-based controller with perfect prediction of the inflexible load profiles, perfect models of the EWH and HP and the corresponding domestic hot water and space heating demand profiles, and perfect knowledge of the future EV charging sessions. For EWHs and on-off HPs, the hysteresis controller was explicitly modeled in the optimization, while, for simplicity, the modulating HPs were assumed to be inflexible (6/25 devices). For all schemes, the simulation was performed for 9 days in summer and 9 days in winter. The first two days were discarded in the evaluation to reduce the impact of simulation initializations.

**Injection peaks in summer** Figure 42 presents the simulated TS load profile that resulted from the application of the five approaches on two summer days. It considers the day with the highest (and non-reduced) injection peak during the pilot phase evaluated for the ToU tariff setting. The inflexible load profile, labeled as $P^{\text{inf}}$, was only known in advance by the “Direct perfect knowledge” scheme. The latter is considered the ideal approach; however, it is unachievable in a real implementation.

The ToU tariff approach performed better in the simulation than in the pilot. We conclude that a higher number of devices increases the chances that at least part of the EWHs operate longer and could cover the peak at 13:45. In general, though, Fig. 42 shows that other approaches can adapt better to different inflexible load profiles. We also found that the adjusted DLC performed considerably better than the DLC during the pilot thanks to the better representation of the running time of EWHs when unblocked. Contrary to the pilot DLC, which unblocked most EWHs for the daylight hours even though the devices mainly operated in the mornings, the adjusted version concentrated the EWH demand at the hours of maximum PV injection.

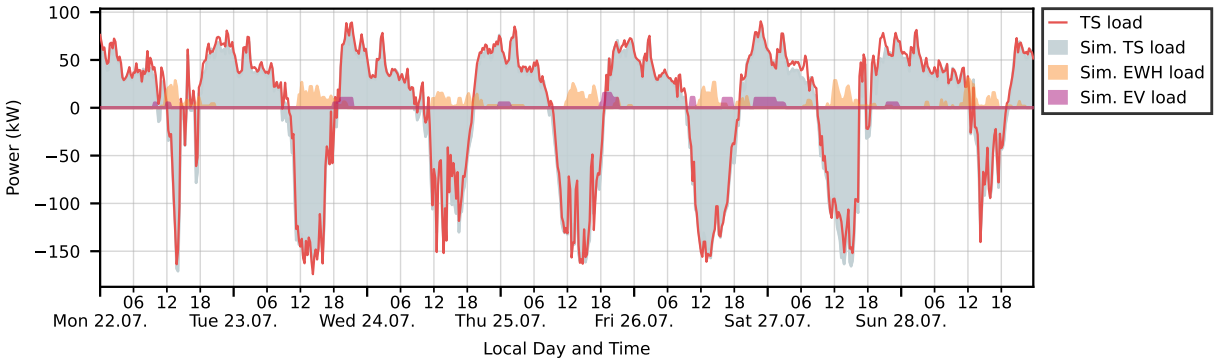


Figure 40: Measured and simulated load for a summer week. The comparison demonstrates that the simulated load is aligned with the measured TS load.

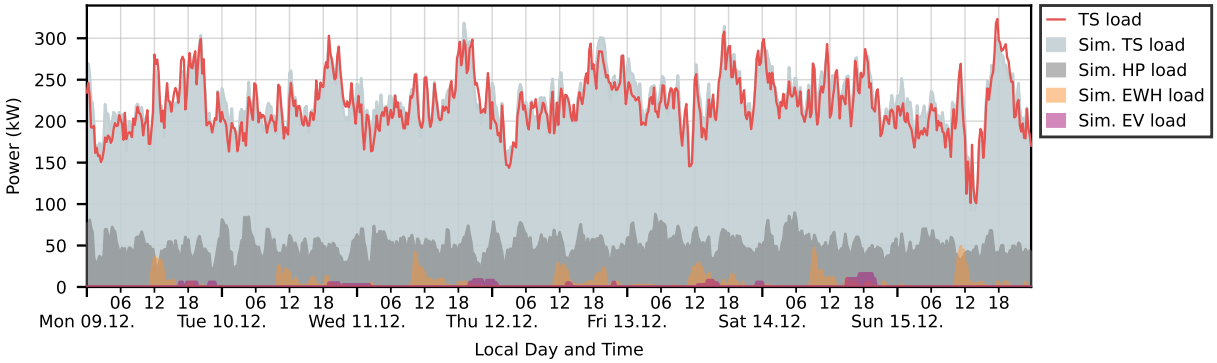


Figure 41: Measured and simulated load for a winter week. The comparison demonstrates that the simulated load is aligned with the measured TS load.

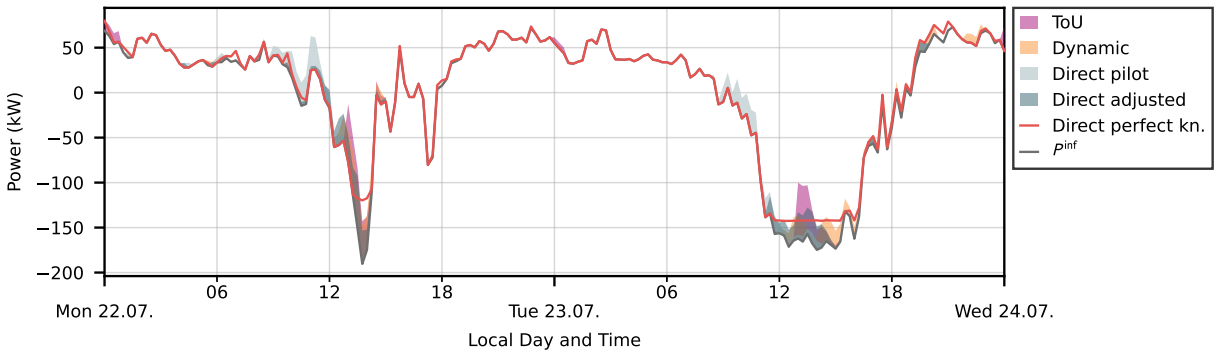


Figure 42: Simulated TS load profiles for different schemes on two summer days. The results illustrate that, unlike the pilot version, the adjusted optimization formulation (Direct adjusted) concentrates the EWH demand at the hours of maximum PV injection. The profiles also show that the Direct and Dynamic schemes can adapt better to different inflexible load profiles than the ToU scheme.

Table 7 presents the results for the summer week, where $P^{\text{max}}$ is the maximum injection peak reported during the simulated week. For a better understanding, we also report the results with no-control and ripple-control schemes. The former resulted in lower injection peaks because it allows flexible loads to operate freely, and some ran at the time of the injection peaks. In most cases, higher reductions were achieved in the simulation environment compared to what was measured during the pilot phase (cf. Table 4). Possible reasons include that in the simulation, communication and other technical issues are neglected and that the simulated EWH demand may be higher than the actual one.

Leaving aside the ideal controller with perfect knowledge, the dynamic tariff performed best in the simulation environment, closely followed by the adjusted DLC and the ToU tariff approaches. The direct pilot approach reported the lowest performance. Further improvements in the inflexible load estimate and EWH demand estimate should lead to a better performance of the DLC compared to the dynamic tariff. Finally, considering the average daily peak reduction $\overline{\Delta P_d^{\text{max}}}$ with respect to the no-control case, the proposed schemes could realize 20-27 % of the potential reduction found with the ideal control scheme, i.e., with perfect knowledge.

Table 7: Simulation results of injection peaks in the summer week; $N_d = 7$, $N^{\text{EWH}} = 16$, $P^{\text{EWH}} = 70.4$ kW.

| | | Comparison to no control | | | Comparison to ripple control | | |
|---|---|---|---|---|---|---|---|
| Scheme | $P^{\text{max}}$ (kW) | $\overline{\Delta P_d^{\text{max}}}$ (kW) | $\overline{\Delta P_d^{\text{max}}}/P^{\text{EWH}}$ (%) | $\overline{\Delta P_d^{\text{max}}/P_d^{\text{max,b}}}$ (%) | $\overline{\Delta P_d^{\text{max}}}$ (kW) | $\overline{\Delta P_d^{\text{max}}}/P^{\text{EWH}}$ (%) | $\overline{\Delta P_d^{\text{max}}/P_d^{\text{max,b}}}$ (%) |
| No control | 176.39 | - | - | - | 5.20 | 7.4 | 2.9 |
| Ripple control | 190.37 | -5.20 | -7.4 | -3.1 | - | - | - |
| ToU | 171.36 | 8.42 | 12.0 | 5.2 | 13.62 | 19.3 | 7.9 |
| Dynamic | 166.42 | 11.61 | 16.5 | 7.1 | 16.81 | 23.9 | 9.8 |
| Direct pilot | 184.37 | -2.39 | -3.4 | -1.5 | 2.81 | 4.0 | 1.6 |
| Direct adjusted | 171.46 | 9.86 | 14.0 | 6.2 | 15.06 | 21.4 | 8.9 |
| Direct perfect kn. | 142.63 | 42.93 | 61.0 | 26.9 | 48.13 | 68.4 | 29.1 |

- The adjusted DLC performed considerably better than the original DLC thanks to the better representation of the running time of EWHs when unblocked.
- In summer, the proposed schemes could realize 20-27 % of the potential reductions found with an ideal controller with perfect knowledge.

**Consumption peaks in winter** Figure 43 presents the simulated TS load profile that resulted from the application of the five approaches on two winter days. The ToU tariff approach performed poorly in the simulation environment as it created a very high consumption peak at 00:00 due to the synchronization of

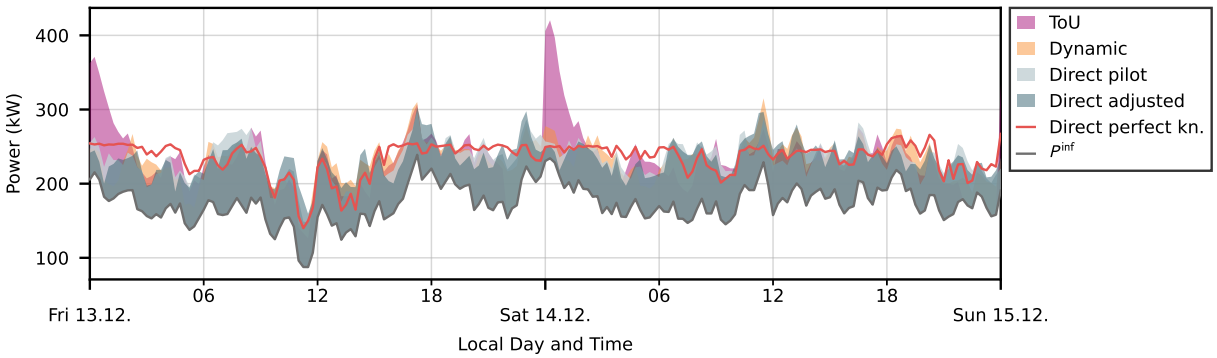


Figure 43: Simulated TS load profiles for different schemes on two winter days. The consumption peaks with the Dynamic and Direct schemes seem comparable, while the ToU scheme leads to significant consumption peaks right after the high-price period.

HPs and EWHs demands right after the high-price period ended. Although the pilot results in Fig. 37(c) also show consumption peaks right after 00:00, the power rebound was less aggressive. This difference is attributable to: a) the number of flexible loads in the simulation ($N^{\text{EWH}} = 16$ and $N^{\text{HP}} = 25$) is considerably larger than in the pilot ToU setting, b) model inaccuracies of hot water and space heating demands, which could result in higher demand and unrealistic synchronization of devices, and c) potential technical issues leading to fewer devices being blocked during the high-price period in the pilot. Finally, the dynamic tariff and the DLC approaches (pilot and adjusted) seem comparable in terms of consumption peak reductions.

Table 8 presents the results for the winter week. We also report the results with no-control and ripple-control schemes. In agreement with the pilot results, the no-control case is preferred over the ripple control to reduce consumption peaks. Without considering the ideal centralized controller, the adjusted DLC performed best, followed by the pilot DLC and the dynamic tariff. Unlike the pilot results, the simulations show that the OrtsNetz schemes could perform better than no control in winter, excluding the ToU tariff approach. Finally, considering $\overline{\Delta P_d^{\text{max}}}$ with respect to the no-control case, the proposed schemes could achieve 8-31 % of the potential reduction found with perfect knowledge. The DLC performance could be enhanced by improving the estimates on the inflexible load, EWH demand, and HP demand. The performance of the dynamic tariff could be improved by using more up-to-date training data for the DSO RL agent. Furthermore, an extension by a peak demand charge or another power-related tariff could incentivize peak reductions on a household level and support consistent peak reductions on a TS level.

Table 8: Simulation results of consumption peaks in the winter week; $N_d = 7$, $N^{\text{EWH}} = 16$, $P^{\text{EWH}} = 70.4$ kW, $N^{\text{HP}} = 25$, $P^{\text{HP}} = 133.5$ kW.

| | | Comparison to no control | | | Comparison to ripple control | | |
|---|---|---|---|---|---|---|---|
| Scheme | $P^{\text{max}}$ (kW) | $\overline{\Delta P_d^{\text{max}}}$ (kW) | $\overline{\Delta P_d^{\text{max}}}/P^{\text{EWH}}$ (%) | $\overline{\Delta P_d^{\text{max}}/P_d^{\text{max,b}}}$ (%) | $\overline{\Delta P_d^{\text{max}}}$ (kW) | $\overline{\Delta P_d^{\text{max}}}/P^{\text{EWH}}$ (%) | $\overline{\Delta P_d^{\text{max}}/P_d^{\text{max,b}}}$ (%) |
| No control | 317.88 | - | - | - | 0.58 | 0.8 | 0.1 |
| Ripple control | 328.03 | -0.58 | -0.8 | -0.2 | - | - | - |
| ToU | 420.38 | -46.84 | -66.5 | -15.2 | -46.26 | -65.7 | -15.0 |
| Dynamic | 315.16 | 3.51 | 5.0 | 1.2 | 4.09 | 5.8 | 1.2 |
| Direct pilot | 305.81 | 8.32 | 11.8 | 2.7 | 8.90 | 12.6 | 2.8 |
| Direct adjusted | 303.08 | 14.23 | 20.2 | 4.6 | 14.81 | 21.0 | 4.7 |
| Direct perfect kn. | 269.31 | 45.52 | 64.7 | 14.8 | 46.10 | 65.5 | 14.9 |

- Unlike the pilot results, the simulations show that the OrtsNetz schemes could perform better than no control in winter, excluding the ToU tariff approach.
- The schemes could achieve 8-31 % of the potential reductions found with the ideal controller.

## 4.3 Battery Energy Storage System control

This section presents the BESS results for the period from 15.11. to 20.11.2024. Before this period, the BESS algorithm ran with a less optimal scenario generation approach than the one described in Section 3.3.6, and after this period, individual BESS modules disconnected due to technical issues. At the given TS, the load peaks typically occur in the evening hours. Thus, for simplicity, the minimum threshold value is reset daily at 15:00 local time, and 15:00 is considered as the start of a new test day $d$. The minimum and maximum SoC limits were specified as 10 % and 90 %, respectively.

Figure 44 shows the scenarios at 17:00 on each day and demonstrates that the daily maximum peaks are captured well. Figure 45 shows the resulting power and SoC profiles for the 5-day test period. Besides the real-world measurements, it includes the simulation results for the same period and the ideal threshold when assuming perfect foresight of the load. Different from the evaluation of the DSM schemes in Section 4.2, the load with and without BESS can be directly compared using the two separately measured profiles in the same period. On average, the algorithm achieved daily peak reductions of $\overline{\Delta P_d^{\text{max}}} = 26.7$ kW and 55.6 % of the ideal reductions. The comparison between the simulation and the real-world results shows that the simulation generally aligns with the real-world data, except for day 4, when a BESS-internal alarm led to delayed charging. The comparison between the applied and the ideal threshold illustrates the trade-off between choosing a conservative and an overly optimistic threshold. On days 1, 3, and 5, the BESS capacity is not fully used as the threshold is higher than the ideal threshold, while on day 4, the threshold is slightly too low, such that the BESS reaches the minimum SoC before the end of the peak.

To put the BESS results in relation to the results obtained with the investigated DSM schemes, the average daily peak reduction is divided by the BESS rated power of 50 kW, i.e., $\overline{\Delta P_d^{\text{max}}}/P^{\text{B,rated}} = 53.3$ %. This value is significantly higher than the ones obtained for $\overline{\Delta P_d^{\text{max}}}/P^{\text{EWH}}$ in Section 4.2, which indicates that the BESS is more effective in using the available flexible power for peak reductions. Note that the meaning of the metric $\overline{\Delta P_d^{\text{max}}}/P^{\text{B,rated}}$ is limited by the fact that the BESS capacity also impacts the peak reduction. The reduction may be smaller than the rated power if the peak duration is high and the BESS capacity is the limiting factor (e.g., the ideal reduction on day 4 in Fig. 45 is 31 kW).

- The BESS algorithm works generally well in the field and achieves 55.6 % of the theoretical ideal reduction with perfect foresight.
- The BESS uses its available flexibility more effectively than the other DSM schemes with a power ratio of $\overline{\Delta P_d^{\text{max}}}/P^{\text{B,rated}} = 53.3$ %. This is expected since the BESS has fewer operating constraints and its behavior is more predictable.

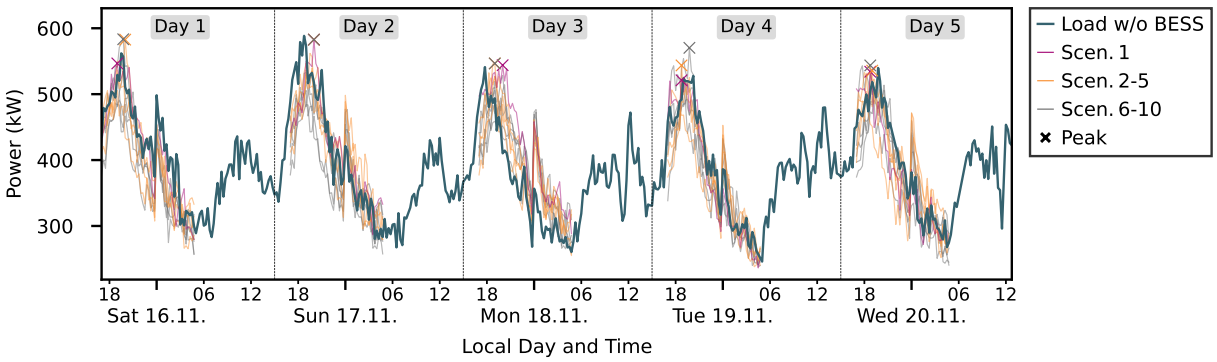


Figure 44: Actual 15-min average load without BESS and scenarios generated during real-world deployment at 17:00. Scenarios 1-5 were used in the optimization. The daily maximum peaks are captured well.

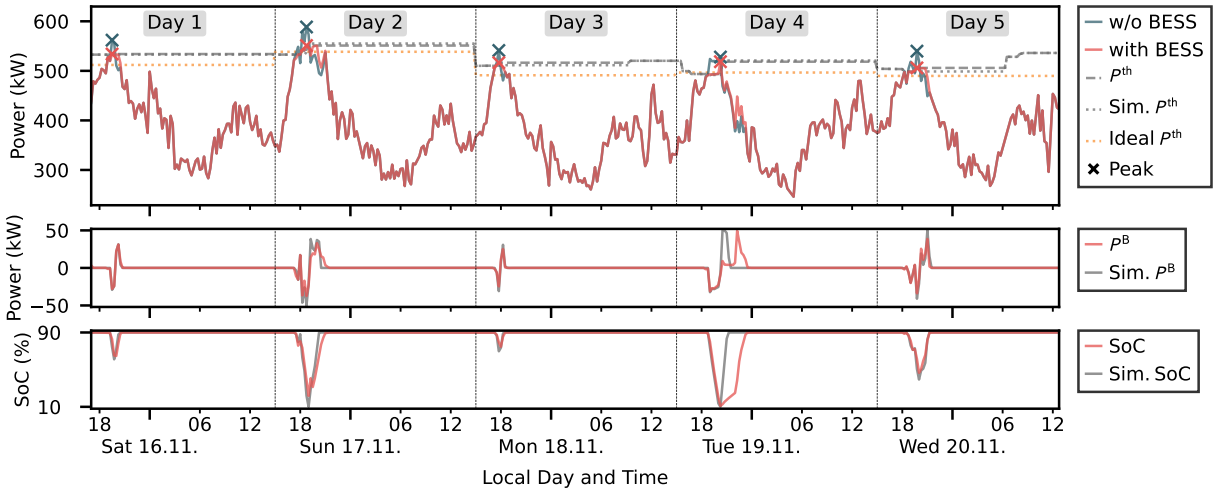


Figure 45: Real-world results and corresponding simulation for 15.-20.11.2024. 'w/o BESS', 'with BESS', $P^{B}$, SoC, and $P^{th}$ are the real-world measurements and applied threshold value. Profiles labeled as 'Sim.' show the results when running the simulation with the scenarios generated in real-time. They are generally aligned with the real-world data. 'Ideal $P^{th}$' shows the ideal threshold with perfect foresight of the load. The comparison with the applied threshold illustrates the trade-off between a conservative and an overly optimistic threshold.

# 5 Conclusions and outlook

In this final section, we summarize and discuss the key findings from the pilot project and provide an outlook on potential future work.

## 5.1 Key findings

**Customer behavior indicates a clear difference between Opt-in and Not Opt-out participants:**

- Opt-in participants had a small but clearly observable change in energy consumption during the project, especially during times with a high tariff. This demonstrates a general responsiveness of these customers to the tariffs. Furthermore, they were more engaged on the platform — which they found more usable, in the voluntary solar market, and during the participant survey.
- Only 12.9 % of targeted customers could be reached by opt-in. In contrast, 97 % of targeted Not opt-out participants could be reached, but these showed a significantly lower response to the tariffs. This aligns with their passive behavior during recruitment.
- This finding has important consequences for the interpretation of future research studies and the roll-out of new tariffs to the wider public. Research projects often feature opt-in recruiting and might find a high effectiveness of novel tariffs. However, based on the differences demonstrated in this project, we show that such effects are caused more by the fact that participants opted in and less by the actual tariffs. Thus, to determine the effectiveness of novel tariff schemes, they must be tested in the wider public through opt-out studies.
- In contrast to the rather small impact on observed behavior, survey responses across all participant groups indicate a strong interest in innovative tariffs. In turn, they expected clear financial savings.
- The findings on customer behavior are limited by two facts: The project was heavily advertised in the community. An opt-in roll-out to the wider public would likely see an even lower participation rate. Furthermore, the best-accounting policy, which ensured participants could only benefit financially, likely influenced participation and engagement across participant groups.

**Interest in smart charging is generally high, while interaction with the charging system is low:**

- A large share of all EV owners in the pilot area indicated interest in the smart charging offer.
- During the automatic load control phase, response rates were much lower and customers who initially registered their vehicle could not be reached anymore. Thus, for a wide roll-out seamless on-boarding and clear communication are key.
- Customers with optimized charging generally made few manual adjustments to the charging system as long as the system functioned.

**The proposed automated load control schemes reduced injection peaks in summer:**

- On average, the ToU tariff scheme reduced injection peaks in summer due to the shift of the EWH load from night hours to the start of the low-price period. However, the highest injection peaks observed with the ToU tariff setting were similar to those in the baseline load profiles. This happened because the operation of flexible devices was highly synchronized and did not necessarily align in time with the injection peaks.
- In the dynamic real-time tariff scheme, the EWH load was more spread out than in the ToU setting on summer days. This resulted in greater peak reductions, including the highest peaks.

- The DLC unblocked the EWHs during most daylight hours in summer. However, as the EWHs mainly operated at the start of the unblocking periods, lower peak reductions were observed compared to the dynamic tariff scheme. Simulation results show that an improved optimization formulation could achieve greater reductions.
- The dynamic real-time tariff achieved the largest peak reductions, followed by the DLC scheme and the ToU tariff. The dynamic tariff setting and the DLC scheme can adjust better to varying shapes of the inflexible load profile compared to the ToU tariff.

**In winter, the pilot results indicate no clear advantages of the evaluated schemes regarding reducing consumption peaks:**

- The ToU tariff setting in winter did not result in a positive mean value of peak reductions. This is because most of the consumption peaks at the TS level were observed around 06:00, but the ToU tariff did not target the morning peaks. This result, together with the observation that there are noticeable differences in the load profiles and peak hours between TSs, indicates that tariff profiles and direct control schemes must be adapted per TS to realize peak reductions and, therefore, cost savings on this level.
- The dynamic tariff setting did not consistently reduce the consumption peaks in winter. The highest peak values occurred in the early evening hours. One possible reason for low price values during these hours is that the learned policy of the DSO RL agent mainly targeted reducing the flexible load at night instead of in the evenings. This result highlights the importance of up-to-date training data or accounting for more scenarios during the training stage, as TS load profiles are considerably changing.
- The DLC spread out the flexible load in winter days, yet insufficient to significantly reduce the highest consumption peaks observed during the pilot phase. The performance of the DLC was affected by the uncertainty of how much power the flexible loads would consume once unblocked, as well as the limited time given to the solver to return a solution. While the DLC reduced the consumption peaks compared to ripple control, its performance was comparable to the case without control.
- None of the schemes performed better than the no-control case. The results further suggest that removing the ripple control can lead to consumption peak reductions. It is expected that a larger fleet of controllable electric vehicles would make the benefits of the schemes more evident.

**BESSs can effectively shave consumption peaks:**

- The proposed BESS algorithm was evaluated for a short winter period and achieved 55.6 % of the theoretical ideal reduction with perfect foresight.

**The technology for deployment of both direct and indirect control schemes is ready:**

- The real-world implementation of the proposed algorithms highlighted the importance of a robust infrastructure with real-time communication and remote update capability. The automated load control results show that the majority of the price signals and switching commands were successfully received and applied with the proposed communication and hardware infrastructure.
- Technical challenges like support for specific vehicle brands and limited wireless connectivity remain hurdles regarding reliable smart charging of EVs.

## 5.2 Main learnings from a DSO perspective

- Even though the value of flexibility, as shown in the project, is not as high as a naive view would assume, the results of the project show that both dynamic tariff schemes and direct control contribute to peak reduction. However, they cannot completely replace the need for additional grid reinforcement. EKZ will adopt dynamic tariffs in 2026 based on OrtsNetz results and plans to replace the ripple control system with an intelligent direct control system.
- Regarding customer adoption, the results show that Opt-In schemes cannot achieve broad adoption in the population. Therefore, estimates of access to flexibility, directly or indirectly via tariffs in the future by DSOs, need to be reassessed. It is also important to keep tariff schemes as simple and understandable as possible.

## 5.3 Outlook

Building on the presented results, the following list outlines potential directions for future work:

- As mentioned above, the estimates of access to flexibility should be reassessed.
- Simulation results indicate that the performance of the dynamic tariff scheme and the direct load control could be improved to achieve reductions for the given setting also in winter.
- In this regard, it is essential to note that the shape of the inflexible load profile and the ratio between the flexible and inflexible load significantly impact the performance, particularly for price-based schemes. If the inflexible load profile cannot accommodate synchronized operation of flexible loads, it is recommended to extend the dynamic tariff by a peak demand charge or another power-related tariff. This could incentivize consumption peak reductions on a household level and support consistent peak reductions on a TS level.
- The project focused on time-variable grid usage tariffs. An extension to time-variable feed-in tariffs or other feed-in specific tariff schemes is likely to give PV owners a stronger incentive to reduce their injection peaks.
- Price-based schemes could promote the installation of home energy management systems and batteries, as well as further developments by corresponding providers and device manufacturers. This would shift the development efforts from DSOs alone to other entities and enable innovative solutions through market-based competition.

# 6 National and international cooperation

Besides the collaboration between the project partners at ETH Zurich and EKZ, there was an active exchange with the chair of Information Systems and Energy Efficient Systems at the University of Bamberg, which is led by Prof. Thorsten Staake. Furthermore, EKZ collaborated with Virtual Global Trading (OrtsNetz platform), Aveniq (IT), Swistec (LCD), enersuisse (billing and metering), Netinium (HES), Neuron (LCSA), Enode (EV connection), HSLU (data analysis) and ewz (HES).

# 7 Communication

The following list presents the events and articles related to the OrtsNetz project:

- EKZ information event, “Ein innovativer, lokaler Strommarkt für Winkel”, Winkel, 6 September 2021
- Newspaper article, Zürcher Unterländer, “Strom aus Winkel für Winkel”, 19 September 2021
- TV report, Tele Z, “Winkel: Lokales Solarstromförderungsprojekt OrtsNetz der EKZ”, 22 September 2021
- Newspaper article, Unterland Zeitung, “Die Energiegemeinschaft «OrtsNetz» handelt lokal mit dem eigenen Strom”, 10 October 2021
- Multiple Newspaper articles and information, Winkel “dorfziitig”, Articles in October 2021, October 2022, November 2022, January 2023, April 2023, May 2023, July 2023, August 2023, September 2023, December 2023, May 2024, June 2024, January 2024, February 2024, May 2024
- Press release, Virtual Global Trading AG, “Partnerschaft zwischen EKZ und VGT zur Realisierung einer Peer-to-Peer Plattform”, March 2022
- Information material, EKZ, “Strom – aus Winkel für Winkel”, July 2022
- Press release, Virtual Global Trading AG, “Solarstrom lokal produzieren und in der Nachbarschaft nutzen?”, August 2022
- Press release, Swistec Systems AG, “Pilotprojekt «OrtsNetz»”, August 2022
- Community event, “Winkel Neuzuzügeranlass”, Winkel, 9 September 2022
- Aufsichtskommission über die wirtschaftlichen Unternehmen (AWU), Visitation EKZ and OrtsNetz, 16 November 2022
- ZHAW Lecture, Lecture on “Intelligente Mess- und Steuersysteme”, 20 April 2023
- Zukunft des ZEVs, Presentation on OrtsNetz, course on ZEV, GBS St. Gallen, 9 May 2023
- Verein Zürich Erneuerbar, Presentation on OrtsNetz, 12 May 2023
- EKZ Betriebsleitertagung, Presentation on OrtsNetz, all utility companies connected to the EKZ grid are invited, 12 May 2023
- GLP Thalwil, Presentation on OrtsNetz, 16 May 2023
- EKZ information event, Winkel, 11 September 2023
- Newspaper article, Zürcher Unterländer, ”Winkel testet das Stromnetz der Zukunft und spart Geld dabei”, 20 September 2023
- Zukunft des ZEVs, Presentation on OrtsNetz, course on ZEV, Primeo Energie Kosmos (Basel), 7 November 2023

- G3 PLC Alliance, Presentation on OrtsNetz, 28 November 2023
- Netzimpuls, Presentation on OrtsNetz, 20 March 2024
- ZHAW Lecture, Lecture on ”Intelligente Mess- und Steuersysteme”, 4 April 2024
- ZHAW Lecture, Lecture on ”Wie Daten und KI die Energieversorgung transformieren”, 17 April 2024
- EKZ Betriebsleitertagung, Presentation on OrtsNetz, all utility companies connected to the EKZ grid are invited, 13 May 2024
- Science Corner BDEW Kongress, Presentation on dynamic grid-usage tariffs, 6 June 2024
- Verteilnetzforum, Presentation on OrtsNetz, 26 June 2024
- EPFL Lecture, Presentation on OrtsNetz, 20 November 2024
- e-mobile Online Forum, Presentation on OrtsNetz EV as part of a smart grid including main results, 19 February 2025
- Abonax Energieforum, Presentation on OrtsNetz, including main results, 27 February 2025
- EKZ closing event of project OrtsNetz, Winkel, 6 March 2025

# 8 Publications

The following list presents the scientific publications that resulted from OrtsNetz to date:

- T. Brudermueller and M. Kreft, “Smart meter data analytics: Practical use-cases and best practices of machine learning applications for energy data in the residential sector,” in *ICLR 2023 Workshop on Tackling Climate Change with Machine Learning*, 2023
- K. Kaiser, M. Kreft, E. Stai, M. González Vayá, T. Staake, and G. Hug, “Reducing power peaks in low-voltage grids via dynamic tariffs and automatic load control,” in *27th International Conference on Electricity Distribution (CIRED 2023)*, (Rome, Italy), June 2023
- E. Stai, K. Kaiser, J. Stoffel, M. González Vayá, and G. Hug, “Automatic load management in active distribution grids using reinforcement learning,” in *IEEE PES ISGT Europe 2023*, (Grenoble, France), October 2023
- K. Kaiser and G. Hug, “Dynamic Grid Tariffs for Power Peak Reduction Using Reinforcement Learning,” in *2024 International Conference on Smart Energy Systems and Technologies (SEST)*, (Torino, Italy), September 2024
- M. Kreft, T. Brudermueller, T. Anderson, and T. Staake, “Identifying electric water heaters from low-resolution smart meter data,” in *2024 IEEE Conference on Technologies for Sustainability (SusTech)*, pp. 128–135, 2024
- M. Kreft, T. Brudermueller, E. Fleisch, and T. Staake, “Predictability of electric vehicle charging: Explaining extensive user behavior-specific heterogeneity,” *Applied Energy*, vol. 370, no. 123544, 2024

# 9 References


[1] C. Winzer, S. Auer, and P. Ludwig, “Kostenwahrheit im Verteilnetz.” https://www.bulletin.ch/de/news-detail/kostenwahrheit-im-verteilnetz.html, 2021. Accessed: 11 October 2023.

[2] Bundeskanzlei, Bundeshaus, 3003 Bern, “Bundesgesetz über die Stromversorgung.” https://www.fedlex.admin.ch/eli/cc/2007/418/de, 2007. Accessed: 11 October 2023.

[3] Kanton Zürich, “Gemeindeporträt Winkel.” https://www.zh.ch/de/politik-staat/gemeinden/gemeindeportraet.html. Accessed: 26 February 2025.

[4] Bundesamt für Statistik, “Strassenfahrzeuge – Bestand, Motorisierungsgrad.” https://www.bfs.admin.ch/bfs/de/home/statistiken/mobilitaet-verkehr/verkehrsinfrastruktur-fahrzeuge/fahrzeuge/strassenfahrzeuge-bestand-motorisierungsgrad.html, 2024. Accessed: 26 February 2025.

[5] Eidgenössische Elektrizitätskommission ElCom, “Strompreise Schweiz.” https://www.strompreis.elcom.admin.ch, 2023. Accessed: 25 October 2023.

[6] K. Kaiser, M. Kreft, E. Stai, M. González Vayá, T. Staake, and G. Hug, “Reducing power peaks in low-voltage grids via dynamic tariffs and automatic load control,” in *27th International Conference on Electricity Distribution (CIRED 2023)*, (Rome, Italy), June 2023.

[7] I. Soares, M. J. Alves, and C. H. Antunes, “A bi-level optimization approach to define dynamic tariffs with variable prices and periods in the electricity retail market,” in *Advances in Evolutionary and Deterministic Methods for Design, Optimization and Control in Engineering and Sciences*, pp. 1–16, Cham: Springer, 2021.

[8] M. Fischetti, I. Ljubić, M. Monaci, and M. Sinnl, “A new general-purpose algorithm for mixed-integer bilevel linear programs,” *Operations Research*, vol. 65, no. 6, p. 1615–1637, 2017.

[9] I. Soares, M. J. Alves, and C. H. Antunes, “A deterministic bounding procedure for the global optimization of a bi-level mixed-integer problem,” *European Journal of Operational Research*, vol. 291, p. 52–66, 2021.

[10] T. Kleinert, M. Labbé, I. Ljubić, and M. Schmidt, “A Survey on Mixed-Integer Programming Techniques in Bilevel Optimization,” *EURO Journal on Computational Optimization*, vol. 9, 2021.

[11] M. Pereira, S. Granville, M. Fampa, R. Dix, and L. Barroso, “Strategic bidding under uncertainty: a binary expansion approach,” *IEEE Trans. on Power Systems*, vol. 20, no. 1, p. 180–188, 2005.

[12] Gurobi Optimization, LLC, “Gurobi Optimizer Reference Manual,” 2023.

[13] B. Mahoney, “Design and Performance Evaluation of Time-of-Use Electricity Tariffs,” *Master Thesis, ETH Zurich*, 2023.

[14] M. González Vayá, *Optimizing the electricity demand of electric vehicles. Creating value through flexibility*. Doctoral thesis, ETH Zurich, 2015.

[15] J. Z. Kolter and M. J. Johnson, “Redd : A public data set for energy disaggregation research,” 2011.

[16] Elektrizitätswerke des Kantons Zürich (EKZ), “Tarife Privatkunden.” https://www.ekz.ch/de/privatkunden/strom/tarife/stromtarife, 2023. Accessed: 20 October 2023.

[17] K. Kaiser and G. Hug, “Dynamic Grid Tariffs for Power Peak Reduction Using Reinforcement Learning,” in *2024 International Conference on Smart Energy Systems and Technologies (SEST)*, (Torino, Italy), September 2024.

[18] H. v. Hasselt, A. Guez, and D. Silver, “Deep Reinforcement Learning with Double Q-learning,” 2015. arXiv:1509.06461v3.

[19] E. Stai, K. Kaiser, J. Stoffel, M. González Vayá, and G. Hug, “Automatic load management in active distribution grids using reinforcement learning,” in *IEEE PES ISGT Europe 2023*, (Grenoble, France), October 2023.

[20] T. Haarnoja, A. Zhou, P. Abbeel, and S. Levine, “Soft Actor-Critic: Off-Policy Maximum Entropy Deep Reinforcement Learning with a Stochastic Actor,” *Proc. of the 35 th Int’l Conf. on Machine Learning*, 2018.

[21] L. C. Hau and Y. S. Lim, “Proposed method for evaluating controllers of battery-based storage system in maximum demand reductions,” *Journal of Energy Storage*, vol. 46, p. 103850, 2022.

[22] R. Mutschler, M. Rüdisüli, P. Heer, and S. Eggimann, “Benchmarking cooling and heating energy demands considering climate change, population growth and cooling device uptake,” *Applied Energy*, vol. 288, no. 116636, 2021.

[23] J. Brooke *et al.*, “Sus-a quick and dirty usability scale,” *Usability evaluation in industry*, vol. 189, no. 194, pp. 4–7, 1996.

[24] T. Brudermueller and M. Kreft, “Smart meter data analytics: Practical use-cases and best practices of machine learning applications for energy data in the residential sector,” in *ICLR 2023 Workshop on Tackling Climate Change with Machine Learning*, 2023.

[25] M. Kreft, T. Brudermueller, T. Anderson, and T. Staake, “Identifying electric water heaters from low-resolution smart meter data,” in *2024 IEEE Conference on Technologies for Sustainability (SusTech)*, pp. 128–135, 2024.

[26] M. Kreft, T. Brudermueller, E. Fleisch, and T. Staake, “Predictability of electric vehicle charging: Explaining extensive user behavior-specific heterogeneity,” *Applied Energy*, vol. 370, no. 123544, 2024.

[27] A. Heider, L. Kundert, B. Schachler, and G. Hug, “Grid reinforcement costs with increasing penetrations of distributed energy resources,” in *2023 IEEE Belgrade PowerTech*, (Belgrade, Serbia), June 2023.

# 10 Appendix

## 10.1 Simulation environment

**Inflexible load** The inflexible load profile $P^{\text{inf}}$ is computed by subtracting the SM profiles of households with a controllable EWH and/or HP from the overall TS load. Furthermore, the EV load of controllable charging sessions is subtracted. To account for the inflexible consumption of the given households, the average SM profile of customers without electric heating, EWH, EV, and PV is scaled to the number of simulated households. Finally, a PV generation profile is subtracted to account for PV installations of simulated households and potential additional PV (Section 3.3.2). This PV profile is either based on weather data (Section 3.3.2), or measurements of two PV installations in Winkel (Section 4.2.5).

**EWH and HP simulation** EWHs and HPs are modeled as described in [17], except that (i) in the simulation environment used in Sections 3.3.2 and 4.2.5, the water storage tank of HPs is sized to be able to bridge between 1 and 2 hours of blocking at the maximum heat demand, similar to [27], and (ii) HPs with a nominal electrical power greater than or equal to 7 kW are modeled as modulating heat pumps. All other heat pumps are assumed to be on-off-controlled with a 5 K hysteresis, as in [17].

**Simulation of EV charging** The simulation of EV charging is based on real-world data from OrtsNetz. In the simulation, each EV has a fixed charging power, charging efficiency and battery capacity. The EV plug-in times, SoC at plug-in, and SoC at departure are used to determine the requirements for each session. In Section 4.2.5, only sessions during which the EV was controlled in the pilot are considered (all other sessions are part of the inflexible load). During training of the DSO agent (Section 3.3.2), charging was assumed to be flexible for all charging sessions at home.

## 10.2 Adapted DLC formulation

This formulation is an improved version of the DLC introduced in Section 3.3.4 to address the deficiency identified during the pilot in summer days, where most EWHs demanded power before the injection peaks. Therefore, a new expression for the flexible load and a revised set of EWH constraints are introduced. The adapted DLC was implemented in the simulations presented in Section 4.2.5. In this formulation, the HP and EV flexibility constraints remain unchanged. For brevity, only the new parameters and variables are defined.

**Objective function** We penalize the deviations from a reference value $P^{\text{ref}}$ of the total demand $P^{\text{tot}}$ at any time $t$ of the 24-hour horizon.

$$\min_{\mathbf{u},\rho^{\text{EWH}},\mathbf{s}^{\text{EV}},\mathbf{SoC}^{\text{EV}}} \quad \sum_{t=0}^{K-1} (P_t^{\text{tot}} - P^{\text{ref}})^2 \tag{52}$$

where $P_t^{\text{tot}} = P_t^{\text{inf}} + P_t^{\text{flx}}$, and the flexible load is now estimated as:

$$P_t^{\text{flx}} = \sum_{c=1}^{N_{\text{customers}}} \left(0.1 u_{c,t}^{\text{EWH}} + 0.9 \rho_{c,t}^{\text{EWH}}\right) \cdot P_{c,\text{nom}}^{\text{EWH}} + \sum_{c=1}^{N_{\text{customers}}} u_{c,t}^{\text{HP}} \cdot \rho_t^{\text{HP}} \cdot P_{c,\text{nom}}^{\text{HP}} + \sum_{c=1}^{N_{\text{customers}}} u_{c,t}^{\text{EV}} \cdot P_{c,\text{nom}}^{\text{EV}} \quad \forall t \tag{53}$$

The decision variable $\rho_{c,t}^{\text{EWH}}$ is introduced to model the times when the EWH runs (demands power) while the device is unblocked, i.e., $\rho_{c,t}^{\text{EWH}} = 1$ when running or $\rho_{c,t}^{\text{EWH}} = 0$ when not, while $u_{c,t}^{\text{EWH}} = 1$. We assume that the EWH only runs during the first $K_{c,\text{EWH}}^{\text{run}}$ intervals[12] of the unblocking period and demands the nominal power. We also assume that the EWH demands 10 % of the nominal power in the remaining intervals, i.e., when $u_{c,t}^{\text{EWH}} = 1$ and $\rho_{c,t}^{\text{EWH}} = 0$. The objective function in (52) is subject to the following constraints:

[12] The input parameter $K_{c,\text{EWH}}^{\text{run}}$ was set to 6, meaning that the EWH runs the first 1.5 hours of the unblocking period.

### EWH flexibility constraints

$$\sum_{i=0}^{t} u_{c,i}^{\text{EWH}} + \sum_{i=1}^{K-1-t} u_{c,-i}^{\text{EWH}} \geq K - K_{c,\text{EWH}}^{\text{block,24h}}, \quad 0 \leq t \leq K-2 \tag{54}$$

$$\sum_{t=0}^{K-1} u_{c,t}^{\text{EWH}} \geq K - K_{c,\text{EWH}}^{\text{block,24h}} \tag{55}$$

$$\sum_{i=0}^{K_{c,\text{EWH}}^{\text{min,block}} - N_{c,\text{EWH}}^{\text{blocked}} - 1} u_{c,i}^{\text{EWH}} \leq 0, \quad \text{if } u_{c,-1}^{\text{EWH}} = 0 \text{ and } t = 0 \tag{56}$$

$$\sum_{i=t}^{t+K_{c,\text{EWH}}^{\text{min,block}}-1} (1 - u_{c,i}^{\text{EWH}}) \geq K_{c,\text{EWH}}^{\text{min,block}} \cdot (u_{c,t-1}^{\text{EWH}} - u_{c,t}^{\text{EWH}}), \quad 0 \leq t \leq K - K_{c,\text{EWH}}^{\text{min,block}} \tag{57}$$

$$\sum_{i=t}^{K-1} (1 - u_{c,i}^{\text{EWH}}) \geq (K-t) \cdot (u_{c,t-1}^{\text{EWH}} - u_{c,t}^{\text{EWH}}), \quad K - K_{\text{min,block}}^{\text{EWH}} + 1 \leq t \leq K-2 \tag{58}$$

$$\sum_{i=0}^{K_{c,\text{EWH}}^{\text{min,unblock}} - N_{c,\text{EWH}}^{\text{unblocked}} - 1} u_{c,i}^{\text{EWH}} \geq K_{c,\text{EWH}}^{\text{min,unblock}} - N_{c,\text{EWH}}^{\text{unblocked}}, \quad \text{if } u_{c,-1}^{\text{EWH}} = 1 \text{ and } t = 0 \tag{59}$$

$$\sum_{i=t}^{t+K_{c,\text{EWH}}^{\text{min,unblock}}-1} u_{c,i}^{\text{EWH}} \geq K_{c,\text{EWH}}^{\text{min,unblock}} \cdot (u_{c,t}^{\text{EWH}} - u_{c,t-1}^{\text{EWH}}), \quad 0 \leq t \leq K - K_{c,\text{EWH}}^{\text{min,unblock}} \tag{60}$$

$$\sum_{i=t}^{K-1} u_{c,i}^{\text{EWH}} \geq (K-t) \cdot (u_{c,t}^{\text{EWH}} - u_{c,t-1}^{\text{EWH}}), \quad K - K_{\text{min,unblock}}^{\text{EWH}} + 1 \leq t \leq K-2 \tag{61}$$

$$\sum_{i=0}^{-N_{c,\text{EWH}}^{\text{unblocked}} + K_{c,\text{EWH}}^{\text{max, unblock}}} 1 - u_{c,i}^{\text{EWH}} \geq 1, \quad \text{if } u_{c,-1}^{\text{EWH}} = 1, t = 0,\ K_{c,\text{EWH}}^{\text{min, unblock}} < N_{c,\text{EWH}}^{\text{unblocked}} \tag{62}$$

$$\sum_{i=t+K_{c,\text{EWH}}^{\text{min, unblock}}}^{t+K_{c,\text{EWH}}^{\text{max, unblock}}+1} 1 - u_{c,i}^{\text{EWH}} \geq u_{c,t}^{\text{EWH}} - u_{c,t-1}^{\text{EWH}}, \quad \text{if } 0 \leq t \leq K - K_{c,\text{EWH}}^{\text{max, unblock}} - 2 \tag{63}$$

$$\sum_{i=t}^{t+K_{c,\text{EWH}}^{\text{run}}-1} \rho_{c,i}^{\text{EWH}} \geq K_{c,\text{EWH}}^{\text{run}} \cdot \left(u_{c,t}^{\text{EWH}} - u_{c,t-1}^{\text{EWH}}\right), \quad \text{if } 0 \leq t \leq K - K_{c,\text{EWH}}^{\text{run}} \tag{64}$$

$$\sum_{i=t}^{K-1} \rho_{c,i}^{\text{EWH}} \geq (K-t) \cdot \left(u_{c,t}^{\text{EWH}} - u_{c,t-1}^{\text{EWH}}\right), \quad \text{if } K - K_{c,\text{EWH}}^{\text{run}} + 1 \leq t \leq K-2 \tag{65}$$

$$\sum_{i=0}^{-N^{\text{running}}_{c,\text{EWH}}+K^{\text{EWH}}_{\text{max, unblock}}-1} \rho^{\text{EWH}}_{c,i} \leq K^{\text{run}}_{c,\text{EWH}} - N^{\text{running}}_{c,\text{EWH}},$$

$$\text{if } \rho^{\text{EWH}}_{c,-1} = 1, t = 0 \tag{66}$$

$$\sum_{i=0}^{-N^{\text{EWH,unblocked}}_{c}+K^{\text{EWH}}_{\text{max, unblock}}-1} \rho^{\text{EWH}}_{c,i} \leq 0,$$

$$\text{if } K^{\text{EWH}}_{\text{max, unblock}} > N^{\text{EWH,unblocked}}_{c}, \rho^{\text{EWH}}_{c,-1} = 0, u^{\text{EWH}}_{c,-1} = 1, t = 0 \tag{67}$$

$$\sum_{i=t}^{t+K^{\text{EWH}}_{\text{max, unblock}}-1} \rho^{\text{EWH}}_{c,i} \leq K^{\text{run}}_{c,\text{EWH}},$$

$$\text{if } 0 \leq t \leq K - K^{\text{EWH}}_{\text{max, unblock}} \text{ and } u^{\text{EWH}}_{c,-1} = 0 \tag{68}$$

$$\sum_{i=t}^{K-1} \rho^{\text{EWH}}_{c,i} \leq K^{\text{run}}_{c,\text{EWH}}, \quad \text{if } K - K^{\text{EWH}}_{\text{max, unblock}} + 1 \leq t \leq K - 2 \tag{69}$$

$$\sum_{i=0}^{-N^{\text{running}}_{c,\text{EWH}}+K^{\text{run}}_{c,\text{EWH}}-1} \rho^{\text{EWH}}_{c,i} \geq (K^{\text{run}}_{c,\text{EWH}} - N^{\text{running}}_{c,\text{EWH}}) \cdot u^{\text{EWH}}_{c,t},$$

$$\text{if } \rho^{\text{EWH}}_{c,-1} = 1, t = 0, \text{ and } N^{\text{running}}_{c,\text{EWH}} < K^{\text{run}}_{c,\text{EWH}} \tag{70}$$

$$\rho^{\text{EWH}}_{c,t} \leq u^{\text{EWH}}_{c,t}, \quad \forall t \tag{71}$$

$$\rho^{\text{EWH}}_{c,t} \in \{0, 1\}, \quad \forall t \tag{72}$$

$$u^{\text{EWH}}_{c,t} \in \{0, 1\}, \quad \forall t. \tag{73}$$

The constraints (54)-(55) ensure that a maximum number of blocking intervals $K^{\text{block,24h}}_{c,\text{EWH}}$ is not exceeded in any 24-hour window. The constraints (56)-(58) specify a minimum duration of a blocking instance. Similarly, the constraints (59) - (61) ensure that the EWHs remain unblocked for the specified number of time steps between two blocking events. We also introduced constraints (62) - (63) to limit the duration of the unblocking sessions to no more than $K^{\text{max, unblock}}_{c,\text{EWH}}$ intervals. We must choose $K^{\text{max, unblock}}_{c,\text{EWH}} > K^{\text{min, unblock}}_{c,\text{EWH}}$. The constraints (64)-(69) ensure that the EWH runs only the first $K^{\text{run}}_{c,\text{EWH}}$ intervals right after a blocking event. Likewise, (70) forces the EWH to operate during the first intervals of the horizon if it was running in the past and $K^{\text{run}}_{c,\text{EWH}} > N^{\text{running}}_{c,\text{EWH}}$, where $N^{\text{running}}_{c,\text{EWH}}$ is the number of previous consecutive intervals the EWH of customer $c$ was running.

**HP flexibility constraints** They were defined in (32) - (42).

**EV flexibility constraints** They were defined in (43) - (50).

## 10.3 Additional figures for the manual customer reaction

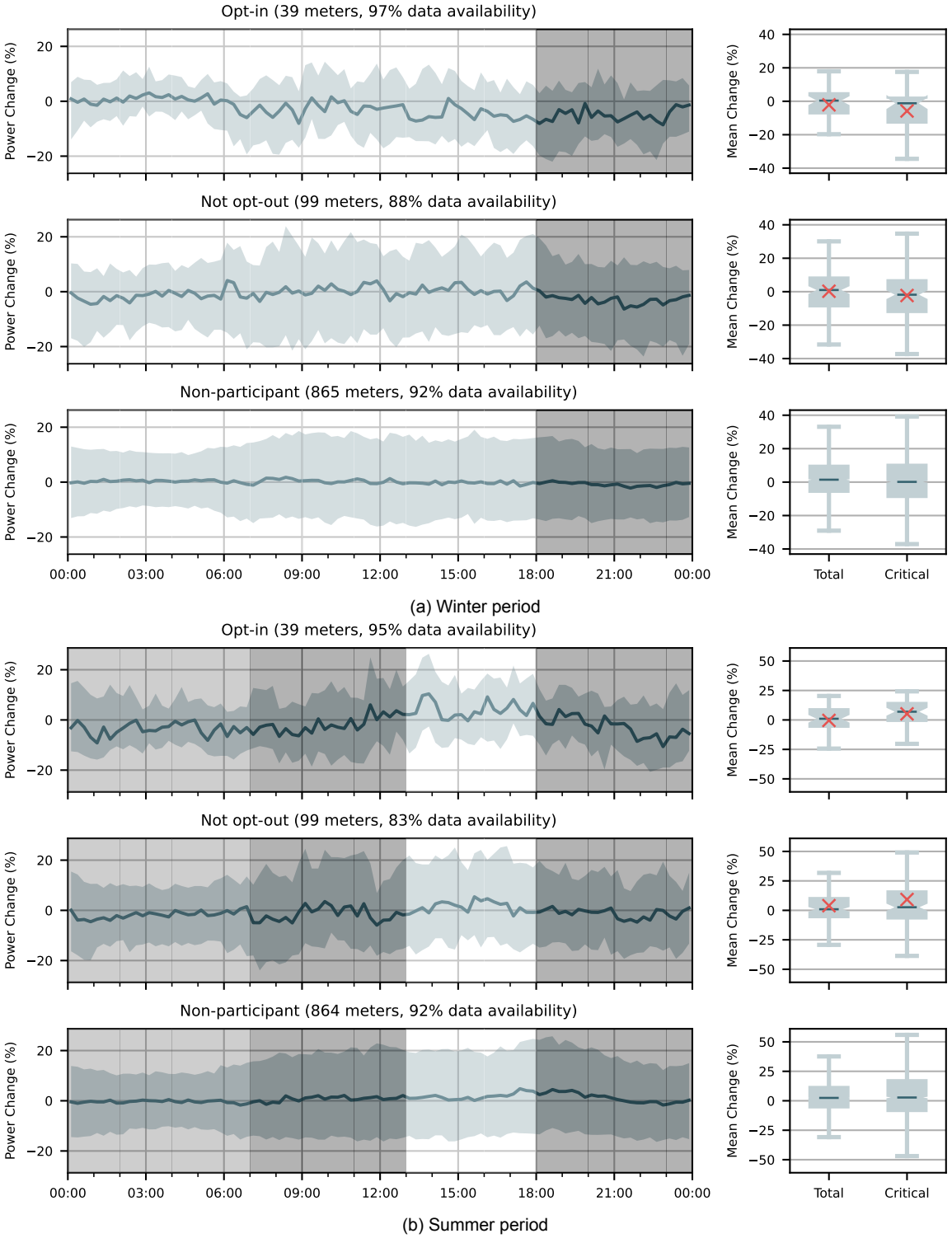


Figure 46: Manual response in power consumption of customers with the time of use tariff. The relative change in the average power profile is calculated from before to after the project start within the winter (a) and summer (b) tariff period. Solid lines show the median across households and shaded areas the quartiles. The box plot labeled Total represents the average across the whole day, the one labeled Critical the average across the hours with the highest/lowest (winter/summer) tariff.

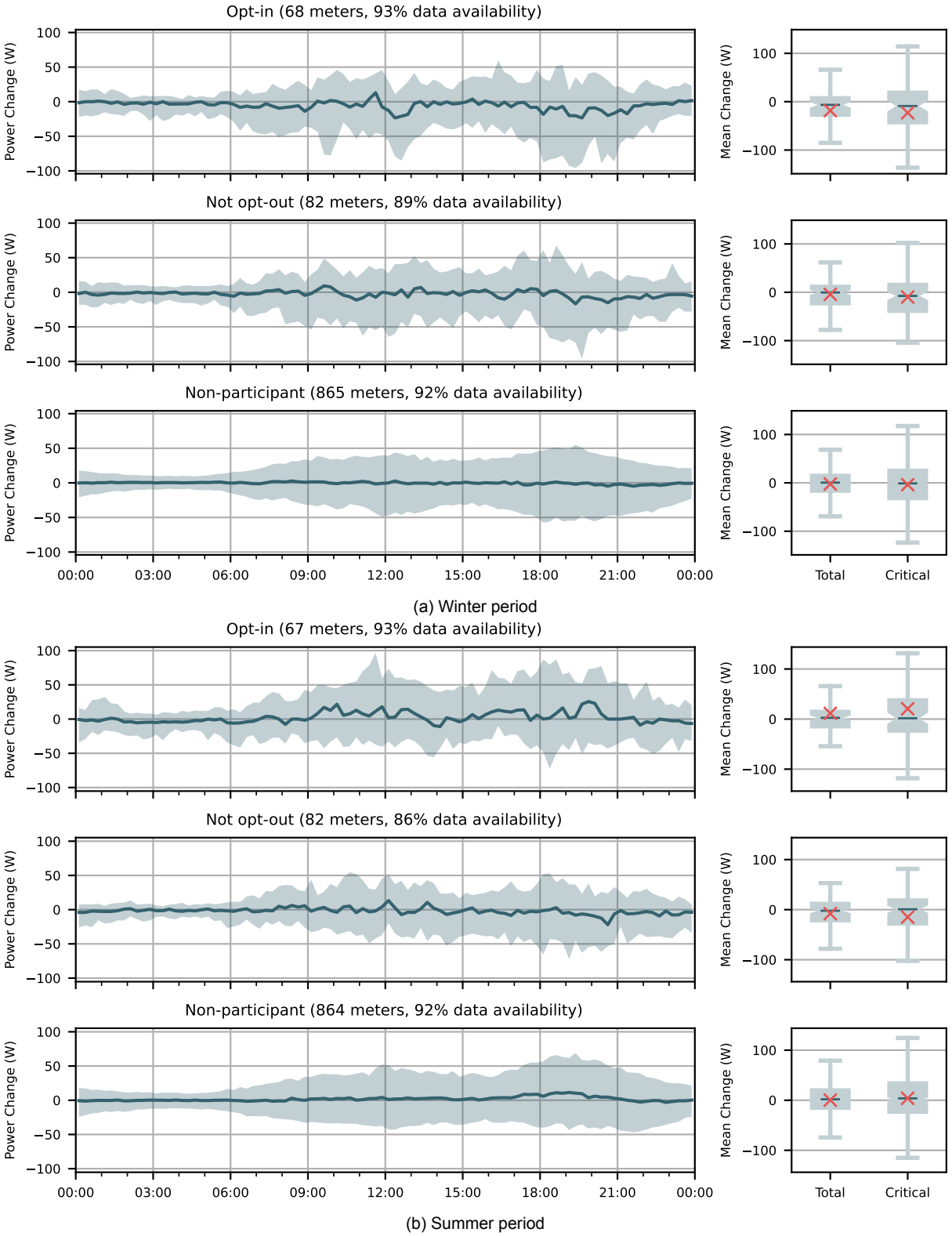


Figure 47: Manual response in power consumption of customers with the dynamic tariff. The change in the average power profile is calculated from before to after the project start within the winter (a) and summer (b) tariff period. Solid lines show the median across households and shaded areas the quartiles. The box plot labeled “Total” represents the average across the whole day, the one labeled “Critical” the average across the evening/noon (winter/summer) hours.

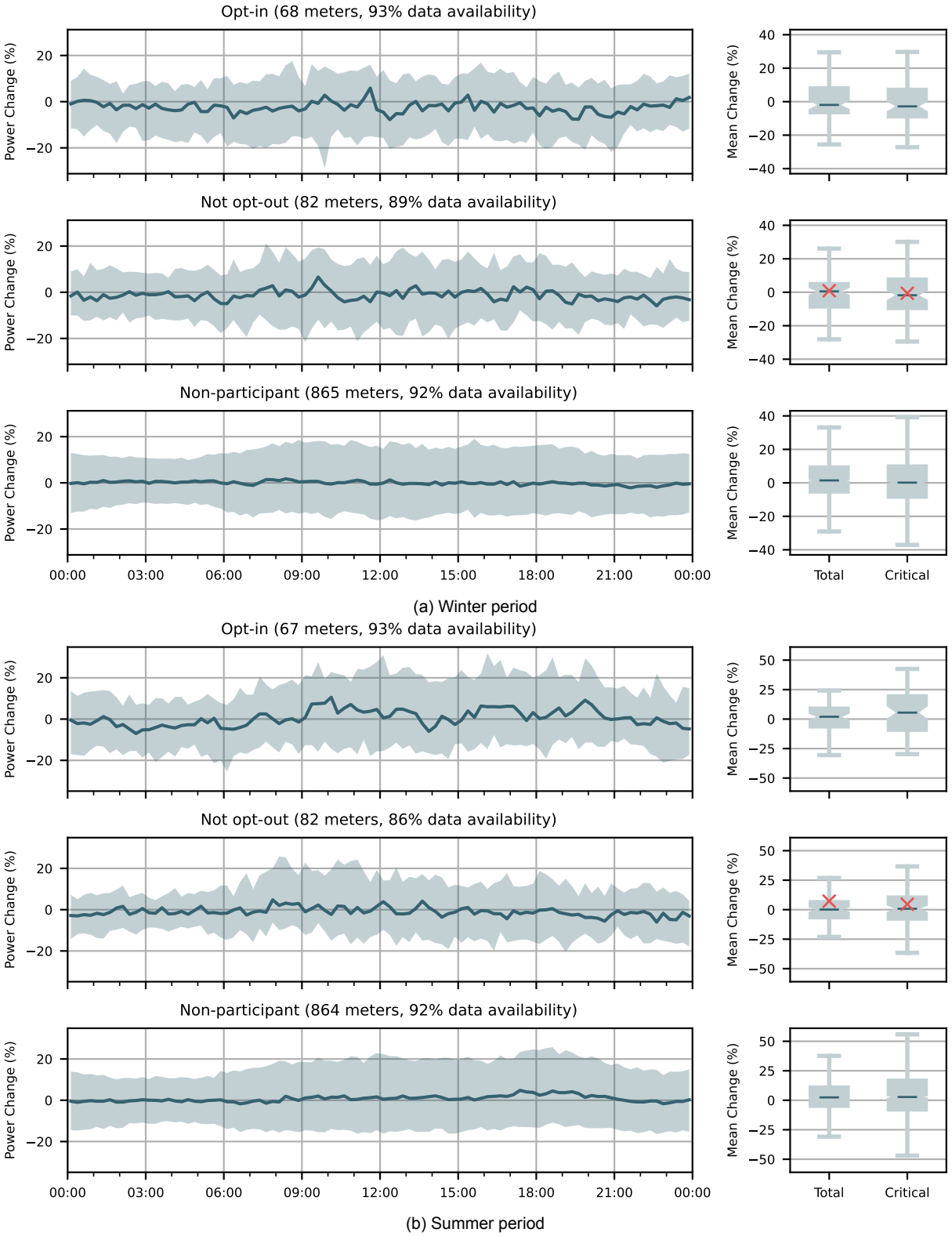


Figure 48: Manual response in power consumption of customers with the dynamic tariff. The relative change in the average power profile is calculated from before to after the project start within the winter (a) and summer (b) tariff period. Solid lines show the median across households and shaded areas the quartiles. The box plot labeled “Total” represents the average across the whole day, the one labeled “Critical” the average across the evening/noon (winter/summer) hours.

## 10.4 Exact wording of questions in the final survey

Here, we report the exact wording of questions asked in the final survey on a 5-point Likert scale (from “1 = stimme überhaupt nicht zu” to “5 = stimme sehr zu”):

- “Der neue Stromtarif war für mich verständlich”
- “Die Höhe der Gutschrift war angemessen”
- “Ich habe mich bemüht, meinen Stromverbrauch auf Zeiten zu verschieben, in denen der Strom besonders günstig war”
- “Ein Energieversorger sollte neuartige Stromtarife vergleichbar mit denen im Projekt OrtsNetz anbieten”

and on an a 5-point Likert scale (“sehr unzufrieden – eher unzufrieden – weder noch – eher zufrieden – sehr zufrieden“): “Wie zufrieden sind Sie mit dem Projekt OrtsNetz?”